Trisections of non-orientable 4–manifolds

by

Patrick Naylor

A thesis
presented to the University of Waterloo
in fulfillment of the
thesis requirement for the degree of
Doctor of Philosophy
in
Pure Mathematics

Waterloo, Ontario, Canada, 2021

Examining Committee Membership

The following served on the Examining Committee for this thesis. The decision of the Examining Committee is by majority vote.

External Examiner:	David Gay Professor Mathematics Department University of Georgia
Supervisor:	Doug Park Professor Department of Pure Mathematics University of Waterloo
Internal Member:	Jason Bell Professor Department of Pure Mathematics University of Waterloo
Internal Member:	Ben Webster Associate Professor Department of Pure Mathematics University of Waterloo
Internal-External Member:	Jon Yard Associate Professor Department of Combinatorics and Optimization University of Waterloo

Author's Declaration

This thesis consists of material all of which I authored or co-authored: see the Statement of Contributions included in the thesis. This is a true copy of the thesis, including any required final revisions, as accepted by my examiners.

I understand that my thesis may be made electronically available to the public.

Statement of Contributions

I am the sole author of Chapter 1 and 2, which are intended as an introduction to the theory of trisections. Chapters 3 and 4 are based on the article [59] (a preprint may be found at arXiv:2010.07433), which is a joint project with Maggie Miller.

Abstract

Broadly, this thesis is concerned with trying to understand 4–manifolds through 3–dimensional techniques. From the point of view of smooth manifolds, dimension four is quite unique; one striking illustration of this is the fact that $\mathbb{R}^n$ admits either one (if $n \neq 4$) or uncountably many (if $n = 4$) smooth structures. There are many remaining questions about the differences between topological and smooth categories in dimension four: for instance, the last remaining Poincaré conjecture asks whether S^4 admits a unique smooth structure. Nonetheless, one might attempt to use tools from lower dimensions to gain some insight.

One highly useful tool in dimension three is the notion of a *Heegaard splitting*: a symmetric decomposition of a closed 3–manifold into two handlebodies that meet along an embedded closed surface. Originally introduced by Heegaard in 1898, they connect 3–manifolds to fundamental objects like mapping class groups groups and the curve complex. Recent techniques like Heegaard Floer homology theories have shown that they are also an effective computational tool that can be used to distinguish 3–manifolds.

In analogy with Heegaard splittings, Gay and Kirby recently introduced the idea of a *trisection* of an orientable closed 4–manifold: a decomposition into three 4–dimensional handlebodies with controlled intersection data. Because a trisection is largely determined by lower-dimensional information, one would hope to use 3–dimensional techniques to understand 4–dimensional phenomena. Trisections have already been used to reprove fundamental results in gauge theory, and define new invariants for 4–manifolds. In this thesis, we complete the theory of trisections for non-orientable 4–manifolds.

Chapter 1 gives the necessary preliminaries for the rest of the thesis. Chapter 2 is a self-contained introduction to trisections that summarizes the current state of the literature and contains many motivating examples.

Chapter 3 is concerned with developing the 3– and 4–dimensional results necessary to carefully extend the theory of trisections to the non-orientable setting. In particular, we prove an analogue of a theorem of Laudenbach-Poénaru which does not seem to appear in the literature. We also give a non-orientable version of Waldhausen's theorem on Heegaard splittings of $\#S^2 \times S^1$ which may be of independent interest.

In Chapter 4, we extend the theory of trisections to non-orientable 4–manifolds. By adapting the orientable case and results from §3, we give proofs of existence and stable uniqueness, along with many examples. We also cover non-orientable relative trisections (for 4–manifolds with boundary) and bridge trisections (for embedded surfaces in 4–manifolds).

Acknowledgements

Firstly, I would like to thank my supervisor, Doug Park. You have been a constant source of guidance, patience, and wisdom. This thesis certainly would not have been possible without your support– for that I am extremely grateful.

I am also grateful for the warm and friendly atmosphere in the Department of Pure Mathematics. To my friends in Waterloo– Blake, Diana, Graeme, Ian, Nick, Ragini, Shubham, and Ty– thank you for your encouragement and support. My office mate Zack Cramer deserves special thanks: for mathematical advice, several years of coffee trips to C&D, and being an excellent departmental BBQ co-chef. So too does Anton Mosunov: for five years of mathematical conversations, being able to live with me while I wrote this thesis, and putting up with my baking. I would also like to extend my gratitude to the department secretaries: Lis D'Alessio, Jackie Hilts, Nancy Maloney, and Pavlina Penk, who make the department such a great place to work.

The members of my examining committee– Jason Bell, David Gay, Ben Webster, and Jon Yard– deserve a special thank you for taking the time to read and provide comments on this thesis.

I owe a debt of gratitude to the members of the ever-growing trisection community. You have been my mathematical mentors and colleagues for the past few years, and collectively taught me a great deal. David Gay originally welcomed me to this community, and for that I am very grateful. To Alex, Gabe, Hannah, Jason, Jeff, Sarah, and Vince: thank you for your friendship, conversations about topology, and time well spent singing karaoke. To Maggie Miller in particular: thank you for your interest in this project, and for the contents of a box labelled "blanket, yarn."

Lastly, I would like to extend my sincere gratitude to my friends in Winnipeg (and elsewhere) for their encouragement. I would also like to thank my family, who gave their constant support to a mathematician living over a thousand miles away.

Dedication

This thesis is dedicated to my grandmother, Brenda.

Table of Contents

List of Figures

Chapter 1

Decompositions of smooth manifolds

This thesis is concerned with decompositions of 3– and 4– dimensional manifolds. One of the most useful ways to study smooth manifolds arises through the study of *Morse functions*, i.e. smooth functions from a manifold to $\mathbb{R}$. This naturally leads to the idea of a handle decomposition: a way of "building" a manifold from standard pieces. In particular, 3–manifolds admit special handle decompositions called *Heegaard splittings*. The theory of trisections attempts to emulate these ideas for 4–manifolds.

While we will assume familiarity with Morse theory and handle decompositions, we review the basic definitions in this chapter for convenience and in preparation for a brief treatment of trisections in Chapter 2. Manifolds in this thesis are generally assumed to be smooth, compact, and connected unless otherwise noted. Since non-orientable manifolds will play a large role in this thesis, we will indicate whether manifolds must be assumed to be orientable.

1.1 Morse functions and handle decompositions

Given a smooth manifold X, the study of smooth maps $f : X \to \mathbb{R}$ provides considerable insight into the topology of X. In this section, we review handle decompositions. For more details, see [28, Part 2] and [60].

Definition 1.1.1. Let X be a smooth, closed, and connected manifold of dimension n. Let $f : X \to \mathbb{R}$ be a smooth function, and $p \in X$ be a critical point for f, i.e $Df_p = 0$. Fixing a local coordinate system $(x_1, \ldots, x_n)$ near p, the Hessian matrix at p is the symmetric

matrix of second order partial derivatives

$$H_p = \left[\frac{\partial^2 f}{\partial x_i \partial x_j}(p) \right].$$

The point p is called a *non-degenerate critical point* if H_p is non-singular; one can show that this property does not depend on the choice of coordinates.

Definition 1.1.2. Let X be a smooth, closed, and connected manifold of dimension n. A smooth function $f : X \to \mathbb{R}$ is called *Morse* if it has no degenerate critical points.

Any given compact manifold X admits many Morse functions. In fact, being Morse is a generic property: Morse functions form an open dense subset of $C^\infty(X; \mathbb{R})$ with the compact-open topology.

In what follows, we will fix a compact connected manifold X and a Morse function $f : X \to \mathbb{R}$. By a version of the implicit function theorem, the preimage $f^{-1}(a)$ of any regular value $a \in \mathbb{R}$ is a smooth compact manifold that we will denote $X_{[a]} \subset X$. On the other hand, if a is a critical value, we can understand $f^{-1}(a)$ via the famous Morse lemma.

Lemma 1.1.3. *Let X be a smooth, closed, and connected manifold of dimension n, and let $f : X \to \mathbb{R}$ be a Morse function. If $a \in \mathbb{R}$ is a critical value for f, then there are local coordinates $(x_1, \ldots, x_n)$ in a neighbourhood U of p and an integer k so that $x_i(p) = 0$ for all i, and on U we have*

$$f(z) = f(p) - (x_1(z))^2 - \cdots - (x_k(z))^2 + (x_{k+1}(z))^2 + \cdots + (x_n(z))^2.$$

The number k is called the index *of f at p.*

If a and b are two regular values of f, then $f^{-1}([a, b]) \subset X$ is a cobordism (i.e. an n manifold with boundary $f^{-1}(a) \sqcup f^{-1}(b)$) between the manifolds $X_{[a]}$ and $X_{[b]}$. In fact, if $[a, b]$ contains no critical values, then one can show that $f^{-1}([a, b])$ is diffeomorphic to the product $X_{[a]} \times [a, b]$ (and in particular, $X_{[a]} \cong X_{[b]}$). If $[a, b]$ contains a single critical point, then Lemma 1.1.3 gives a local model for the cobordism $f^{-1}([a, b])$ called a *handle attachment*.

Lemma 1.1.4. *Let $f : X \to \mathbb{R}$ be a Morse function, and let a and b be regular values for f. If $[a, b]$ contains no critical values, then $f^{-1}([a, b])$ is diffeomorphic to $f^{-1}(a) \times [a, b]$. If $[a, b]$ contains a single critical value of index k, then $f^{-1}([a, b])$ is diffeomorphic to an* n–dimensional k–handle *attached to $f^{-1}([a, a + \epsilon])$ (for some small $\epsilon > 0$).*

Since each critical point is isolated, the manifold X can built as a union of these specific kinds of cobordisms, i.e. by Lemma 1.1.4, by *attaching handles*. In what follows, we will set $D^k = [-1,1]^k$.

Definition 1.1.5. Let $0 \leq k \leq n$. An n–dimensional k–handle h is the attachment of $D^k \times D^{n-k}$ to the boundary of an n–manifold along $S^{k-1} \times D^{n-k}$. Here, we are using the decomposition

$$\partial(D^k \times D^{n-k}) = S^{k-1} \times D^{n-k} \cup D^k \times S^{n-k-1}.$$

The *attaching sphere* of h is the image of $S^{k-1} \times \{0\}$, and the *core* of h is the image of $D^k \times \{0\}$. The *belt sphere* of h is the image of $\{0\} \times S^{n-k-1}$, and the co-core of h is the image of $\{0\} \times D^{n-k}$.

An n–dimensional handle is always abstractly diffeomorphic to D^n, but each index corresponds to a different kind of attachment. For a fixed n and k, an n–dimensional k–handle h is generally determined by two things: the isotopy class of the attaching sphere and a framing, i.e. a specific trivialization of neighbourhood of the the attaching sphere of h. Once a trivialization is fixed, then any other trivialization differs from it by an element of $\pi_{k-1}(GL(n-k))$. Thus, isotopy classes of framings of n–dimensional k–handles are in (non-canonical) bijection with $\pi_{k-1}(GL(n-k))$. This is a known (and sometimes trivial) group for small n and k. Applying a transversality argument to the attaching spheres, one can show that all handles of index k may be assumed to be attached before any handles of index $k+1$, and we will usually assume this is the case.

Some handles are illustrated in Figure 1.1 for small k and n. In each case, the attaching sphere is colored red and the belt sphere is colored blue (when they are non-empty).

In some cases, we need surprisingly little information to specify a handle attachment. In what follows, suppose that X is an n–dimensional manifold. A 0–handle is "attached" to X along $S^{-1} \times D^n = \emptyset$; we interpret this as taking the disjoint union with D^n. An n–handle is attached to X along $S^{n-1} \times D^0$, and by the above discussion there is a unique way to frame an $(n-1)$– sphere in ∂X. For $n \leq 4$, any orientation preserving diffeomorphism of S^{n-1} is smoothly isotopic to the identity map (though this is highly non-trivial when $n = 4$), and so there is a unique way to attach an n–handle in these dimensions.

The attaching sphere of a 1–handle is $S^0 \times \{0\}$, i.e. two points. If ∂X is connected, then there is a unique embedding of S^0 in ∂X up to isotopy. A framing corresponds to an element of $\pi_0(GL(n-1)) \cong \mathbb{Z}_2$ (for $n \geq 2$), and so there are two ways to attach a 1–handle to ∂X, depending on whether the loop determined by the core of the 1–handle is orientation preserving or not.

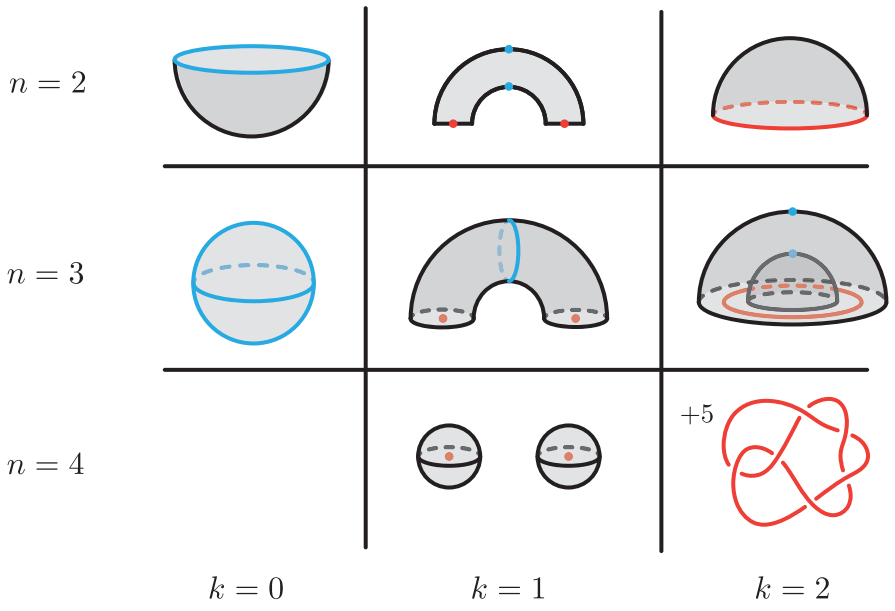

Figure 1.1: Various handles for small k and n. Each handle is diffeomorphic to an n–ball, but attached along a neighbourhood of the attaching sphere (in red). A 4–dimensional 0–handle is a 4–ball. We "draw" the boundary by visualizing the page as most of S^3. Similarly, we only draw the "feet" of a 4–dimensional 1–handle, indicated by two 3–balls. We only draw the attaching sphere for a 4–dimensional 2–handle (drawn in $\partial B^4 = S^3$). The framing is indicated with an integer.

If $n = 3$, then the attaching sphere of a 2–handle is an embedding of S^1 (into a surface). A framing corresponds to an element of $\pi_1(GL(1)) \cong \{1\}$, and so a 2–handle attachment is completely determined by the isotopy class of an embedded circle (the image of $S^1 \times \{0\}$) in ∂X.

If $n = 4$, then 2–handles are still attached along a knot K in ∂X (which is now a 3–manifold), but framings are now in bijection with $\pi_1(GL(2)) \cong \mathbb{Z}$. Various conventions exist to keep track of the framings of 2–handles; for more details see [28]. In the case that 2–handles are attached to $\partial B^4 = S^3$, one solution is to declare the 0–framing to be the one which intersects a Seifert surface $F \subset S^3$ for K zero times. Then, one can assign an integer to a framing by counting the number of times a pushoff of K intersects F.

It is natural to ask how two handle decompositions of M are related. Note that since $\mathbb{R}$ is contractible any two Morse functions are at least homotopic. Such a homotopy cannot be taken to be Morse at all times, but Theorem 1.1.6 guarantees that there are only finitely

many times where it fails to be Morse. At such times, there are two possible local models for the change in the function, called *handle cancellation*, and *handle sliding*.

Theorem 1.1.6 ([18], e.g. see [28, §4])**.** *Given any two handle decompositions (ordered in levels of increasing index) corresponding to a Morse function $f : M \to \mathbb{R}$, it is possible to get from one to the other by a sequence of the following moves:*

1. *Isotopy of handles within levels. This corresponds to an isotopy of the corresponding Morse function.*
2. *Creating/cancelling a k– and $(k+1)$–handle pair. In this case, there are local coordinates $(x_1, \dots, x_n)$ on on a neighbourhood $U \subset M$ so that the homotopy f_t has the form*
$$f_t(x_1, \dots, x_n) = -x_1^2 - \cdots - x_k^3 - (t - t_0)x_{k+1} + x_{k+2}^2 + \cdots + x_n^2$$
for some $t_0 \in \mathbb{R}$. If the attaching sphere of a $(k+1)$–handle and the belt sphere of the k–handle intersect in exactly one point, then they can be cancelled.
3. *A handle slide of a k–handle over another k–handle. In this case, two critical points cross at some $t_0 \in \mathbb{R}$. On the level of handles, this is given by pushing the attaching sphere of one handle through the belt sphere of the other handle; at the time t_0, the spheres will intersect in a single point.*

In the 2–dimensional case, a cancelling handle pair is illustrated in Figure 1.2, and a handle slide is illustrated in Figure 1.3.

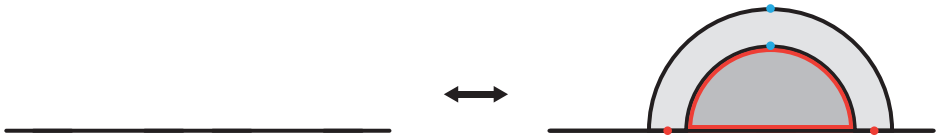

Figure 1.2: A creation/cancellation of a 2–dimensional 1– and 2–handle. The attaching sphere of the 2–handle (S^1) intersects the belt sphere of the 1–handle (S^0) transversely in a single point. Attaching this pair of handles is diffeomorphic to attaching none at all.

The reader is referred to [28] for more details on handle decompositions, particularly in low dimensions.

1.2 Heegaard splittings of 3–manifolds

An essential tool for studying 3–manifolds is a *Heegaard splitting*. We will now specialize §1.1 to the case of 3–manifolds.

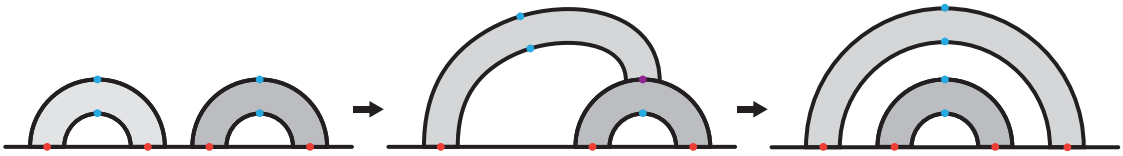

Figure 1.3: A handle slide of 2–dimensional 1–handles. We slide the attaching sphere of the left 1–handle through the belt sphere of the right 1–handle. In the middle time slice, the attaching sphere of the left 1–handle intersects the belt sphere of the right 1–handle transversely in a single point (purple). While the resulting manifolds are diffeomorphic, they have been presented differently.

Definition 1.2.1. A *handlebody* of genus g is a compact manifold which can be built with a single 0–handle and g 1–handles. Equivalently, an n–dimensional orientable handlebody is a manifold which is diffeomorphic to a regular neighbourhood of a wedge of g circles in $\mathbb{R}^n$.

Definition 1.2.2. Let M be a smooth, closed, and connected 3–manifold. A *Heegaard splitting* $\mathcal{H} = (\Sigma; H_1, H_2)$ of M is a decomposition $M = H_1 \cup_\Sigma H_2$, where $\Sigma \subset M$ is an embedded surface, and H, H' are 3–dimensional handlebodies. If Σ has genus g, we will call this a *genus g splitting*.

One imagines cutting a 3–manifold "in half," or into two equal pieces. We will generally *not* assume that M (and consequently H and H') are orientable.

Note. The boundary of a 3–dimensional handlebody is either a closed orientable surface of genus g, or decomposes as a connected sum of an *even* number of $\mathbb{RP}^2$ summands. If Σ is non-orientable and $\chi(\Sigma)$ is even, then to make certain statements simpler (e.g. Proposition 1.3.12) we will define the genus of Σ by $g(\Sigma) = \frac{1}{2}(2 - \chi(\Sigma))$. Equivalently, this is half the number of $\mathbb{RP}^2$ summands appearing in a connected sum decomposition. For example, this means that we will declare the "genus" of the Klein bottle to be equal to one.

Definition 1.2.3. Let M be a closed, connected 3–manifold, and suppose that $\mathcal{H} = (\Sigma; H_1, H_2)$ and $\mathcal{H}' = (\Sigma'; H_1', H_2')$ are two Heegaard splittings of M. We say that $\mathcal{H}$ and $\mathcal{H}$ are *equivalent* if there is a diffeomorphism $\phi : M \to M$ sending $\mathcal{H}$ to $\mathcal{H}'$. If ϕ is isotopic to id_M, then $\mathcal{H}$ and $\mathcal{H}'$ are called *isotopic*.

Since a Heegaard splitting is entirely determined by the splitting surface, $\mathcal{H}$ and $\mathcal{H}'$ are isotopic if and only if Σ and Σ' are ambiently isotopic. For brevity, we will occasionally omit reference to the handlebodies in the decomposition.

Given a Heegaard splitting of M, there is an easy way to produce another Heegaard splitting of higher genus.

Definition 1.2.4. Let $\mathcal{H} = (\Sigma; H_1, H_2)$ be a Heegaard splitting of a 3–manifold M. Let $\alpha \subset H_1$ be a properly embedded and boundary parallel arc, and define a new Heegaard splitting $\mathcal{H}'$ of M by:

- $H_1' = H_1 \setminus \nu(\alpha)$;
- $H_2' = H_2 \cup \overline{\nu(\alpha)}$;
- $\Sigma' = \partial H_1' = \partial H_2'$,

where $\nu(\alpha)$ is an open tubular neighbourhood of α. We say that $\mathcal{H}'$ is a *stabilization* of $\mathcal{H}$, or that $\mathcal{H}$ is a *destabilization* of $\mathcal{H}'$.

It is easy to check that $\mathcal{H}'$ is a Heegaard splitting of M, and that the isotopy class of $\mathcal{H}'$ does *not* depend on the choice of the arc α. Moreover, reversing the roles of H_1 and H_2 does not affect the resulting Heegaard splitting up isotopy.

While these decompositions may appear quite specialized, the following theorem of Reidemeister and Singer guarantees that *every* closed 3-manifold admits a Heegaard splitting, and that such decompositions are unique up to stabilization. We will only outline a proof of existence.

Theorem 1.2.5 ([64], [68], e.g. see [50])**.** *Any closed and connected 3–manifold M admits a Heegaard splitting. Any two Heegaard splittings for M are stably isotopic, i.e. become isotopic after some number of stabilizations.*

Proof Sketch (Existence). Let $f : M \to \mathbb{R}$ be a Morse function. By re-ordering critical points, we can assume that f is self-indexing (i.e. that if x is a critical point of index i, then $f(x) = i$), and so $f(M) = [0, 3]$. We can also assume that f has only a single critical point of index 0 and index 3. Indeed, such critical points can generally be cancelled by index 1 and index 2 critical points. Consequently M admits a handle decomposition consisting of a single 0–handle, some number of 1– and 2–handles, and a single 3–handle. In fact, the argument below shows that M must have the same number of 1– and 2–handles.

Note that $f^{-1}([0, 3/2])$ is a handlebody, since it is the result of attaching 1–handles to B^3. Similarly, by considering the Morse function $-f$ we see that $f^{-1}([3/2, 3])$ is also a handlebody. These two handlebodies meet along the common surface $f^{-1}(3/2)$, and so give a Heegaard splitting for M. □

Remark 1.2.6. The existence of Heegaard splittings may also be deduced from the triangulability of 3–manifolds due to Moise [61]. Indeed, given a triangulation of M, a neighbourhood of the 1–skeleton of this triangulation gives one obvious handlebody H_1 for M. The complement $H_2 = M \setminus H_1$ is a regular neighbourhood of the corresponding dual 1–skeleton, and so is also a handlebody.

If $\mathcal{H} = (\Sigma; H_1, H_2)$ and $\mathcal{H}' = (\Sigma'; H_1', H_2')$ are Heegaard splittings of M and M', then there is a natural Heegaard splitting of $M \# M'$ obtained by performing the connected sum at points on the splitting surfaces. In other words, remove a small 3–ball centered on Σ and Σ' from each of M and M', respectively, and form the Heegaard splitting $\mathcal{H}\#\mathcal{H}' = (\Sigma\#\Sigma'; H_1\#H_1', H_2\#H_2')$.

One might ask whether every Heegaard decomposition of $M \# M'$ decomposes in this way. Remarkably, by the following fundamental result (known as Haken's Lemma) this is true.

Haken's Lemma ([29], e.g. see [37, Chapter II])**.** Let M be a (possibly non-orientable) 3–manifold containing an essential 2–sphere. Let Σ be a Heegaard surface for M. Then there exists an essential 2–sphere S in M that intersects Σ in a simple closed curve.

1.3 Heegaard diagrams of 3–manifolds

One of the most useful properties of Heegaard splittings is that they can be represented by diagrams. If $\mathcal{H} = (\Sigma; H_1, H_2)$ is a Heegaard splitting of M, then we can record which curves on Σ bound disks in H_i. By drawing these curves on a model surface (an abstract copy of Σ), we will be able to reconstruct M.

Definition 1.3.1. Let Σ be a (possibly non-orientable) closed surface of genus g. A *cut system of curves* for Σ is a collection C of g disjointly embedded closed curves such that $\Sigma \setminus C$ is a connected planar surface. Equivalently, performing surgery on all curves in C (i.e. attaching 2–handles along each curve in C) gives S^2.

Definition 1.3.2. A Heegaard diagram is a tuple $(\Sigma; \alpha, \beta)$ where Σ is a closed surface of genus g, and α and β are cut systems of curves for Σ.

To distinguish the curves in a Heegaard diagram, the α curves will always be red, and the β curves will always be blue.

Remark 1.3.3. A Heegaard diagram $(\Sigma; \alpha, \beta)$ determines a closed 3–manifold M in the following way. Beginning with $\Sigma \times I$, attach 3–dimensional 2–handles corresponding to the α curves to $\Sigma \times \{0\}$, and 3–dimensional 2–handles corresponding to the β curves to $\Sigma \times \{1\}$. By hypothesis, the resulting 3-manifold has two 2–sphere boundary components, which can uniquely be filled in with 3–balls. We say that $(\Sigma; \alpha, \beta)$ is a *Heegaard diagram for* M.

Note. Since a Heegaard diagram depends on a choice of identification of the splitting surface with a model surface, it can only record information up to diffeomorphism. In particular, Heegaard diagrams do not generally distinguish Heegaard splittings up to isotopy.

If two Heegaard diagrams for M describe the same Heegaard splitting up to diffeomorphism, then there is a complete set of moves relating these diagrams. For example, if we modify either the α or β curves by an isotopy or a *handle slide* (illustrated below; compare with §1.1), then this corresponds to isotopy or a handle slide of the 2–handles in the above construction, and so does not affect the Heegaard splitting up to diffeomorphism. In fact, these are essentially the only required moves.

Definition 1.3.4. Suppose that Σ is a closed surface and C is a cut system of curves for Σ. If $c_1, c_2 \in C$, then we say that a curve c_3 is the result of a handle slide of c_1 over c_2 (or vice versa) if $c_1 \cup c_2 \cup c_3$ bounds an embedded pair of pants $P \subset \Sigma$.

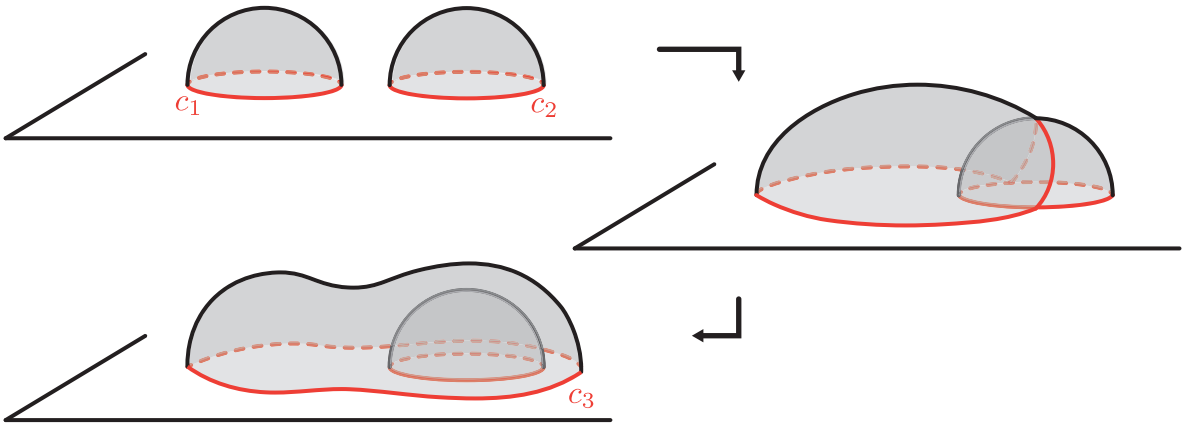

Figure 1.4: The effect on the attaching curves (technically, spheres) when sliding a 3–dimensional 2–handles. For clarity, only the attaching curves and the disks they bound are pictured. The key observation is that the curves c_1, c_2, c_3 bound a pair of pants embedded in Σ.

Proposition 1.3.5 (e.g. see [50]). *Suppose that $\mathfrak{D} = (\Sigma; \alpha, \beta)$ and $\mathfrak{D}' = (\Sigma; \alpha', \beta')$ describe diffeomorphic Heegaard diagrams for a 3–manifold M. Then $\mathfrak{D}$ and $\mathfrak{D}$ describe diffeomorphic Heegaard splittings if and only if they are related by a sequence of isotopies of curves, handle slides (among curves of each type) and surface automorphisms. In other words, there is a natural bijection*

$$\frac{\{\textit{Heegaard diagrams}\}}{\textit{slides, surface automorphism}} \leftrightarrow \frac{\{\textit{Heegaard splittings of 3–manifolds}\}}{\textit{diffeomorphism}}$$

If two diagrams are related by a sequence of handle slides and surface automorphisms, we will call them *slide-diffeomorphic*. We will now give several examples of Heegaard splittings of some familiar closed 3-manifolds.

Example 1.3.6. The simplest Heegaard splitting is the genus zero splitting of the 3–sphere. Viewing S^3 as

$$S^3 = B^3 \cup_{S^2} B^3,$$

i.e. as two 3–balls glued along their boundary by the identity map, we obtain a genus zero Heegaard splitting. Equivalently, viewing S^3 as $\mathbb{R}^3 \cup \{\infty\}$, the unit 2–sphere $S \subset \mathbb{R}^3$ bounds a 3–ball to each side, and so is a genus 0 Heegaard surface. A Heegaard diagram for this splitting is given by S^2 with *no* curves.

A more interesting Heegaard splitting of the 3–sphere has genus one. Again, view S^3 as $\mathbb{R}^3 \cup \{\infty\}$ and define a splitting by:

$$H_1 = \nu(U)$$

where U is the unknotted circle $U = \{(x, y, z) \in \mathbb{R}^3 : x^2 + y^2 = 1 \text{ and } z = 0\}$ and

$$H_2 = S^3 \setminus H_1.$$

It is easy to see that both H_1 and H_2 are solid tori, and so we have exhibited a genus one Heegaard splitting of S^3. A diagram $\mathfrak{T}$ for this splitting is given below[1]; this splitting is a stabilization of the genus zero splitting given above.

It is easy to check that stabilization (Definition 1.2.4) is equivalent to taking the connected sum with the above genus one Heegaard splitting of S^3. Diagrammatically, this corresponds to taking the connected sum with $\mathfrak{T}$ (up to equivalence, the connected sum of diagrams is well defined).

[1]This image is original but inspired by the excellent illustration in [8]

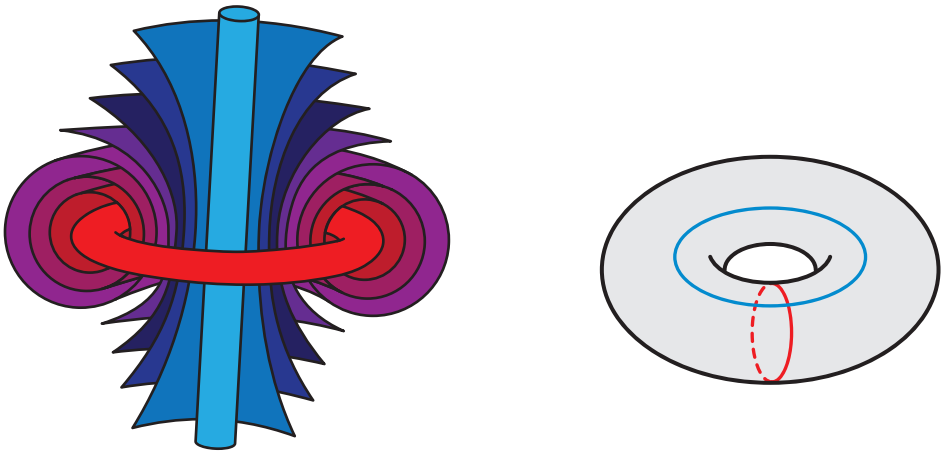

(a) (b)

Figure 1.5: In (a), an illustration of S^3 as the union of concentric tori. The Heegaard diagram $\mathfrak{T}$ in (b) describes the corresponding Heegaard splitting. The curves on the torus bound disks in the corresponding colored handlebodies in S^3.

Definition 1.3.7. Let $\mathfrak{D}$ be a Heegaard diagram. A *stabilization* of $\mathfrak{D}$ is a diagram of the form $\mathfrak{D}\#\mathfrak{T}$. We say that $\mathfrak{D}'$ is a stabilization of $\mathfrak{D}$, or that $\mathfrak{D}$ is a *destabilization* of $\mathfrak{D}'$.

It is generally difficult to check whether a Heegaard diagram $\mathfrak{D}$ is stabilized, since one has to perform handle slides to express $\mathfrak{D}$ as a connected sum of the above form. The Reidemeister-Singer Theorem (Theorem 1.2.5) can also be restated in terms of diagrams.

Theorem 1.3.8. *Any closed and connected 3–manifold M admits a Heegaard diagram. If $\mathfrak{D}$ and $\mathfrak{D}'$ are Heegaard diagrams for M, then for some k and l, $\mathfrak{D}\#(\#^k\mathfrak{T})$ and $\mathfrak{D}'\#(\#^l\mathfrak{T})$ are slide-diffeomorphic.*

Example 1.3.9. The 3–torus $T^3 = S^1 \times S^1 \times S^1$ admits an interesting genus three Heegaard splitting. We will view T^3 as the quotient of $[0,1]^3$ obtained by identifying opposite faces.

There is an obvious handlebody $H_1 \subset T^3$ depicted in Figure 1.6. In fact, $H_2 = T^3 \setminus H_1$ is also a handlebody, since we can find three compressing disks. Thus, H_2 is a handlebody, and we have exhibited a genus three Heegaard splitting of T^3.[2]

[2]The author would like to thank Abigail Thompson for pointing out this highly symmetric planar diagram.

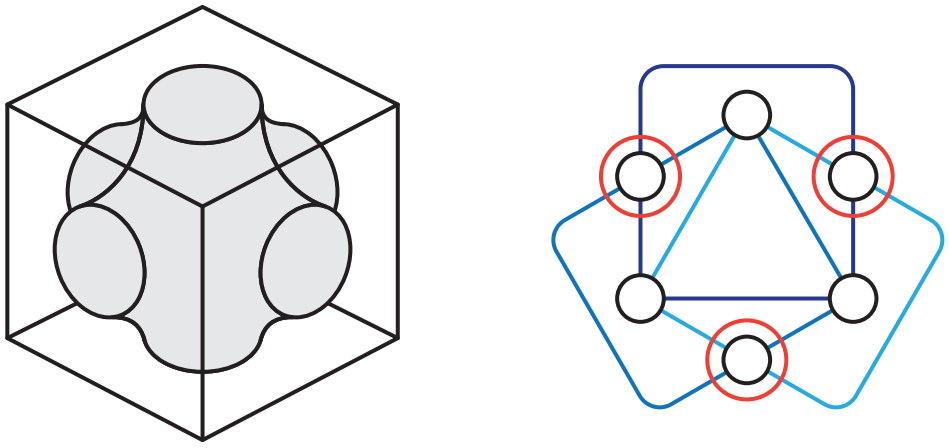

(a) (b)

Figure 1.6: In (a), an illustration of a Heegaard surface for T^3. The edges of the faces of the cubes are identified; the faces of the drawn solid are identified to form a genus 3 handlebody whose complement is also a handlebody. The planar Heegaard diagram in (b) describes this Heegaard splitting. Circles opposite one another are identified to form a genus 3 surface.

This is the lowest genus splitting possible for T^3. In general, each handlebody of a Heegaard splitting generates the fundamental group, and so the genus of any splitting of T^3 is bounded below by the rank of $\pi_1(T^3) = \mathbb{Z}^3$, which is equal to 3.

Example 1.3.10. One of the most important Heegaard splittings that will appear in this thesis is the *standard* Heegaard splitting of $S^2 \times S^1$. Since $S^2 = D^2 \cup_{S^1} D^2$, the surface $S^1 \times S^1$ defines a genus 1 Heegaard splitting of $S^2 \times S^1$. In Figure 1.7, we see that a diagram for this splitting has two parallel curves.

Similarly, there is a standard (non-orientable) Heegaard splitting of $S^2 \tilde{\times} S^1$. Recall that this 2–sphere bundle over S^1 is obtained by gluing the boundary components of $S^2 \times I$ via a reflection (which we will take to be across the equator of S^2). Figure 1.8 illustrates a "genus one" Heegaard splitting. In this case, the surface is a Klein bottle, and the handlebodies are each diffeomorphic to $B^2 \tilde{\times} S^1$. Note that unlike the case of $S^2 \times S^1$, the image of $S^1 \times I$ under the identification of the boundary components is a Klein bottle which is non-separating (and hence does not define a Heegaard splitting in our sense).

Note. In fact, there are only four isotopy classes of essential embedded closed curves

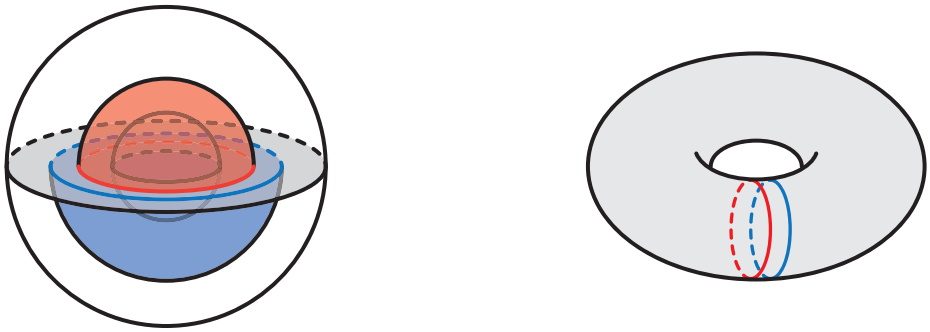

(a) (b)

Figure 1.7: In (a), a schematic of a Heegaard splitting of $S^2 \times S^1$, viewed as $S^2 \times I$ with $S^2 \times \{0\}$ and $S^2 \times \{1\}$ identified. The surface $S^1 \times S^1$ (in grey) is a Heegaard surface. In (b), a diagram for this Heegaard splitting. The schematic in (a) shows that the same curve bounds a disk in both handlebodies.

on the Klein bottle [34]. Only one of these is both non-separating and has an annular neighbourhood, and so Figure 1.8 is the *only* genus one non-orientable Heegaard diagram.

By taking connected sums of these standard Heegaard splittings, we obtain genus k Heegaard splittings of $\#^k S^2 \times S^1$ and $\#^k S^2 \tilde{\times} S^1$, which we will call *standard*. Note that these splittings have minimal genus, but we can also stabilize them to obtain higher genus splittings.

In fact, a theorem of Waldhausen guarantees that these are the *only* Heegaard splittings of $\#^k S^2 \times S^1$. Waldhausen showed that Heegaard splittings of S^3 are unique up to isotopy; combining this with an easy application of Haken's lemma shows that genus g Heegaard splittings of $\#^k S^2 \times S^1$ are unique up to diffeomorphism. Carvalho and Oertel (and more recently Hensel and Schultens) have shown that this is actually true up to isotopy.

Theorem 1.3.11 ([71], see e.g. [10] and [32])**.** *Let $g \geq k \geq 0$. Any genus g Heegaard splitting of $\#^k S^2 \times S^1$ is isotopic to the result of stabilizing the standard Heegaard surface $g - k$ times.*

In particular, any genus g Heegaard diagram for $\#^k S^2 \times S^1$ is slide-diffeomorphic to the diagram in Figure 2.3.

A version of Theorem 1.3.11 for $\#^k S^2 \tilde{\times} S^1$ may be known to some experts, but does not seem to appear in the literature. We include a proof up to diffeomorphism here. Using

(a) (b)

Figure 1.8: In (a), a schematic of a genus 1 Heegaard splitting of $S^2 \tilde{\times} S^1$, viewed as $S^2 \times I$ with $S^2 \times \{0\}$ and $S^2 \times \{1\}$ identified by a reflection through the equator. The purple curve traces out a separating Klein bottle. In (b), a diagram (on a Klein bottle) for this Heegaard splitting.

the methods of Carvalho and Oertel, we will show that like the orientable case, this result holds up to isotopy (Theorem 3.2.8).

Proposition 1.3.12. *Let $g \geq k \geq 0$. Any genus g Heegaard splitting of $\#^k S^2 \tilde{\times} S^1$ is equivalent to the result of stabilizing the standard Heegaard surface $g-k$ times.*

Proof. The proof will proceed by induction. If $k = 0$, then the claim holds by Waldhausen's theorem on Heegaard splittings of S^3. Write $\Sigma_{g,k}$ to indicate the result of stabilizing the standard genus k surface in $\#^k S^2 \tilde{\times} S^1$ $g-k$ times.

Now fix some $n \geq 1$ and suppose the claim holds whenever $k < n$. Let Σ be some genus g Heegaard surface in $M := \#^n S^2 \tilde{\times} S^1$. By Haken's lemma, there is an essential 2–sphere S in M that intersects Σ in a simple closed curve. Let (M', Σ') be the 3–manifold and Heegaard surface obtained by compressing (M, Σ) along S. There are two cases to consider.

Case 1: S is separating.

If S is separating, then M' is a disjoint union $M' = M_1 \sqcup M_2$ with $M_i \cong \#^{k_i} S^2 \times S^1$ or $M_i \cong \#^{k_i} S^2 \tilde{\times} S^1$, and $k_1 + k_2 = n$. Since S is essential, $k_1, k_2 \neq 0$ and so $k_1, k_2 < n$. By Theorem 1.3.11 or the inductive hypothesis, the corresponding components of Σ' are equivalent to Σ_{g_1,k_1} and Σ_{g_2,k_2} for some g_1, g_2 with $g_1 + g_2 = g$. Thus in this case, $(M, \Sigma) \cong (\#^n S^2 \tilde{\times} S^1, \Sigma_{g,n})$.

Case 2: S is non-separating.

If S is non-separating, then either $M' \cong \#^{n-1} S^2 \times S^2$ or $M' \cong \#^{n-1} S^2 \tilde{\times} S^1$. By Theorem 1.3.11 or the inductive hypothesis, Σ' is equivalent to $\Sigma_{g-1,n-1}$. Thus, in this case we also have $(M, \Sigma) \cong (\#^n S^2 \tilde{\times} S^1, \Sigma_{g,n})$.

We conclude the claim holds for $k = n$, so Proposition 1.3.12 holds by induction. □

1.4 Open book decompositions

We will need one more useful decomposition of a 3–manifold in this thesis, called an *open book decomposition*. The reader may wish to skip this very short section; they will only be used in passing for descriptions of trisections, and as a structure on the boundary of a relative trisection in §4.3. For more details, we recommend the extensive treatment by Etnyre in [19].

Definition 1.4.1. Let Y be a closed, connected 3–manifold. An *open book decomposition* of Y is a pair (B, π), where

- $B \subset Y$ is a link called the *binding*;
- $\pi : Y \setminus B \to S^1$ is a fibration. For each $\theta \in S^1$, $\pi^{-1}(\theta)$ is the interior of a compact surface $\Sigma_\theta \subset Y$, and $\partial \Sigma_\theta = B$. The surface Σ_θ is called the *page*.

Abstractly, one can also start with a surface Σ with boundary, together with an automorphism $\phi : \Sigma \to \Sigma$ which is the identity on $\partial\Sigma$. By filling in the resulting boundary components of the mapping torus $\Sigma \times_\phi S^1$ with solid tori, we obtain a closed 3–manifold M_ϕ equipped with a natural open book decomposition.

Like Heegaard splittings, every 3–manifold admits such a decomposition.

Theorem 1.4.2. *Let Y be a closed, connected 3–manifold. Then Y admits an open book decomposition.*

Originally due to Alexander, the proof of this theorem proceeds by showing that every closed 3–manifold arises as the branched cover of link $L \subset S^3$. By braiding L around the unknot in S^3, one obtains a fibration of the desired kind.

Chapter 2

Trisections of 4–manifolds

This thesis deals with extending the theory of *trisections* to non-orientable 4–manifolds. In this chapter we review the orientable theory, and so the experienced reader may wish to skip to later chapters and refer back as necessary.

This chapter is not intended as a complete guide. Rather, it is a brief introduction containing all the fundamental results that will be used in this thesis, along with many examples. For a more complete picture, the reader is encouraged to consult the following excellent references. We will refer to them throughout this chapter, but also present them here as a collection for the interested reader.

- For the original treatment of trisections by Gay and Kirby see [24]. For extensions to 4–manifolds with boundary, see [13], [14]; for extensions to non-orientable 4–manifolds see [59], [69] (as well as Chapter 3 and Chapter 4 of this thesis); for decompositions involving more than three pieces see [36], [47], [67], and [66]. For computations of the homology or intersection form of a closed 4–manifold from a trisection, see [20] and [21]
- For the development of Weinstein trisections and other applications of trisections to symplectic 4–manifolds see [46]; for a trisection-based proof of the Thom conjecture and a proof of the adjunction inequality, see [43] and [44]. For invariants of 4–manifolds that can be defined using trisections, see [15], [41], and [62].
- For the original treatment of bridge trisections see [56] and [58]; for applications to embedded surfaces in 4–manifolds, see [25] [45], and [55].
- For more results on trisection diagrams and their applications to 4–manifolds, see [16], [57], and [65].

For a very first motivating example, we will consider the following decomposition of the 2–sphere. While S^2 is not a 4–manifold, it will be useful to illustrate the basic idea of a trisection. We will identify $S^2 \subset \mathbb{R}^3 = \mathbb{C} \times \mathbb{R}$ as

$$S^2 = \{(re^{i\theta}, z) \in \mathbb{R}^3 : |(re^{i\theta}, z)| = 1\},$$

and imagine cutting S^2 into three wedges (like an orange). Formally, one might define:

$$X_i = \{(re^{i\theta}, z) \in S^2 : 2\pi(i-1)/3 \leq \theta \leq 2\pi i/3\}.$$

Each "sector" X_i is diffeomorphic to a 2–dimensional disk. The triple intersection is $X_1 \cap X_2 \cap X_3 = \{(0,1), (0,-1)\}$, and so is diffeomorphic to S^0. Similarly, $X_i \cap X_j \subset S^2$ is an embedded arc connecting $(0,1)$ and $(0,-1)$, and so is diffeomorphic to B^1. While this example may seem trivial, it will be a useful schematic to keep in mind. In short, we have decomposed S^2 into three 2–dimensional pieces, so that the pairwise and triple intersections are as simple as possible.

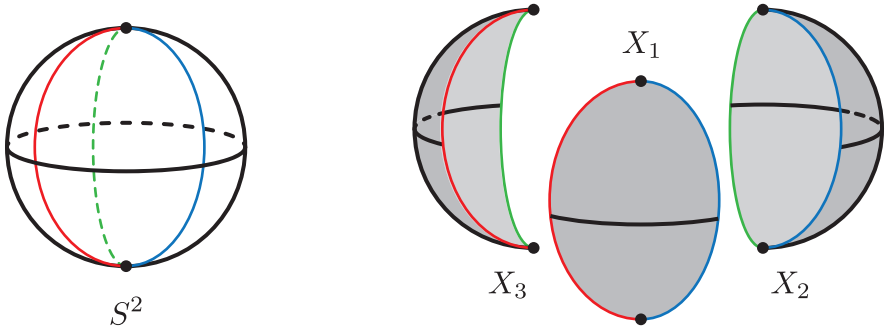

Figure 2.1: A "trisection" of the 2–sphere into three pieces. Each piece is a 2–dimensional disk, each pairwise intersection is a 1–dimensional arc, and the triple intersection is a 0–dimensional.

The 4–dimensional sphere admits a similar decomposition. View $S^4 \subset \mathbb{R}^5 = \mathbb{C} \times \mathbb{R}^3$ as

$$S^4 = \{(re^{i\theta}, x, y, z) \in \mathbb{R}^5 : |(re^{i\theta}, x, y, z)| = 1\}$$

and set

$$X_i = \{(re^{i\theta}, x, y, z) \in S^4 : 2\pi(i-1)/3 \leq \theta \leq 2\pi i/3\}.$$

In this case, each X_i is diffeomorphic to a 4–dimensional ball. As before, the triple intersection is

$$X_1 \cap X_2 \cap X_3 = \{(re^{i\theta}, x, y, z) \in S^4 : r = 0\},$$

and so is diffeomorphic to a 2–dimensional sphere. Similarly, the pairwise intersections are diffeomorphic to 3–dimensional balls. As in the first example, we have decomposed S^4 into three 4–dimensional pieces, so that the pairwise and triple intersections are as simple as possible.

As a slightly more interesting 4–dimensional example, we will describe a trisection of $\mathbb{CP}^2$. Recall that $\mathbb{CP}^2$ is the quotient of $\mathbb{C}^3 \setminus \{0\}$ obtained by identifying lines through the origin, i.e.

$$\mathbb{CP}^2 = \frac{\mathbb{C}^3 \setminus \{0\}}{z \sim \lambda z \text{ for } 0 \neq \lambda \in \mathbb{C}}.$$

Points in $\mathbb{CP}^2$ are described using homogeneous coordinates, i.e. as elements $[z_0 : z_1 : z_2]$, where z_i are not all zero and points can be rescaled. The *moment map* $\mu : \mathbb{CP}^2 \to \mathbb{R}^2$ is defined by:

$$\mu([z_1 : z_2 : z_3]) = \left(\frac{|z_2|}{|z_1| + |z_2| + |z_3|}, \frac{|z_3|}{|z_1| + |z_2| + |z_3|} \right).$$

Note that μ is well defined, and that the image of μ is the polytope

$$\Delta = \{(x, y) \in \mathbb{R}^2 : 0 \leq x, 0 \leq y, x + y \leq 1\}.$$

Consider the three "sectors" of $\mathbb{CP}^2$ (indices taken modulo 3) given by

$$X_i = \{[z_0 : z_1 : z_2] \in \mathbb{CP}^2 : |z_i|, |z_{i+1}| \leq |z_{i+2}|\}.$$

Equivalently, X_i is the preimage under μ of Δ_i in Figure 2.2. By rescaling, it is clear that each X_i is diffeomorphic to a 4–ball. Although the intersections among the X_i are not disks, they are fairly well behaved. For instance, we have:

$$X_1 \cap X_2 \cap X_3 = \{[z_1 : z_2 : z_3] \in \mathbb{CP}^2 : |z_1| = |z_2| = |z_3|\}.$$

By rescaling (e.g. so that $z_1 = 1$), it is easy to see that $X_1 \cap X_2 \cap X_3$ is an embedded torus in $\mathbb{CP}^2$. Similarly, $X_i \cap X_j$ is a 3-dimensional handlebody, i.e. diffeomorphic to $S^1 \times B^2$. Each pairwise intersection $X_i \cap X_j$ has $X_1 \cap X_2 \cap X_3$ as its boundary, but in different ways. If we draw a schematic of $X_1 \cap X_2 \cap X_3$ as a torus Σ, we can record its interaction with $X_i \cap X_j$ by drawing the curve on Σ which bounds a disk in $X_i \cap X_j$ (i.e., a compressing disk). Keeping track of these curves carefully (for details see Example 2.2.10), we might draw the schematic in Figure 2.2.

As in the case of S^4, we have exhibited a decomposition of $\mathbb{CP}^2$ into three simple pieces (4–balls), whose pairwise intersections are 3–dimensional handlebodies, and whose triple intersection is a surface. This is the foundation of the idea of a trisection. Just like a

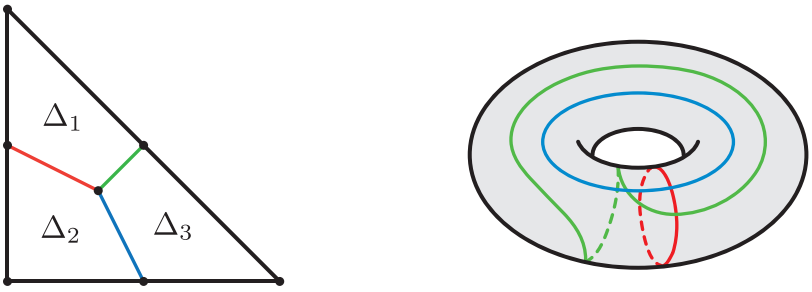

$\Delta = \mu(\mathbb{CP}^2) \subset \mathbb{R}^2$ $\quad$ $\Sigma \cong X_1 \cap X_2 \cap X_3$

Figure 2.2: A schematic of a trisection of $\mathbb{CP}^2$. Each sector $X_i = \mu^{-1}(\Delta_i)$ is a 4–ball. Each of the three coloured curves on Σ bounds a disk in the handlebody $X_i \cap X_j = \mu^{-1}(\Delta_i \cap \Delta_j)$ of the same color.

Heegaard splitting, much of the data of a trisection is carried by how the sectors intersect along the surface, and so schematics like the one in Figure 2.2 will be very useful.

The outline of this chapter will be as follows. In §2.1, we will define a trisection of a closed 4–manifold rigorously. In §2.2 we will introduce *trisection diagrams*, a way of describing 4–manifolds via diagrams on surfaces (like Figure 2.2). Lastly, in §2.3 we will briefly review some special kinds of trisections: *relative trisections*, an extension of trisections to 4–manifolds with boundary, and *bridge trisections*, a tool for studying embedded surfaces in trisected 4–manifolds

2.1 Trisections of 4–manifolds

In this section, we rigorously introduce the definition of a trisection of a closed 4–manifold. Later, we will also describe trisections of 4–manifolds with boundary, which are more technical but useful for standard cut-and-paste operations.

In this chapter all manifolds are taken to be orientable, but in Chapter 4 we will relax this assumption. Recall that an orientable handlebody of genus g is a compact manifold which can be built with a single 0–handle and g orientable 1–handles.

Definition 2.1.1 ([24])**.** Suppose that X is a smooth, oriented, closed, and connected 4–manifold. A *trisection* $\mathcal{T}$ of X is a decomposition $X = X_1 \cup X_2 \cup X_3$ such that

- X_i is diffeomorphic to a 4–dimensional handlebody of genus k_i;

- $X_i \cap X_j$ is diffeomorphic to a 3–dimensional handlebody of genus g;
- $\Sigma = X_1 \cap X_2 \cap X_3$ is diffeomorphic to a closed surface of genus g.

We will refer to $\mathcal{T}$ as a $(g; k_1, k_2, k_3)$–trisection of X. When $k_1 = k_2 = k_3 = k$, the trisection is called *balanced*, and we will refer to $\mathcal{T}$ as a $(g; k)$–trisection. Each X_i is called a *sector*, and the triple intersection Σ is called the *central surface* of $\mathcal{T}$.

Note that by definition, for each i the central surface Σ induces a genus g Heegaard splitting of ∂X_i. Since $X_i \cong \natural^{k_i} B^3 \times S^1$, we have $\partial X_i \cong \#^{k_i} S^2 \times S^1$, and so we necessarily have $g \geq k_i$. By the strong version of Waldhausen's theorem on Heegaard splittings of $\#^{k_i} S^2 \times S^1$ (Theorem 1.3.11), every such Heegaard splitting is standard, i.e. isotopic to a stabilization of the standard genus k_i splitting.

Remark 2.1.2. An Euler characteristic calculation shows that if X admits a $(g; k_1, k_2, k_3)$–trisection, then $\chi(X) = g + 2 - k_1 - k_2 - k_3$.

If $\mathcal{T}$ and $\mathcal{T}'$ are (g, k_1, k_2, k_3)– and $(g'; k_1', k_2', k_3')$– trisections of X and X', then there is a natural trisection of $X \# X'$ obtained by performing the connected sum at points on the central surfaces. In other words, remove a trisected 4–ball from each of X and X' and identify the resulting boundary components by a diffeomorphism which respects this trisection structure. The result is a $(g + g'; k_1 + k_1', k_2 + k_2', k_3 + k_3')$–trisection of $X \# X'$.

Like Heegaard splittings, there is a natural stabilization operations for trisections.

Definition 2.1.3. Suppose that $\mathcal{T}$ is a $(g; k_1, k_2, k_3)$–trisection of a 4–manifold X, with sectors X_1, X_2, X_3. Let $\alpha \subset X_1 \cap X_2$ be a properly embedded and boundary parallel arc, and define a new trisection $\mathcal{T}'$ of X by:

- $X_1' = X_1 \setminus \nu(\alpha)$;
- $X_2' = X_2 \setminus \nu(\alpha)$;
- $X_3' = X_3 \cup \overline{\nu(\alpha)}$.

One can check that this defines a $(g{+}1; k_1, k_2, k_3{+}1)$–trisection of X, and that this operation is well defined up to isotopy of trisections. The trisection $\mathcal{T}'$ is called a 3–*stabilization* (or simply *stabilization*) of $\mathcal{T}$; 1– and 2– stabilizations are defined analogously. Conversely, $\mathcal{T}$ is called a *destabilization* of $\mathcal{T}'$.

Note that (e.g. in the case of 3–stabilization) this procedure stabilizes the Heegaard splittings of ∂X_1 and ∂X_2, while adding an $S^1 \times S^2$ summand to ∂X_3.

The reader may wish to compare this definition to the stabilization operation for Heegaard splittings in §1.2. Unlike the 3–dimensional case, each kind of stabilization produces a *distinct* kind of trisection. However, i– and j– stabilization commute up to isotopy.

As in the 3–dimensional case, one may also define stabilization as the connected sum (respecting the trisection structure) of $\mathcal{T}$ with one of the three genus one trisections that arise by 1–, 2– or 3–stabilizing the unique genus 0 trisection of S^4. For more details, see Definition 2.2.4.

The following fundamental theorem of Gay and Kirby allows us to study closed 4–manifolds via trisections:

Theorem 2.1.4 ([24])**.** *Every smooth, oriented, closed, and connected 4–manifold X admits a $(g;k)$–trisection for some $0 \leq k \leq g$. Any two trisections of X become isotopic after sufficiently many stabilizations.*

For convenience, we give a short handle-theoretic proof of the existence of trisections. This proof is well known, and various versions appear in [24] and [58]. One can also give a proof via Morse 2–functions (i.e. generic maps to $\mathbb{R}^2$), but we will not discuss this point of view.

Proof sketch of Theorem 2.1.4 (Existence). Begin with a self-indexing Morse function $f : X \to [0,4]$, inducing a handle decomposition for X with a single 0– and 4– handle, h_1 1–handles, h_2 2–handles, and h_3 3–handles, and fix a gradient-like vector field ∇ for f. From this handle decomposition, we will build a trisection of X. For convenience, we will write $X_{[a,b]}$ for the cobordism $f^{-1}([a,b])$, and simply write $X_{[c]} = f^{-1}(c)$. If $Y \subset X_{[a]}$, we will write $Y_{[a,b]}$ for the trace of flowing $Y \subset X_{[a]}$ along gradient flow lines to $X_{[b]}$.

Note that $X_{[0,3/2]} \cong \natural^{h_1} B^3 \times S^1$ since it contains only critical points of index 0 or 1, and so in particular $X_{[3/2]} \cong \#^{h_1} S^2 \times S^1$. The descending manifolds of the index 2 critical points intersect $X_{[3/2]}$ in h_2 closed curves; this is the attaching link L for the 2–handles of X, viewed in $X_{[3/2]}$. Choose a genus g Heegaard splitting $X_{[3/2]} = H \cup_\Sigma H'$ so that each component of L is a core of H, i.e. is dual to a properly embedded disk in H that does not intersect any other component of L. We claim that the following decomposition is now a $(g; h_1, g-h_2, h_3)$–trisection of X.

- $X_1 = X_{[0,3/2]} \cup H'_{[3/2,2]}$;

- $X_2 = H_{[3/2,5/2]} = X \setminus (X_1 \cup X_3)$;
- $X_3 = H'_{[2,5/2]} \cup X_{[5/2,4]}$.

Since $H'_{[3/2,2]}$ and $H'_{[2,5/2]}$ deformation retract onto $H'_{[3/2]}$ and $H'_{[5/2]}$, respectively, we have $X_1 \cong \natural^{h_1} B^3 \times S^1$ and $X_3 \cong \natural^{h_3} B^3 \times S^1$. Lastly, we may view X_2 as built from $\nu(H_{[3/2]}) \cong (\natural^g B^2 \times S^1) \times I$ by the addition of h_2 2–handles. This is a genus g handlebody; by construction these 2–handles geometrically cancel h_2 of the 1–handles and so $X_2 \cong \natural^{g-h_2} B^3 \times S^1$. Thus the advertised decomposition is a trisection of X. □

Note. A quick sanity check of this proof using Remark 2.1.2 shows that

$$\chi(X) = g + 2 - h_1 - (g - h_2) - h_3 = 1 - h_1 + h_2 - h_3 + 1$$

as expected.

The above proof shows that a handle decomposition induces a trisection. Conversely, we can also extract a handle decomposition from a trisection.

Proposition 2.1.5 ([24, Lemma 13])**.** *Suppose that $\mathcal{T}$ is a $(g; k_1, k_2, k_3)$–trisection of X. Then X admits a handle decomposition with a single 0– and 4– handle, k_1 1–handles, $g-k_2$ 2–handles, and k_3 3–handles.*

Proof. Let the sectors of $\mathcal{T}$ be X_1, X_2, and X_3, and let $X_1 \cap X_2 \cap X_3 = \Sigma$. Since $X_1 \cong \natural^{k_1} B^3 \times S^1$, it is a handlebody, which we will take this to be the 0– and 1–handles of a handle decomposition for X.

The sector X_2 may now be viewed as a cobordism (of manifolds with boundary) of $X_1 \cap X_2$ to $X_2 \cap X_3$. Note that the surface Σ is a genus g Heegaard splitting for $\partial X_2 \cong \#^{k_2} S^2 \times S^1$. By Waldhausen's theorem, this Heegaard splitting is standard, and so we can find a collection L of $g - k_2$ curves on Σ which bound disks in $X_2 \cap X_3$ and are dual to curves that bound disks in $X_1 \cap X_2$. We are now in a position to appeal to the following well known lemma.

Lemma 2.1.6. *Let H be a handlebody, and suppose that $\gamma \subset \partial H$ is a curve so that $|\gamma \cap \partial D| = 1$ for some properly embedded disk $D \subset H$. Then, the result of pushing γ into H and doing surgery is still a handlebody. If we surger γ with the surface framing, then γ bounds a disk in the new surgered handlebody.*

Thus, attaching 2–handles to $\nu(X_1 \cap X_2) \cong (X_1 \cap X_2) \times I \cong \natural^g B^3 \times S^1$ along L is a cobordism from $X_1 \cap X_2$ to $X_2 \cap X_3$. In fact, since the 2–handles are geometrically dual to $g - k_2$ of the 1–handles of $\nu(X_1 \cap X_3)$, this cobordism is diffeomorphic to $\natural^{k_2} B^3 \times S^1$. By Theorem 3.0.1, any two ways of attaching $\natural^{k_2} B^3 \times S^1$ are equivalent, and so we may take X_2 to be this specific cobordism. In other words, $X_1 \cup X_2$ consists of k_1 1–handles together with $g - k_2$ 2–handles attached along a link $L \subset X_1 \cap X_2$ with surface framing.

All that remains is the sector $X_3 \cong \natural^{k_3} B^3 \times S^1$, which we will take to be the 3– and 4–handles of a handle decomposition for X. □

The above arguments essentially give a correspondence between handle decompositions and trisections. Via Cerf theory, any two handle decompositions of a fixed 4–manifold X are related via handle slides and handle creation/cancellation, i.e. births and deaths of pairs of handles. Like the 3–dimensional case, the stable equivalence statement in Theorem 2.1.4 can be proved by realizing changes in handle decompositions by stabilizations of the corresponding trisections. The reader is referred to [24, Theorem 11] for more details; in Chapter 4 we will give a version of their proof that also works in the non-orientable setting.

Remark 2.1.7. The above construction is highly symmetric in the sectors X_1, X_2, and X_3. We can take any X_i to be the 1–handles of a handle decomposition, and any other X_j to be the 2–handles. This is one of the most interesting features of trisections: a trisection induces up to six different handle decompositions. By comparison, one can only turn a Kirby diagram "upside down" to get a new handle decomposition. This gives potentially new ways to show that various 4–manifolds (i.e. homotopy spheres) are standard.

In particular, if a 4–manifold X admits a $(g; k_1, k_2, k_3)$–trisection with some $k_i = 0$, then X admits a handle decomposition without 1–handles and is therefore simply connected.

2.2 Trisection diagrams and examples

A main feature of trisections is that, like Heegaard splittings, they can be described diagrammatically. In this section, we review the definition of a trisection diagram. We also give many examples of trisected 4–manifolds and their associated diagrams.

Definition 2.2.1. A $(g; k_1, k_2, k_3)$–*trisection diagram* is a tuple $\mathfrak{D} = (\Sigma; \alpha, \beta, \gamma)$, where Σ is a closed orientable surface of genus g, and α, β, and γ are collections of g embedded closed curves such that:

- Each of α, β, and γ is a cut system of curves for Σ;

- Each pair of curves is standard, i.e. each of $(\Sigma;\alpha,\beta)$, $(\Sigma;\beta,\gamma)$, and $(\Sigma;\gamma,\alpha)$ is a genus g Heegaard diagram for $\#^{k_i} S^1\times S^2$. Equivalently, each pair of curves is *standardizable*, i.e. can be made to look like the curves in Figure 2.3 after handle slides and possibly a diffeomorphism of Σ.

To distinguish each set of curves in a diagram, we will always draw the α, β, and γ curves in red, blue, and green, respectively.

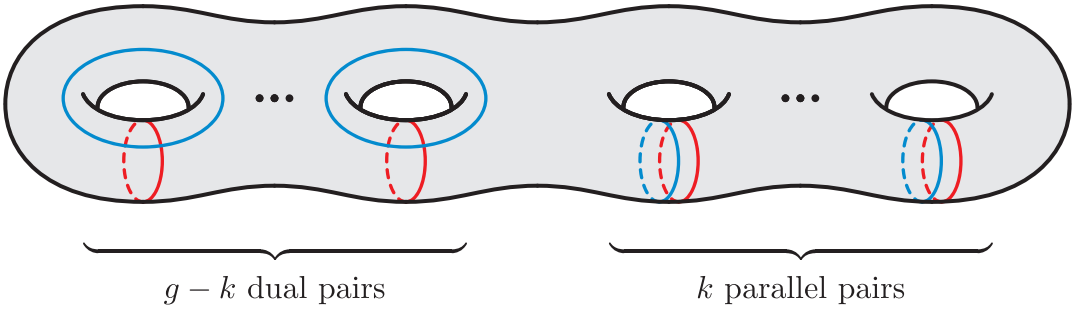

Figure 2.3: A standard diagram for a genus g Heegaard splitting of $\#^k S^2\times S^1$. In a trisection diagram, every pair of curves $(\Sigma;\star,\star)$ is slide-diffeomorphic to this one.

A trisected 4–manifold determines a trisection diagram in the following way. If $\mathcal{T}$ is a trisection of X with sectors X_1, X_2, X_3, then we may choose an identification of $X_1\cap X_2\cap X_3$ with a model surface Σ. Since $X_1\cap X_2\cap X_3$ induces a Heegaard splitting of each ∂X_i, there are cut systems of curves α,β,γ on Σ recording curves that bound disks in each of $X_i\cap X_j$ (which are well defined up to handle slides). Since $\partial X_i\cong \#^{k_i} S^2\times S^1$, these collections of curves pairwise define Heegaard splittings for $\#^{k_i} S^2\times S^1$.

By Theorem 1.3.11, every Heegaard splitting for $\#^{k_i} S^2\times S^1$ is standard, and so after handles slides and possibly a diffeomorphism of Σ, each pair of curves can be *standardized*, i.e. made to look like the curves in Figure 2.3. In general, the three collections of curves cannot be *simultaneously* standardized.

In fact, we can recover a trisected 4–manifold from a trisection diagram. The key ingredient needed to show that a diagram determines a 4–manifold is a theorem of Laudenbach-Poénaru. We will state it here for completeness, but postpone discussing it until Chapter 3. Note that an immediate corollary of Theorem 3.0.1 is that 4–dimensional handlebodies may be attached uniquely, i.e. if a component of ∂X is diffeomorphic to $\#^k S^2\times S^1$, then up to diffeomorphism there is a unique 4–manifold that can be obtained by gluing $\natural^k B^3\times S^1$ to this component. This is strikingly different from the 3–dimensional case, since a solid torus in a 3–manifold may be cut out and re-glued in many in inequivalent ways.

Theorem 3.0.1. Let $p \geq 0$, and suppose that $h : \#^p S^2 \times S^1 \to \#^p S^2 \times S^1$ is a diffeomorphism. Then there is a diffeomorphism $H : \natural^p B^3 \times S^1 \to \natural^p B^3 \times S^1$ such that $H|_\partial = h$.

Proposition 2.2.2 ([24]). *A $(g; k_1, k_2, k_3)$–trisection diagram $\mathfrak{D}$ uniquely determines a trisected 4–manifold $X(\mathfrak{D})$ up to diffeomorphism. Moreover, this trisection of $X(\mathfrak{D})$ induces the trisection diagram $\mathfrak{D}$.*

Proof. Given a trisection diagram $\mathfrak{D}$, we will construct a closed 4–manifold equipped with a natural trisection. Beginning with $\Sigma \times D^2$, attach $H_\alpha \times I$, $H_\beta \times I$, and $H_\gamma \times I$ along $\Sigma \times \{1\}$, $\Sigma \times \{e^{2\pi i/3}\}$, and $\Sigma \times \{e^{4\pi i/3}\}$ respectively, where H_α, H_β, and H_γ are the handlebodies determined by the α, β, and γ curves and we have identified $D \subset \mathbb{C}$. The resulting 4–manifold has three boundary components, each diffeomorphic to $\#^{k_i} S^2 \times S^1$ by construction. By Theorem 3.0.1, we may uniquely fill in these boundary components with $\natural^{k_i} B^3 \times S^1$ to obtain a closed 4–manifold $X(\mathfrak{D})$ up to diffeomorphism. By construction, $X(\mathfrak{D})$ admits a trisection which determines the trisection diagram $\mathfrak{D}$. □

Remark 2.2.3. Note that Proposition 2.2.2 shows that trisection diagrams only describe a trisected 4–manifold up to *diffeomorphism*, and vice versa. While there are interesting questions about the isotopy classes of trisections of a fixed 4–manifold, facts about isotopy are not generally recorded by a trisection diagram.

A connected sum of trisections corresponds directly to taking the connected sum of trisection diagrams. In particular, we can define stabilization of diagrams in the following way.

Definition 2.2.4. Let $\mathfrak{D} = (\Sigma; \alpha, \beta, \gamma)$ be a trisection diagram. A 1–, 2–, or 3–stabilization of $\mathfrak{D}$ is the diagram $\mathfrak{D}'$ obtained by taking the connected sum of $\mathfrak{D}$ with the appropriate trisection diagram of S^4 in Figure 2.4. We say that $\mathfrak{D}'$ is a stabilization of $\mathfrak{D}$, or that $\mathfrak{D}$ is a destabilization of $\mathfrak{D}'$.

Note that the trisection determined by $\mathfrak{D}'$ is precisely a stabilization of the trisection determined by $\mathfrak{D}$ in the sense of Definition 2.1.3. Combining Theorem 2.1.4 and the above discussion about trisection diagrams, we obtain the following fundamental diagrammatic statement about 4–manifolds.

Theorem 2.2.5 ([24]). *Suppose that X is a smooth, oriented, connected and closed 4–manifold. Then X admits a $(g; k)$–trisection diagram for some $g \geq k$. Any two trisection diagrams for X become equivalent after some number of stabilizations.*

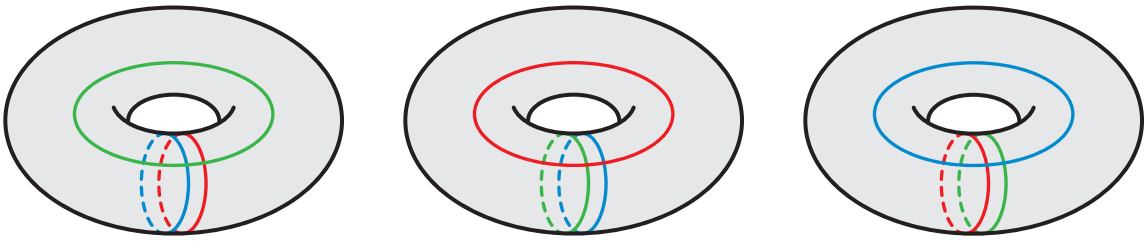

(a) (b) (c)

Figure 2.4: The three (unbalanced) trisection diagrams for S^4, which correspond to the three different kinds of stabilization. Taking the connected sum with (a), (b), or (c) is a 1–, 2–, or 3–stabilization, respectively.

In general, it may not be obvious whether two trisection diagrams describe diffeomorphic 4–manifolds; if they do, arbitrarily many stabilizations might be required to relate them by handle slides. It is also usually difficult to decide if a given trisection diagram can be destabilized. To do so, one must rearrange the curves to realize the diagram as a connected sum with one of the stabilizations in Figure 2.4 above.

We now give several examples of trisections and trisection diagrams.

Example 2.2.6. The simplest trisection is the genus zero trisection of S^4. As described in the introduction to this chapter, we view $S^4 \subset \mathbb{R}^5 = \mathbb{C} \times \mathbb{R}^3$ as

$$S^4 = \{re^{i\theta}, x_3, x_4, x_5) \in \mathbb{R}^5 : |(re^{i\theta}, x_3, x_4, x_5)| = 1\}$$

and define three sectors by

$$X_k = \{(re^{i\theta}, x_3, x_4, x_5) \in S^4 : 2\pi k/3 \leq \theta \leq 2\pi(k+1)/3\}.$$

Equivalently, this trisection may be obtained by projecting S^4 to the unit disk in $\mathbb{C}$, and lifting the pieces of the obvious trisection of D^2. It is easy to check that each X_k is a 4–ball, and that the triple intersection $X_1 \cap X_2 \cap X_3$ is the unknotted 2–sphere in S^4 (it is the the subset of points where $r = 0$). Thus, this is a $(0;0)$–trisection of S^4. A diagram for this trisection is given by a 2–sphere with *no* curves, as in Figure 2.5. In fact, this trisection is unique. Any 4–manifold with a such a trisection is diffeomorphic to S^4, since the result of constructing a 4–manifold from a $(0;0)$–trisection diagram is diffeomorphic to S^4 by Theorem 3.0.1.

One can easily verify that the result of stabilizing the $(0;0)$–trisection of S^4 produces one of the diagrams in Figure 2.4. Up to diffeomorphism these are the *only* possible genus one trisections for S^4.

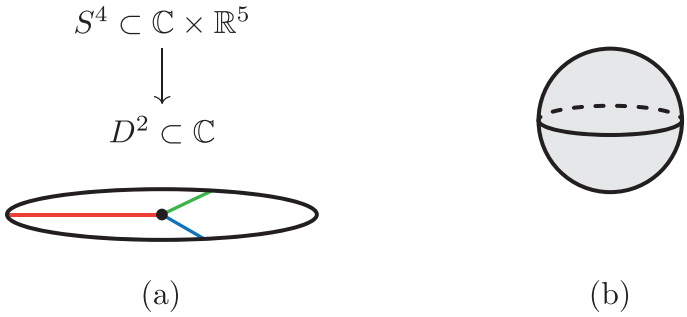

Figure 2.5: In (a), a schematic of projecting S^4 to a 2–dimensional disk. The sectors of the $(0;0)$–trisection of S^4 are obtained by taking preimages of each sector of D^2. In (b), the $(0;0)$–trisection diagram for S^4.

Remark 2.2.7. The equivalence classes of trisections of S^4 are not presently well understood. Like Heegaard splittings of S^3, one might hope that an analogue of Waldhausen's theorem (Theorem 1.3.11) holds for trisections, i.e. that every trisection of S^4 is isotopic (or diffeomorphic) to a stabilization of the $(0;0)$–trisection. To answer this question, one would have to understand the intricate combinatorics of trisections diagrams of S^4. This question is also related to understanding $\pi_0(\mathrm{Diff}^+(S^4))$.

Gay has recently proved the following result[1]: two trisections of S^4 are isotopic if and only if they are diffeomorphic, i.e. their diagrams are slide diffeomorphic. Remarkably, the proof does not give any insight into the structure of $\pi_0(\mathrm{Diff}^+(S^4))$. Instead, one proceeds by showing that if $f : (S^4, \mathcal{T}_1) \to (S^4, \mathcal{T}_2)$ is a diffeomorphism of trisections, then the spines of $\mathcal{T}_1$ and $\mathcal{T}_2$ are isotopic. This isotopy extends to an ambient isotopy of of S^4, and so one concludes that $\mathcal{T}_1$ and $\mathcal{T}_2$ are isotopic. However, the proof does *not* give any indication whether f is isotopic to the identity map. The proof relies heavily on the fact that the ambient manifold is S^4, but one might ask whether the same result is true for any simply connected 4-manifold. There are known to be non-diffeomorphic trisections of some 4–manifolds, but all techniques presently used to distinguish them seem to require a non-trivial fundamental group (e.g. see [35]).

We record these questions below. In Chapter 4, we will make some progress towards an answer to Question 2.2.8.

Question 2.2.8 (Waldhausen's Theorem for trisections of S^4)**.** Are all trisections of S^4 standard? That is, is every trisection of S^4 isotopic to a stabilization of the $(0;0)$–trisection?

[1]Currently unpublished.

Question 2.2.9 (Diffeomorphism vs. isotopy for trisections)**.** Suppose that X is a simply connected 4–manifold. If two trisections of X are diffeomorphic, are they isotopic?

Example 2.2.10. Another simple trisection is of $\mathbb{CP}^2$. As in the introduction to this chapter, we can define three sectors X_1, X_2, and X_3 of $\mathbb{CP}^2$ (in homogeneous coordinates, with indices taken modulo 3) by:

$$X_k = \{[z_1 : z_2 : z_3] \in \mathbb{CP}^2 : |z_k|, |z_{k+1}| \leq |z_{k+2}|\}.$$

By scaling coordinates so that $z_{k+2} = 1$, we see that:

$$X_k = \{[z_1 : z_2 : z_3] \in \mathbb{CP}^2 : |z_k|, |z_{k+1}| \leq 1\}$$

and so X_k is diffeomorphic to a 4-ball. The triple intersection is

$$\Sigma = X_1 \cap X_2 \cap X_3 = \{[z_1 : z_2 : z_3] \in \mathbb{CP}^2 : |z_1| = |z_2| = |z_3|\}.$$

Again, by scaling some coordinate, it is clear that Σ is an embedded torus. Similarly, one can also show that $X_i \cap X_j$ is a genus one handlebody, i.e. $X_i \cap X_j \cong B^2 \times S^1$. Thus, this decomposition defines a $(1; 0)$–trisection of $\mathbb{CP}^2$.

To obtain a diagram for this trisection, we need to identify which curve on Σ bounds a disk in $X_i \cap X_j$. By scaling so that $z_1 = 1$, we can identify Σ with

$$\Sigma \cong \{[1 : z_2 : z_3] \in \mathbb{CP}^2 : |z_2| = |z_3| = 1\}.$$

Then, we see that

$$X_1 \cap X_2 = \{[z_1 : z_2 : z_3] \in \mathbb{CP}^2 : |z_2| \leq |z_3| = |z_1|\}$$

and so the curve $|z_2| = 1$ (i.e. the $(1, 0)$ curve on Σ) bounds a disk in $X_1 \cap X_2$. Similarly, the curve $|z_3| = 1$ (i.e. the $(0, 1)$ curve on Σ) bounds a disk in $X_2 \cap X_3$. In $X_3 \cap X_1$, the curve $|z_2| = |z_3|$ bounds a disk, which is the $(1, 1)$ curve on Σ. Thus, a trisection diagram for $\mathbb{CP}^2$ is given in Figure 2.6 below.

To obtain a diagram for $\overline{\mathbb{CP}}^2$, we can simply take the mirror of the diagram for $\mathbb{CP}^2$, i.e. the image of this diagram under an orientation *reversing* diffeomorphism. This follows from Remark 2.2.11 below.

As in the introduction, we could also have built this trisection of $\mathbb{CP}^2$ by pulling back a trisection of a specific map to D^2. This is not an accident; trisections may be defined via Morse 2-functions (as in [24]), but we will not focus on this aspect of the theory in this thesis.

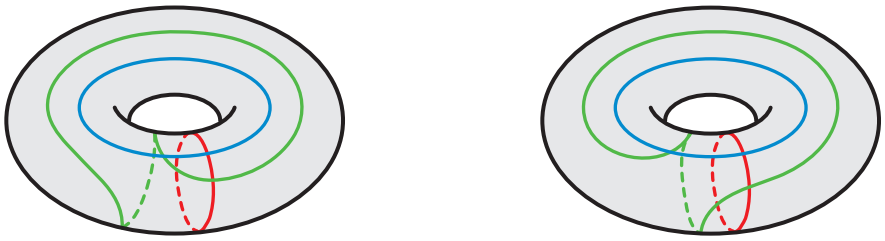

(a) (b)

Figure 2.6: In (a), a $(1;0)$–trisection diagram for $\mathbb{CP}^2$. In (b), a $(1;0)$–trisection diagram for $\overline{\mathbb{CP}}^2$; obtained by reflecting Σ by an orientation reversing diffeomorphism. The γ curve is now the $(1,-1)$ curve.

Remark 2.2.11. The careful reader will note that a trisection is a decomposition of an *oriented* 4-manifold. In general, if $\mathfrak{D} = (\Sigma;\alpha,\beta,\gamma)$ is a $(g;k_1,k_2,k_3)$–trisection diagram for a 4-manifold X, then $\overline{(\Sigma;\alpha,\beta,\gamma)}$ is a $(g;k_1,k_2,k_3)$–trisection diagram for $\overline{X}$. Here, $\overline{X}$ denotes the mirror of X, i.e. X with the opposite orientation. Indeed, an orientation of Σ (implicit when we draw a diagram in $\mathbb{R}^3$) determines an orientation of $X(\mathfrak{D})$ by construction.

Example 2.2.12. As our first example of a trisection of a 4–manifold with a non-trivial fundamental group, we will consider $S^3 \times S^1$. There is a natural trisection arising from the trivial open book decomposition of S^3. Indeed, start with the open book on S^3 with disk pages and binding given by the unknot U. Take three disjoint pages of this open book; these pairwise cobound three 3–balls B_1, B_2, and B_3.

Define $X_i = B_i \times S^1 \subset S^3 \times S^1$. Then $X_i \cong B^3 \times S^1$, and $X_i \cap X_j \cong S^1 \times B^2$. The triple intersection is $X_1 \cap X_2 \cap X_3 = U \times S^1$, which is an embedded torus. Thus, this decomposition defines a $(1;1)$–trisection of $S^3 \times S^1$. Since the curve $U \times \{\star\}$ bounds a disk in each $X_i \cap X_j$, a diagram for this trisection is given in Figure 2.7 below. In fact, this is the only possible $(1;1)$–diagram.

Koenig has shown how to trisect the mapping torus $M \times_\phi S^1$, where $\phi : M \to M$ is an automorphism fixing (or flipping) a Heegaard surface for M [42].

Remark 2.2.13. Given a trisection $\mathcal{T}$ of a 4–manifold X, Proposition 2.1.5 produces a handle decomposition of X. Given a trisection diagram $\mathfrak{D}$ for $\mathcal{T}$, the proof can be refined to produce a Kirby diagram of the corresponding handle decomposition. We remind the reader that a Kirby diagram is simply a drawing of framed 2–handles in $\#S^2 \times S^1$, such

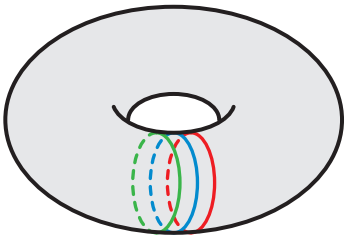

Figure 2.7: A $(1;1)$–trisection diagram for $S^3 \times S^1$.

that their surgery is again $\#S^2 \times S^1$. Thus, our task is to concretely draw the attaching curves for each 2–handle.

By standardizing the α and β curves, we can visualize a concrete copy of $\#S^2 \times S^1$, where the handlebody determined by the α curves is the one "inside" the surface as drawn. The proof of 2.1.5 shows that we can take the 1–handles to be the sector bounded by the α and β curves. The 2–handles are attached along those γ curves which are dual (i.e. not parallel) to the α curves, pushed into the α handle with surface framing.

Diagrammatically, this requires that we know *which* γ curves are dual to α curves, which we might have to check by handle slides. If desired, we can also simply use *all* γ curves as 2–handles as in [24]. Up to slides some will be parallel to the α curves and so will be cancelled by additional 3–handles in the induced handle decomposition (which we do not draw). There are several similar methods in the literature (see e.g. [24], [36],[54] [59]) for extracting a handle decomposition from a trisection, but all are essentially equivalent. One such algorithm is outlined precisely below.

Algorithm 2.2.14 (Converting a trisection diagram to a Kirby diagram)**.** Let $(\Sigma; \alpha, \beta, \gamma)$ be a $(g; k_1, k_2, k_3)$ trisection diagram describing a 4–manifold X. The following procedure produces a Kirby diagram for X.

- **Step 1.** Standardize the α and β curves. In other words, do handle slides among the α and β curves, and apply a diffeomorphism of $(\Sigma; \alpha, \beta, \gamma)$ to arrange that $(\Sigma; \alpha, \beta)$ looks like the curves in Figure 2.3.
- **Step 2.** Slide the γ curves so that $(\Sigma; \gamma, \alpha)$ has a standard intersection pattern, i.e. any γ curve intersects exactly zero or one α curves. Equivalently, $(\Sigma; \gamma, \alpha)$ is diffeomorphic to the curves in Figure 2.3.
- **Step 3.** Draw dotted 1–handles for each α curve that is parallel to a β curve, by pushing the α curve slightly "out" of the surface. Equivalently, draw a 1–handle by placing two 3–balls on either side of disk bounded by the α curve.

- **Step 4.** For each γ curve that is dual to an α curve, draw a 2–handle curve.
- **Step 5.** Give each 2–handle curve its surface framing, i.e. the self linking number of the curve as viewed in $\mathbb{R}^3$.

In many cases, Steps 1 and 2 have already been arranged. In most examples we will consider, all α and β curves will be dual, and so no 1–handles are added. The reader may wish to convert the trisection diagrams obtained thus far into familiar Kirby diagrams.

Example 2.2.15. We could define a trisection as a careful decomposition of $S^2 \times S^2$ as we did for $\mathbb{CP}^2$. Instead, we will reverse engineer a trisection using Algorithm 2.2.14. Applying the algorithm to each of the trisection diagrams in Figure 2.8 and Figure 2.9, we obtain the usual Kirby diagrams for $S^2 \times S^2$ or $S^2 \tilde{\times} S^2$. Thus, $S^2 \times S^2$ and $S^2 \tilde{\times} S^2$ both admit $(2;0)$–trisections.

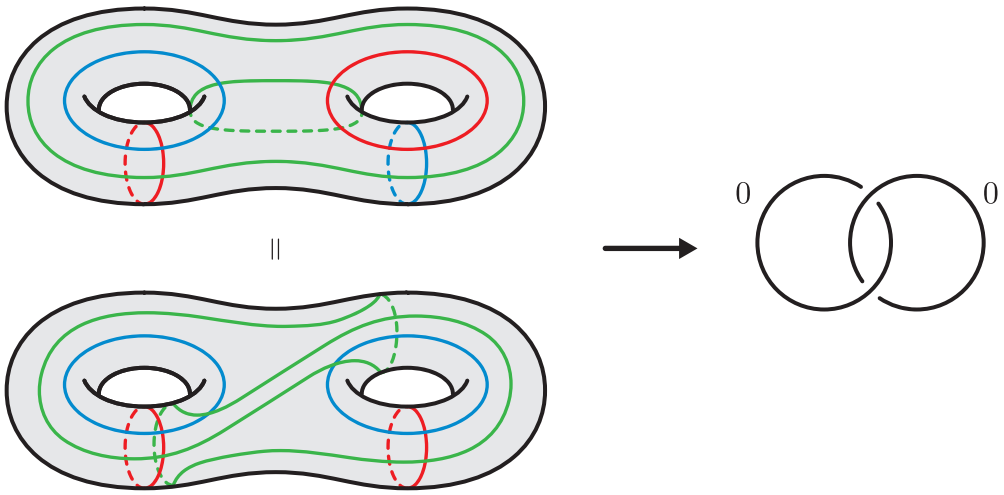

Figure 2.8: On the left, two equivalent trisection diagrams of $S^2 \times S^2$ (related by handle slides and diffeomorphism). By applying Algorithm 2.2.14 to the diagram on the bottom, we obtain the familiar Kirby diagram for $S^2 \times S^2$ on the right.

In fact, the trisection of $S^2 \tilde{\times} S^2$ in Figure 2.9 splits as a connected sum of $(1;0)$–trisections of $\mathbb{CP}^2$ and $\overline{\mathbb{CP}}^2$, giving another proof that $S^2 \tilde{\times} S^2 \cong \mathbb{CP}^2 \# \overline{\mathbb{CP}}^2$.

Remark 2.2.16. So far, we have described the following (balanced) irreducible trisection diagrams: the $(0;0)$–trisection of S^4; the $(1;0)$– trisections of $\mathbb{CP}^2$ and $\overline{\mathbb{CP}}^2$, the $(1;1)$–trisection of $S^3 \times S^1$, and a $(2;0)$–trisection of $S^2 \times S^2$. By a theorem of Meier-Zupan [57], these are all such trisection diagrams. In other words, all trisections of genus less than or

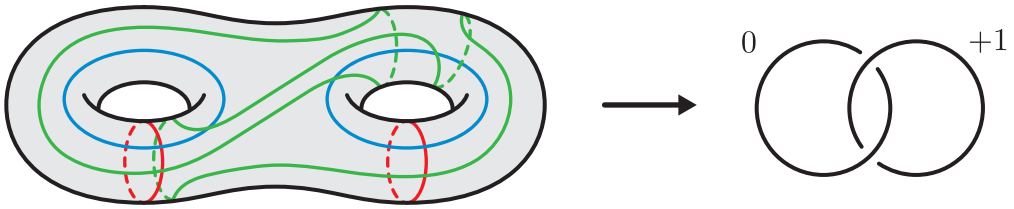

Figure 2.9: Applying Algorithm 2.2.14 to this trisection diagram, we obtain a Kirby diagram for $S^2 \tilde{\times} S^2$.

equal to two are *standard*. While this is easy to see for $g = 1$, their proof in the case that $g = 2$ relies on deep results about genus two Heegaard splittings. This standardness result has important consequences for trisections and exotic 4–manifolds.

Remark 2.2.17. One particularly motivating reason to study trisections might be the following observation from Meier and Lambert-Cole [45]. If Y is a closed 3–manifold, then we can define the Heegaard genus of Y by

$$g(Y) = \min\{g : Y \text{ admits a genus } g \text{ Heegaard splitting}\}.$$

A remarkable property is that this invariant is additive for connected sums, i.e. $g(Y\#Y') = g(Y) + g(Y')$. Indeed, this follows from Haken's lemma: any Heegaard splitting $(Y\#Y', \Sigma)$ for a non-trivial sum $Y\#Y'$ contains an essential 2–sphere which meets Σ in a single curve, and so $(Y\#Y', \Sigma) = (Y, \Sigma_Y)\#(Y', \Sigma_{Y'})$ for some Heegaard splittings of Y and Y'. In particular, $g(Y\#Y') \geq g(Y) + g(Y')$. Since the other inequality holds trivially, we obtain the desired equality.

We can define a similar invariant for trisections. If X is a smooth, oriented, closed, and connected 4–manifold, then we can define the *trisection genus* of X to be

$$g(X) = \min\{g : X \text{ admits a } (g; k)\text{–trisection}\}.$$

One might ask the seemingly innocuous question: is trisection genus additive under connected sum? In fact, this would have remarkably strong consequences. If X and X' are an exotic pair of 4–manifolds (i.e. homeomorphic but not diffeomorphic), then a theorem of Gompf [27] or Wall [72] (in the simply connected case) shows that for some $m \geq 0$,

$$X\#(\#^m S^2 \times S^2) \cong X'\#(\#^m (S^2 \times S^2).$$

That is, X and X' are stably diffeomorphic. If the trisection genus invariant were additive under connected sum, we would have:

$$g(X) + m \cdot g(S^2 \times S^2) = g(X') + m \cdot g(S^2 \times S^2)$$

and so $g(X) = g(X')$. However, since trisections of genus at most two are known to be standard, this would imply that there does not exist an exotic $S^2 \times S^2$, $\mathbb{CP}^2$, $\overline{\mathbb{CP}}^2$, $\mathbb{CP}^2 \# \overline{\mathbb{CP}}^2$, nor most notably an exotic S^4. Interestingly, this lies on the edge of current technology, since there *is* an exotic manifold homeomorphic to $\mathbb{CP}^2 \# 2\overline{\mathbb{CP}}^2$ [4].

The trisection genus invariant is not expected to be additive in general, but this discussion shows that these decompositions have deep connections to exotic 4–manifolds.

2.3 Special kinds of trisections

Trisections can be adapted to more specialized settings. In this section, we briefly outline some extensions. In §2.3.1, we describe the structure of a *relative trisection* of a 4–manifold with boundary. These structures connect trisections with open book decompositions of 3–manifolds, and can be used to understand surgery along embedded submanifolds. In §2.3.2, we discuss *bridge trisections* of embedded surfaces, introduced by Meier and Zupan in [56]. Both of these topics are treated in detail in Chapter 4.

2.3.1 Relative trisections

If X is a smooth, oriented, connected 4–manifold with non-empty boundary, there is a notion of a *relative trisection* of X. These were introduced by Gay and Kirby in [24], and subsequently studied in detail by Castro [12]. We will define these decompositions more carefully in Chapter 4, and also extend them to the case when X is non-orientable.

As in the closed case, a relative trisection is a decomposition of a 4–manifold X into three 4–dimensional handlebodies that meet in a prescribed way. However, the boundary of each handlebody X_i now intersects ∂X as well as the other handlebodies.

If Z is a 4–dimensional handlebody, then one can define a decomposition of ∂Z into two parts: $\partial Z = \partial_{\text{in}} Z \cup \partial_{\text{out}} Z$, where $\partial_{\text{in}} Z$ admits a natural (generalized) Heegaard splitting into two compression bodies (see §4.3 for the definition of a compression body), i.e. $\partial_{\text{in}} Z = Y_- \cup Y_+$. With such a decomposition in mind, one defines a relative trisection in the following way.

Definition 4.3.3. Let X be a smooth, connected, oriented 4–manifold with connected non-empty boundary. A relative trisection $\mathcal{T}$ of X is a a decomposition $X = X_1 \cup X_2 \cup X_3$ such that:

- There are diffeomorphisms $\phi_i : X_i \to Z$ such that $\phi_i(X_i \cap \partial X) = \partial_{\text{out}} Z$,
- For each i, $\phi_i(X_i \cap X_{i-1}) = Y^-$ and $\phi_i(X_i \cap X_{i+1}) = Y^+$.

A very rough schematic of this decomposition is illustrated in Figure 2.10 below.

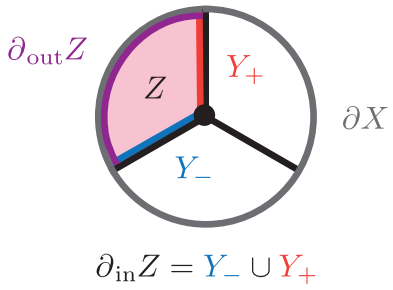

Figure 2.10: A schematic of a relative trisection. Each sector is a 4–dimensional handlebody which meets both the boundary and the other handlebodies.

One advantage of this structure is that it naturally induces an open book on ∂X with binding $L = \partial(X_1 \cap X_2 \cap X_3)$, for which the surfaces $X_i \cap X_j \cap \partial X$ are pages. If X and Y are relatively trisected 4–manifolds with boundary, and $f : \partial X \to \partial Y$ is a diffeomorphism respecting the open book decompositions, then the following theorem of Castro [12] guarantees that there is a natural trisection of $X \cup_f Y$.

Definition 4.3.8 ([12])**.** Let $\mathcal{T}$ and $\mathcal{T}'$ be relative trisections of 4–manifolds X and X', respectively. Denote the open book decompositions induced on ∂X and $\partial X'$ by $\mathcal{O}$ and $\mathcal{O}'$, respectively. Suppose that there is a diffeomorphism $f : \partial X \to \partial X'$, and that $f(\mathcal{O})$ is isotopic to $\mathcal{O}'$. Then there is a naturally induced trisection $\mathcal{T} \cup \mathcal{T}'$ of $X \cup_f X'$.

There is also a notion of a *relative trisection diagram*. A relative trisection can be described by a surface with non-empty boundary, together with three cut systems of curves. An example is given in Figure 2.11 below. The monodromy of the induced open book decomposition can be computed diagrammatically, and there is an analogue of the gluing theorem for diagrams. A complete discussion of relative trisection diagrams, their uses, and many examples are given in Chapter 4.

One reason that the definition of a relative trisection is noticeably more technical is the absence of a "Waldhausen's theorem" for compression bodies. Consequently, one must take care to define the decompositions so that they are determined up to diffeomorphism by a diagram, and vice versa.

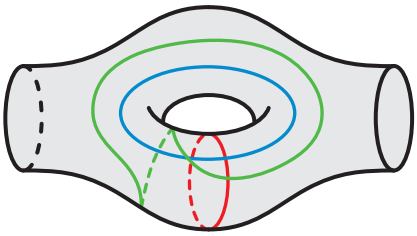

Figure 2.11: A relative trisection diagram of B^4 inducing the Hopf open book on S^3.

2.3.2 Bridge trisections

In [56] and [58], Meier and Zupan generalized bridge splittings of knots in S^3 to knotted surfaces in 4–manifolds. Recall that a knot $K \subset S^3$ is in *b–bridge position* if it intersects the equatorial 2–sphere in $2b$ points, and each 3–ball in boundary parallel arcs. Equivalently, all local minima appear before maxima (with respect to the radial height function on S^3). An example is given in Figure 2.12 below.

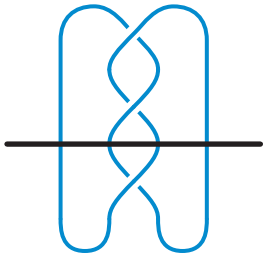

Figure 2.12: A 2–dimensional schematic of a bridge splitting of the trefoil knot in S^3.

We will denote the three sectors of the $(0;0)$–trisection of S^4 by X_1, X_2, and X_3, the pairwise intersections by X_{12}, X_{23}, and X_{31}, and the central surface by Σ.

Definition 4.4.5 ([56])**.** A smoothly embedded surface $S \subset S^4$ is in *bridge position* in S^4 if:

- $S \cap X_i = \mathcal{D}_i$ is a trivial c_i–disk system,
- $S \cap X_{ij} = \tau_{ij}$ is a trivial b–tangle,
- $S \cap \Sigma$ is a collection of $2b$ points.

Here, a trivial c_i–disk system is a collection of c_i properly embedded and boundary parallel disks in X_i, and a trivial b–tangle is a collection of b properly embedded and boundary parallel arcs in X_{ij}. The surface S is said to be in $(b; c_1, c_2, c_3)$–*bridge trisected position*.

Note that since each $\mathcal{D}_i$ is boundary parallel, the union of any pair of tangles in $X_{ij} \cong S^3$ is necessarily an unlink. In fact, the unlink bounds a unique collection of boundary parallel disks in B^4 up to isotopy (rel the unlink), and so a bridge trisection is completely determined by the union $\tau_{12} \cup \tau_{23} \cup \tau_{31}$. A schematic of this kind of decomposition is given in Figure 2.13.

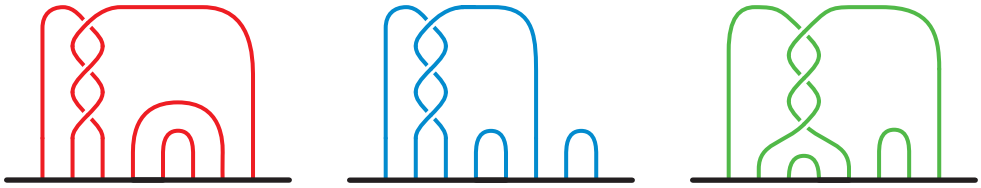

Figure 2.13: A "triplane" diagram for the spun trefoil $S \subset S^4$ from [56]. This schematic describes this embedded surface by recording the intersection of S with each X_{ij}.

This decomposition can also be generalized to a smoothly embedded surface in a trisected 4–manifold. In [58], Meier and Zupan show that if X is a 4–manifold with trisection $\mathcal{T}$, and S is an embedded surface, then S can be isotoped to lie in bridge trisected position with respect to $\mathcal{T}$. Analogous to the natural stabilization operation for bridge splittings of knots in S^3, there is also a stabilization operation for bridge trisections with respect to a fixed trisection [56]. Hughes, Kim, and Miller [33] have shown that any two bridge trisections for $S \subset X$ can be made isotopic after some number of stabilizations.

In Chapter 4, we define these decompositions carefully, give several examples, and explain how the theory can be modified to extend bridge trisections to non-orientable 4–manifolds.

Chapter 3

Diffeomorphisms of 1–handlebodies

A fundamental tool for the modern-day study of 4–manifolds is the following theorem of Laudenbach-Poénaru [51].

Theorem 3.0.1. *Let $p \geq 0$, and suppose that $h : \#^p S^2 \times S^1 \to \#^p S^2 \times S^1$ is a diffeomorphism. Then there is a diffeomorphism $H : \natural^p B^3 \times S^1 \to \natural^p B^3 \times S^1$ such that $H|_\partial = h$.*

One application is the following useful re-statement. A common slogan is that "4–dimensional handlebodies can be attached uniquely."

Corollary 3.0.2 ([51])**.** *Suppose that X is a 4–manifold and that ∂X has a component diffeomorphic to $\#^p S^2 \times S^1$. Then up to diffeomorphism, there is a unique smooth 4–manifold that can be obtained by gluing an orientable 4–dimensional handlebody to this boundary component.*

In particular, this theorem is critical for the usual descriptions of 4–manifolds via Kirby diagrams.

A more complete description will be given in §3.2.2, but we remind the reader of how a Kirby diagram determines a closed 4–manifold. One begins with a Morse function $f : X \to \mathbb{R}$; the critical points of f can be re-organized to have increasing index, and we may assume that f has a single 0– and 4–handle. Passing to a handle decomposition, we see that X may be built from a single 0–handle (a 4–ball), followed by the attachment of 1– and 2–handles. The remaining 3–handles and 4–handle are a 4–dimensional handlebody, and so by Corollary 3.0.2 this portion is attached uniquely. Thus, to completely describe a closed 4–manifold, we only need to specify the attaching regions of the 1– and 2–handles.

A Kirby diagram is a framed link diagram in $\#S^2 \times S^1$ whose surgery is again $\#S^2 \times S^1$, and thus describes a closed 4–manifold.

Theorem 3.0.1 is also extremely important for the description of 4–manifolds via trisection diagrams. In a similar fashion, one needs to guarantee that certain handlebodies are attached uniquely.

In this chapter, we show that the same method may be used to study non-orientable 4-manifolds. In §3.1, we give a self contained proof of a non-orientable analogue of Theorem 3.0.1. In §3.2, we give some applications, including a non-orientable version of Waldhausen's theorem for $\#S^2 \tilde{\times} S^1$ (up to isotopy). In §3.2.2 we illustrate how to describe non-orientable 4–manifolds via Kirby diagrams with several examples.

3.1 Gluing non-orientable 1–handlebodies

In this section, we will give a self-contained proof of a non-orientable analogue of Theorem 3.0.1.

Theorem 3.1.1. *Let $p \geq 0$, and suppose that $h : \#^p S^2 \tilde{\times} S^1 \to \#^p S^2 \tilde{\times} S^1$ is a diffeomorphism. Then there is a diffeomorphism $H : \natural^p B^3 \tilde{\times} S^1 \to \natural^p B^3 \tilde{\times} S^1$ such that $H|_\partial = h$.*

While it may be known to experts, a proof of this theorem does not seem to appear in the literature and is critical for diagrammatic descriptions of closed, non-orientable 4–manifolds. In particular, Akbulut has used this result to draw difficult Kirby diagrams of exotic non-orientable 4–manifolds, see e.g. [2].

The proof will proceed similarly to the orientable case in [51], with some modifications. We begin by first reducing to the case that h acts trivially on $\pi_1(\#^p S^2 \tilde{\times} S^1)$ and $\pi_2(\#^p S^2 \tilde{\times} S^1)$. Then, we use Laudenbach's theorem on homotopy and isotopy of 2–spheres in 3–manifolds [48] together with Cerf's theorem on diffeomorphisms of the 3–sphere [17] to isotope h to a diffeomorphism which obviously extends to $\natural^p B^3 \tilde{\times} S^1$. In fact, the case when $p = 0$ follows directly from Cerf's theorem: every orientation preserving diffeomorphism of S^3 is isotopic to the identity, and so extends to a diffeomorphism of B^4.

Theorem 3.1.2 ([17])**.** *Any orientation preserving diffeomorphism of S^3 (resp. D^3, or D^3 rel S^2) is smoothly isotopic to the identity map on S^3 (resp. D^3, or D^3 rel S^2).*

Specifically, we will use the following remarkable theorem of Laudenbach.[1]

[1]The author would like to thank François Laudenbach for his correspondence regarding this theorem.

Theorem 3.1.3 ([48]). *Let S and S' be embedded 2–spheres in a 3–manifold Y (which may be non-orientable and have nonempty boundary). If S and S' are homotopic, then they are isotopic.*

The careful reader will note that the hypothesis that S and S' are 2–spheres is certainly necessary; embedded tori in the 3–sphere are rarely isotopic (consider any pair of non-isotopic knots in S^3).

Before proving Theorem 3.1.1, we will prove several lemmas. For convenience, we will denote $Y_p := \#^p S^2 \tilde{\times} S^1$, and $X_p = \natural^p B^3 \tilde{\times} S^1$. Given a map $f : X \to Y$, we will write $f_k^{\#} : \pi_k(X) \to \pi_k(Y)$ and $f_k^* : H_k(X;\mathbb{Z}) \to H_k(Y;\mathbb{Z})$ for the maps induced by f on the homotopy or homology groups of X and Y.

Observe that we have the following commutative triangle, where A and B are the maps that send a diffeomorphism of X_p to its induced map on $\pi_1(Y_p)$ or $\pi_1(X_p)$.

$$\begin{array}{ccc} & \pi_0(\mathrm{Diff}(X_p)) & \\ {\scriptstyle A}\swarrow & & \searrow{\scriptstyle B} \\ \mathrm{Aut}(\pi_1(X_p)) & \xrightarrow[\mathrm{id}]{} & \mathrm{Aut}(\pi_1(Y_p)) \end{array}$$

Lemma 3.1.4. *The maps A and B are surjective.*

Proof. It is sufficient to show that the map A is surjective. Since $\pi_1(S^2 \tilde{\times} S^1) \cong \mathbb{Z}$, it follows that $\pi_1(Y_p) = \star^p \mathbb{Z}$. That is, $\pi_1(Y_p)$ is a free group, with generators $a_1, \ldots, a_p$ corresponding to loops around the S^1 factor of each summand. These loops are also generators for $\pi_1(X_p)$, using the inclusion $Y_p \hookrightarrow \partial X_p$.

Thus, automorphisms of $\pi_1(Y_p)$ are generated by elementary automorphisms (sometimes called Nielsen transformations) of the form:

(a) $a_i \mapsto a_i^{-1}$, i.e. replacing a generator with its inverse;

(b) $a_i \mapsto a_j$, $a_j \mapsto a_i$, i.e. switching two generators;

(c) $a_i \mapsto a_i a_j$, i.e. multiplying one generator by another.

These are all realizable by elements of $\mathrm{Diff}(X_p)$. In particular, they correspond to either isotopy or handle slides of the 4–dimensional 1–handles of X_p. Moves of type (a) may be achieved by "interchanging the feet of a 1–handle," and moves of type (b) may be achieved

by interchanging two 1–handles. Moves of type (c) are slightly more difficult to visualize; these correspond to a handle slide of a 1–handle over another. Each move is illustrated in Figure 3.1 below. □

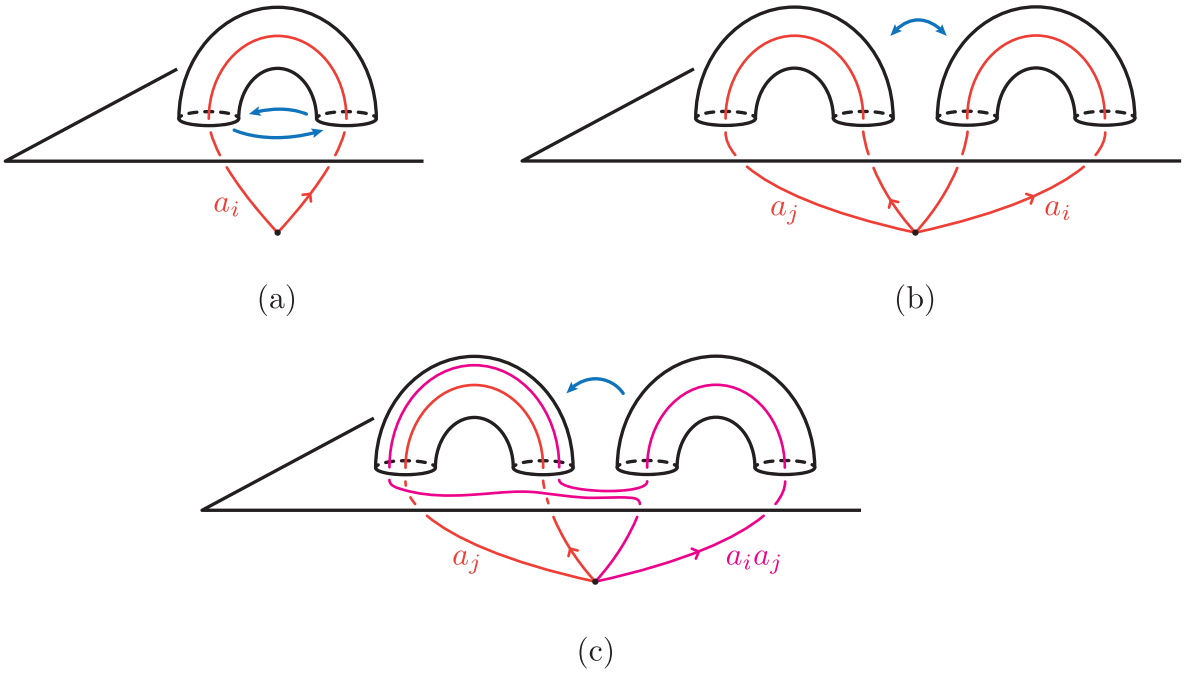

Figure 3.1: A 3–dimensional schematic (inspired by the one in [49]) illustrating each type of move. Moves (a) and (b) are realized by the isotopy indicated by the blue arrows. Move (c) is realized by a handle slide, i.e. the diffeomorphism which is the result of dragging one foot of a 1–handle over another (here, the pink 1–handle slides over the red 1–handle).

By Lemma 3.1.4, we can choose a diffeomorphism $\phi : X_p \to X_p$ so that $(\phi|_\partial \circ h)_1^\# : \pi_1(Y_p) \to \pi_1(Y_p)$ is the identity. Since $(\phi|_\partial \circ h)$ extends to a diffeomorphism of X_p if and only if h does, we may assume without loss of generality that $h_1^\# = \mathrm{id}$. In fact, the following lemma shows that this implies that $h_2^\# = \mathrm{id}$.

Lemma 3.1.5. *Suppose that a diffeomorphism $h : Y_p \to Y_p$ is such that $h_1^\# : \pi_1(Y_p) \to \pi_1(Y_p)$ is the identity map. Then $h_2^\# : \pi_2(Y_p) \to \pi_2(Y_p)$ is also the identity map.*

We will split the proof of Lemma 3.1.5 into several smaller lemmas. We will need the corresponding orientable version from [51]. For completeness, we include the proof.

Lemma 3.1.6 ([51], Lemma 3, see also [7])**.** *Suppose that Y is an orientable 3–manifold and that an orientation preserving diffeomorphism $f : Y \to Y$ is such that $f_1^{\#} : \pi_1(Y) \to \pi_1(Y)$ is the identity. Then $f_2^{\#} : \pi_2(Y) \to \pi_2(Y)$ is also the identity.*

Proof of Lemma 3.1.6. The map $f : Y \to Y$ lifts to a map $\tilde{f} : \widetilde{Y} \to \widetilde{Y}$ of the universal cover of Y, and so by the Hurewicz theorem (since $\widetilde{Y}$ is simply connected) we have the following diagram.

$$\begin{array}{ccc} H_2(\widetilde{Y};\mathbb{Z}) & \xrightarrow{\tilde{f}_2^*} & H_2(\widetilde{Y};\mathbb{Z}) \\ \cong\downarrow & & \downarrow\cong \\ \pi_2(Y) & \xrightarrow[f_2^{\#}]{} & \pi_2(Y) \end{array}$$

This lemma now follows from the more general statement in Lemma 3.1.7 below. □

Lemma 3.1.7 ([51], Lemma 4)**.** *Let X be a closed n–dimensional topological manifold. Suppose that $f : X \to X$ is an orientation preserving homeomorphism such that $f_1^{\#} : \pi_1(X) \to \pi_1(X)$ is the identity map. Then $\tilde{f}_{n-1}^* : H_{n-1}(\widetilde{X};\mathbb{Z}) \to H_{n-1}(\widetilde{X};\mathbb{Z})$ is also the identity map.*

Proof of Lemma 3.1.7. For convenience, let $G = \pi_1(X)$. By Poincaré duality, $H_{n-1}(\widetilde{X};\mathbb{Z})$ is isomorphic to $H_c^1(\widetilde{X};\mathbb{Z})$, via an isomorphism which is functorial for (orientation preserving) maps preserving the fundamental class of $\widetilde{X}$. We will also use the fact (without proof) that $H^k(X;\mathbb{Z}[G]) \cong H^k(\widetilde{X};\mathbb{Z})$.

A spectral sequences argument[2] shows that for any $\mathbb{Z}[G]$-module R we have the following short exact sequence:

$$0 \to \mathrm{Ext}_R^1(H_0(X;R),R) \to H^1(X;R) \to \mathrm{Ext}_R^0(H_1(X;R),R) \to 0.$$

We will simply apply this sequence in the case that $R = \mathbb{Z}[G]$. Since $H_0(X;\mathbb{Z}[G]) \cong H_0(\widetilde{X};\mathbb{Z}) = \mathbb{Z}$, by definition of group cohomology we have

$$\mathrm{Ext}_{\mathbb{Z}[G]}^1(H_0(X;\mathbb{Z}[G]),\mathbb{Z}[G]) \cong \mathrm{Ext}_{\mathbb{Z}[G]}^1(\mathbb{Z},\mathbb{Z}[G]) = H^1(G;\mathbb{Z}[G]).$$

[2]The author would like to thank Patrick Orson for very helpful correspondence regarding the proof of this lemma.

Moreover, $H_1(\widetilde{X};\mathbb{Z}) = 0$ since $\widetilde{X}$ is simply connected and so

$$\mathrm{Ext}^0_{\mathbb{Z}[G]}(H_1(X;\mathbb{Z}[G]),\mathbb{Z}[G]) = \mathrm{Ext}^0_{\mathbb{Z}[G]}(H_1(\widetilde{X};\mathbb{Z}),\mathbb{Z}[G]) = 0.$$

Applying these two facts to the short exact sequence above, we conclude that

$$H^1(G;\mathbb{Z}[G]) \cong H^1(X;\mathbb{Z}[G]) \cong H^1_c(\widetilde{X},\mathbb{Z}) \cong H_{n-1}(\widetilde{X};\mathbb{Z}).$$

Since $f_1^{\#} : G \to G$ is the identity, it induces the identity map on $H^1(G;\mathbb{Z}[G])$. By functoriality of the above isomorphisms, f induces the identity map on $H_{n-1}(\widetilde{X};\mathbb{Z})$. □

We can now prove Lemma 3.1.5.

Proof of Lemma 3.1.5. Since $h_1^{\#}$ is the identity map, h lifts to a diffeomorphism $\tilde{h} : \#^{2p-1}S^2 \times S^1 \to \#^{2p-1}S^2 \times S^1$ of the orientation double cover $\widetilde{Y}_p$ of Y_p. In fact, there are only two lifts: one of which is orientation preserving, and one of which is orientation reversing. We will let $\tilde{h}$ be the orientation preserving lift, and $\tilde{h} \circ \tau$ be the orientation reversing lift, where $\tau : \#^{2p-1}S^2 \times S^1 \to \#^{2p-1}S^2 \times S^1$ is the (orientation reversing) deck transformation.

In fact, we can describe this covering explicitly. Using the identification $Y_p = S^2 \tilde{\times} S^1 \#(\#^{p-1}S^2 \times S^1)$, let S be a 2–sphere of the form $S^2 \times \{\mathrm{pt}\} \subset S^2 \tilde{\times} S^1 \subset Y_p$. By cutting Y_p along S, we obtain a twice punctured copy of $\#^{p-1}S^2 \times S^1$. The orientation double cover is obtained by gluing two such copies together; the deck transformation is the map which interchanges them, and so $\#^p S^2 \tilde{\times} S^1 = (\#^{2p-1}S^2 \times S^1)/\tau$.

Since the fundamental domain (i.e. one of the two copies of a twice punctured $\#^{p-1}S^2 \times S^1$ above) only has two boundary components, it is easy to check that $\tilde{h}_1^{\#} = \mathrm{id}$. Indeed, we can choose the basepoint x for $\pi_1(Y_p)$ on S, and also assume that h preserves a small neighbourhood of this basepoint. Up to homotopy, any element of $\pi_1(\widetilde{Y}_p;\tilde{x})$ is a union of arcs starting and ending at one of x or $\tau(x)$. Since the lift of h is simply the result of applying h to each fundamental domain, we see that $\tilde{h}_1^{\#} = \mathrm{id}$ and that $\tilde{h}$ is orientation preserving.

Consequently, we have the following commutative diagram.

$$\begin{array}{ccc} \pi_2(\#^{2p-1}S^2 \times S^1) & \xrightarrow{\tilde{h}_2^{\#}} & \pi_2(\#^{2p-1}S^2 \times S^1) \\ \cong\downarrow & & \downarrow\cong \\ \pi_2(Y_p) & \xrightarrow[h_2^{\#}]{} & \pi_2(Y_p) \end{array}$$

By Lemma 3.1.6, $\tilde{h}_2^{\#}$ is the identity. Since the covering map induces an isomorphism on the second homotopy groups of Y_p and $\widetilde{Y}_p$, we conclude that $h_2^{\#}$ is also the identity map. □

Consider the p essential 2–spheres $S_1, \ldots, S_p$ of the form $S^2 \times \{\star\} \subset \#^p S^2 \tilde{\times} S^1$. By Lemma 3.1.5, we know that $h(S_i)$ is homotopic to S_i for each $1 \leq i \leq p$. By Laudenbach's theorem on 2–spheres in 3–manifolds (Theorem 3.1.3), we conclude that $h(S_i)$ is *isotopic* to S_i for each $1 \leq i \leq p$. In fact, we will show that the collections $\{h(S_1), \ldots, h(S_p)\}$ and $\{S_1, \ldots, S_p\}$ are isotopic in Y_p. To do this, we will need the following lemma.

Lemma 3.1.8. *Let Y be a (possibly non-orientable) 3–manifold whose boundary is a disjoint union of 2–spheres, and let W be a 3–manifold obtained by gluing $S^2 \times I$ to Y along two boundary components B_1, B_2 of Y. Suppose S_1 and S_2 are 2–spheres in Y that are not homotopic to each other or to B_1 or B_2. Then S_1 and S_2 are also not homotopic in W.*

Proof. Let $\widetilde{Y}$ denote the universal cover of Y, and let $\widetilde{B}_i \subset \widetilde{Y}$ be the collection of lifts of B_i. Note that the universal cover $\widetilde{W}$ of W may be constructed in the following recursive way. To begin, attach $S^2 \times I$ to any element of $\widetilde{B}_1$, along with a copy of $\widetilde{Y}$ attached to the remaining boundary component along an element of $\widetilde{B}_2$. Then, infinitely iterate this process. In particular, this process yields an inclusion of $\widetilde{Y}$ in $\widetilde{W}$.

Towards a contradiction, suppose that S_1 and S_2 are homotopic in W. In particular, some lifts L_1 and L_2 of S_1 and S_2 cobound an immersion A of $S^2 \times I$ in $\widetilde{W}$, with $\partial A = L_1 \cup L_2$. Now, let A' denote the (one or two) components of $A \setminus \widetilde{B}_1 \cup \widetilde{B}_2$ with L_i as a boundary component. Note that since S_1 and S_2 are *not* homotopic in Y, $A' \neq A$.

Now, suppose that $A \setminus A'$ intersects a copy of $\widetilde{Y}$ non-trivially. Then it follows that the boundary components B_1 and B_2 are not free generators in $\pi_2(Y)$. This implies that $Y \cong S^2 \times I$, which contradicts the assumption that S_1 and S_2 are not homotopic.

Thus, $A \setminus A' \cong S^2 \times I$, and so A' consists of an immersed copy of $S^2 \times I$ connecting L_1 to an element of $\widetilde{B}_1 \cup \widetilde{B}_2$, and a similar copy of $S^2 \times I$ connecting L_2 to a corresponding element of $\widetilde{B}_1 \cup \widetilde{B}_2$. But this implies that S_1 and S_2 are each homotopic to some B_i, a contradiction.

We conclude that S_1 and S_2 are not homotopic in W. □

Lemma 3.1.9. *Let $h : Y_p \to Y_p$ be a diffeomorphism. If $h(S_i)$ is isotopic to S_i for each $1 \leq i \leq p$, then h is isotopic to a diffeomorphism which is the identity on each S_i.*

Proof. The proof will proceed by induction. Since S_1 and $h(S_1)$ are isotopic, we can isotope h so that $h|_{S_1} = \mathrm{id}_{S_1}$. Now suppose that for some $k \geq 1$, we have $h|_{S_i} = \mathrm{id}\,|_{S_i}$ for

all $1 \leq i \leq k$. We will show that $h(S_{k+1})$ can be isotoped to S_{k+1} in the complement of $\{S_1, \ldots, S_k\}$.

Note that $[S_{k+1}] = [h(S_{k+1})]$ is not a linear combination of $\{[S_1], \ldots, [S_k]\}$ in $H_2(Y_p; \mathbb{Z})$. By Lemma 3.1.8, since S_{k+1} and $h(S_{k+1})$ are homotopic in Y_p they are also homotopic in $Y_p \setminus \{S_1 \cup \cdots \cup S_k\}$, a 3–manifold with $2k$ boundary spherical boundary components. By Laudenbach's theorem (3.1.3), S_{k+1} and $h(S_{k+1})$ are isotopic in $Y_p \setminus \{S_1 \cup \cdots \cup S_k\}$. In other words, h can be further isotoped in the complement of $\{S_1, \ldots, S_k\}$ so that $h|_{S_{k+1}} = \mathrm{id}\,|_{S_{k+1}}$. Thus, h is isotopic to a diffeomorphism such that $h|_{S_i} = \mathrm{id}\,|_{S_i}$ for all $1 \leq i \leq p$. □

For $\alpha \in \pi_1(SO(3))$, let H_α denote the diffeomorphism of $S^2 \times I$ defined by $H_\alpha(x, t) = (\alpha(t) \cdot x, t)$. Since $\pi_1(SO(3)) = \mathbb{Z}/2\mathbb{Z}$, there are only two possibilities for such a map up to isotopy rel boundary (depending on the homotopy class of α). If $S \subset Y$ is a 2–sphere embedded in a 3–manifold Y, we will use $H_\alpha(S)$ to denote H_α applied to the neighbourhood $\nu(S) \cong S^2 \times I \subset Y$, and call this a *sphere twist* of S. Note that this map has order two up to isotopy, i.e. $H_\alpha(S)^2 = \mathrm{id}$ as an element of $\mathrm{Diff}^+(Y)$.

We need one more lemma to complete the proof. Let $S(k)$ denote the 3–manifold with spherical boundary obtained by removing k open 3–balls from S^3. The following lemma asserts that the diffeotopy group of $S(k)$ is generated by sphere twists along boundary components. When $k = 0$ (or $k = 1$) this is precisely Cerf's celebrated theorem (Theorem 3.1.2, [17]) on diffeomorphisms of S^3. In fact, when $k = 1$ any such diffeomorphism is isotopic to the identity (i.e. no sphere twist is necessary).

While relatively standard, the proof has a somewhat different flavour than the arguments used thus far. Rather than proving it here, we will refer the reader to [7] for a modern proof. The idea is to use a certain fiber bundle associated to gluing a 3–ball to a puncture, and the long exact sequence in homotopy to show that $\pi_0(\mathrm{Diff}^+(S(k); \partial S(k)) \cong (\mathbb{Z}_2)^{k-1}$, generated by sphere twists along pushoffs of the boundary components. In fact, a twist about *every* components is isotopic to the identity.

Lemma 3.1.10 ([17], see e.g. [7] or [49])**.** *Any diffeomorphism of $S(k)$ which is the identity on $\partial S(k)$ is isotopic rel boundary (i.e. through diffeomorphisms which are the identity on $\partial S(k)$) to a composition of sphere twists along pushoffs of elements of $\partial S(k)$.*

We can now prove Theorem 3.1.1.

Proof of Theorem 3.1.1. Note that the result of cutting Y_p along $S_1, \ldots, S_p$ is exactly $S(2p)$. Moreover, since h is the identity on each S_i, h induces an orientation preserving diffeomorphism $f : S(2p) \to S(2p)$ which is the identity on all boundary components. By Lemma

3.1.10, f is isotopic (via an isotopy which is the identity on all boundary components) to a composition of sphere twists along pushoffs of boundary components. Thus h is isotopic to a composition of sphere twists about $S_1, \dots, S_p$, i.e. for some $\alpha_1, \dots, \alpha_p \in \pi_1(SO(3))$ we have

$$h \cong H_{\alpha_p}(S_p) \circ \cdots \circ H_{\alpha_1}(S_1).$$

Any diffeomorphism of Y_p of the form $H_\alpha(S_i)$ extends to X_p, since the rotation of S_i extends to the 3–ball that it bounds in X_p. Thus, up to isotopy h extends to a diffeomorphism H of Y_p. This completes the proof of Theorem 3.1.1. □

3.2 Applications

Theorem 3.1.1 has several applications in this thesis. The main application will be to ensure that trisection diagrams of non-orientable 4–manifolds determine a unique closed 4–manifold. However, there are other applications to non-orientable 3– and 4–manifolds. In §3.2.1, we extend Theorem 3.1.1 to a statement about diffeomorphisms of $\#^p S^2 \tilde{\times} S^1$. We also give an analogue of Waldhausen's Theorem (see Theorem 1.3.11) for Heegaard splittings of $\#^p S^2 \tilde{\times} S^1$ up to isotopy, which may be of independent interest. In §3.2.2, we discuss the implications of Theorem 3.1.1 for Kirby diagrams of non-orientable 4–manifolds, and illustrate several examples.

3.2.1 Diffeomorphisms and splittings of $\#\mathbf{S^2 \tilde{\times} S^1}$

We can adapt the proof of Theorem 3.1.1 to give a statement about diffeomorphisms of $\#^p S^2 \tilde{\times} S^1$. It seems likely that this theorem may have been known to experts, but it does not seem to appear in the literature. As in §3.1, we will write $Y_p = \#^p S^2 \tilde{\times} S^1$, and $S_1, \dots, S_p$ for the p 2–spheres of the form $S^2 \times \{\star\} \subset Y_p$.

Theorem 3.2.1. *Let $h : \#^p S^2 \tilde{\times} S^1 \to \#^p S^2 \tilde{\times} S^1$ be a diffeomorphism homotopic to the identity. Then h is isotopic to the identity.*

The reader will recall that the proof of Theorem 3.1.1 begins by assuming that a diffeomorphism $h : Y_p \to Y_p$ acts as the identity on $\pi_1(Y_p)$. Under this hypotheses, we show (Lemma 3.1.10) that h is isotopic to a diffeomorphism of the form

$$H_{\alpha_p}(S_p) \circ \cdots \circ H_{\alpha_1}(S_1),$$

for some elements $\alpha_1, \ldots, \alpha_p \in \pi_1(SO(3))$. If h is a diffeomorphism of Y_p homotopic to the identity map (i.e. not just the identity on $\pi_1(Y_p)$ and $\pi_2(Y_p)$), then this same conclusion certainly still follows, and is the starting point for the proof of Theorem 3.2.1.

Note that the assumption that h is honestly homotopic to the identity is necessary, since the map $H_{\alpha_i}(S_i)$ is non-trivial, yet *does* act trivially on $\pi_1(Y_p)$ and $\pi_2(Y_p)$.

Proof of Theorem 3.2.1. By Lemma 3.1.10, the map h is isotopic to a diffeomorphism of the form

$$H_{\alpha_p}(S_p) \circ \cdots \circ H_{\alpha_1}(S_1).$$

Applying the following general proposition due to Laudenbach completes the proof. For the convenience of the reader (particularly for one who does not read French), we include a short proof. □

Proposition 3.2.2 ([49], Appendix II)**.** *Let Y be a (possibly non-orientable) 3–manifold, and let $S_1, \ldots, S_p \subset Y$ be disjointly embedded 2–spheres. Suppose that S_1 does not separate $Y \setminus \{S_2 \cup \cdots \cup S_p\}$ and that the map $H := H_{\alpha_p}(S_p) \circ \cdots \circ H_{\alpha_1}(S_1)$ is homotopic to the identity. Then $\alpha_1 = 0$.*

Proof. Since S_1 does not separate $Y \setminus \{S_2 \cup \cdots \cup S_p\}$, there is an embedded loop $\gamma \subset Y \setminus \{S_2, \ldots, S_p\}$ which intersects S_1 once. Let N be a tubular neighbourhood of γ, and note that this determines a splitting $Y \cong E \# Y'$, where E is a 2–sphere bundle over S^1, and Y' is another 3–manifold. Indeed, $\nu(S_1) \cup N$ is homeomorphic to either $S^2 \times S^1$ or $S^2 \tilde{\times} S^1$ with a 3–ball removed, so this gives the advertised connected sum decomposition. Moreover, by choosing γ to pass through the points fixed by the rotation of $H_{\alpha_1}(S_1)$, we may assume that H preserves γ pointwise and N setwise. We will first prove the proposition in the case that Y is orientable; if Y is non-orientable we will carefully surger the orientation double cover in order to reduce to the orientable case.

Case 1: N is orientable, i.e. $N \cong D^2 \times S^1$ and $E \cong S^2 \times S^1$.

Let $T_0 : D^2 \times S^1 \to N$ be a trivialization of N, and let $T_1 = T_0 \circ dH$ be the trivialization induced by H. Since H is homotopic to the identity, there is an embedded (framed) annulus $A : (D^2 \times S^1) \times I \to Y \times \mathbb{R}$ with

$$A|_{D^2 \times S^1 \times \{0\}} = T_0$$

and

$$A|_{D^2 \times S^1 \times \{1\}} = T_1.$$

In other words, A is the trace of N throughout the homotopy. Moreover, using the normal bundle of A, T_0 and T_1 extend to trivializations R_0 and R_1 of $\nu_{Y\times\mathbb{R}}(\gamma)$, and R_0 and R_1 are homotopic. Note that such trivializations are in correspondence with $\pi_1(SO(3)) = \mathbb{Z}_2$.

If $\alpha_1 = 1$, then when we view R_0 and R_1 as elements of $\pi_1(SO(3))$ we see that they differ exactly by a full 2π rotation about some axis. That is, R_0 and R_1 correspond to different elements and so cannot be homotopic. We conclude that $\alpha_1 = 0$. Note that if Y is orientable then N is always orientable, and so we have successfully proved the proposition in the case that Y is orientable.

Case 2: N is non-orientable, i.e. $N \cong D^2 \tilde{\times} S^1$ and $E \cong S^2 \tilde{\times} S^1$.

Let $p : \widetilde{Y} \to Y$ be the orientation double cover of Y, with deck transformation $\tau : \widetilde{Y} \to \widetilde{Y}$. For $1 \leq i \leq p$, let $\widetilde{S}_i$ denote one of the two possible lifts of S_i. The map H lifts to a map

$$\widetilde{H} = H_{\alpha_p}(\widetilde{S}_p) \circ \cdots \circ H_{\alpha_1}(\widetilde{S}_1) \circ H_{\alpha_p}(\tau(\widetilde{S}_p)) \circ \cdots \circ H_{\alpha_1}(\tau(\widetilde{S}_1)).$$

Since H is homotopic to the identity, $\widetilde{H}$ must be homotopic to either the identity or τ. However, $\widetilde{H}$ is orientation preserving while τ is orientation reversing, and so it must be the case that $\widetilde{H}$ is also homotopic to the identity. Since $\widetilde{Y}$ is orientable, our goal will be to apply the first case to $\widetilde{H}$. Since $\widetilde{S}_1$ may actually separate $\widetilde{Y} \setminus \{\widetilde{S}_2, \ldots \widetilde{S}_p, \tau(\widetilde{S}_1), \ldots, \tau(\widetilde{S}_p)\}$, we will carefully add another $S^2 \times S^1$ summand to $\widetilde{Y}$ to guarantee that $\widetilde{S}_1$ meets the non-separating hypothesis. For a visualization of why this is necessary, consider the schematic in Figure 3.2 below.

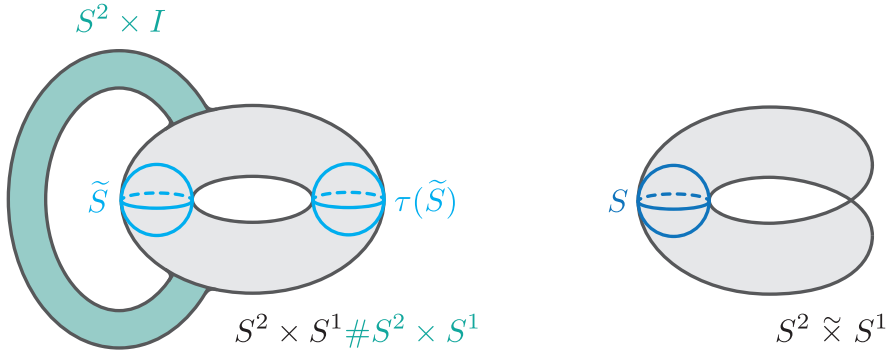

Figure 3.2: A schematic in the case that $p = 1$. The 2–sphere $S \subset S^2 \tilde{\times} S^1$ lifts to the 2–spheres $\widetilde{S}, \tau(\widetilde{S}) \subset S^2 \times S^1$; note that $\widetilde{S}$ *does* separate $S^2 \times S^1 \setminus \tau(\widetilde{S})$. By adding another $S^2 \times S^1$ summand (green), we will ensure that $\widetilde{S}$ is non-separating.

To this end, let B be a small 3–ball centered on a point $x_0 \in E$, chosen so that B is fixed by H.

Lemma 3.2.3. *There exists a homotopy h_t from H to id_Y so that $h_t^{-1}(B) = B$ and $h_t^{-1}(x_0) = \{x_0\}$ for all t. In other words, h_t fixes B setwise and x_0 pointwise.*

Proof of Lemma 3.2.3. Consider any homotopy g_t from H to id_Y. The loop $g_t(x_0)$ traces out some element η of $\pi_1(Y; x_0)$. If $[\eta]$ is trivial, then we can contract η to obtain a new homotopy of the desired form. There are two cases to consider.

Case (a): $Y = E$, and so $\pi_1(V; x_0) \cong \mathbb{Z}$.

Since H is homotopic to the identity, η lifts to a loop $\tilde{\eta} \in \pi_1(S^2 \times S^1; \tilde{x}_0) \cong \mathbb{Z}$, where $\tilde{x}_0$ is a lift of x_0. Thus, $[\tilde{\eta}] \in 2\mathbb{Z}$.

Now, consider the homotopy f_t of $S^2 \tilde{\times} S^1$ given by pushing $S^2 \times \{\star\}$ around the S^1 factor *twice*. Then the trace of $f_t(x_0)$ as t varies is the class $[2] \in \pi_1(S^2 \tilde{\times} S^1; x_0)$. Thus, by composing g_t with some number of copies of f_t or its inverse, we may assume that $[\eta] = 0$.

Case (b): $Y \neq E$, and so $\pi_1(V; x_0) \cong \mathbb{Z} \star \pi_1(Y')$.

Since H is homotopic to the identity, the action of conjugation of $[\eta]$ on $\pi_1(Y; x_0)$ is trivial. Thus, $[\eta]$ is in the center of $\pi_1(V; x_0)$. Since $V \neq E$, we know $Y' \ncong S^3$ and so by the 3–dimensional Poincaré conjecture, $\pi_1(Y')$ is non-trivial. Thus, the center of $\mathbb{Z} \star \pi_1(Y')$ is trivial, which implies that $[\eta] = 0$. □

Remark 3.2.4. The apparently casual use of the 3–dimensional Poincaré conjecture in the proof of Lemma 3.2.3 is not without reason. In fact, Laudenbach's original work on 2–spheres in 3–manifolds [48] (in particular Theorem 3.1.3) assumed this conjecture, and so we have effectively already used it in this section. By the remarkable work of Perelman, we know that this conjecture is indeed true.

By Lemma 3.2.3, there is a homotopy h_t from H to id_Y which fixes x_0 pointwise and B setwise. Let $\widetilde{B} \subset \widetilde{Y}$ be a lift of B. Now, fix some identification $\phi : S^2 \to \partial B$ and consider the manifold W obtained by removing the interior of $\widetilde{B}$ and $\tau(\widetilde{B})$ and gluing in $S^2 \times I$, i.e.,

$$W = \frac{(\widetilde{Y} \setminus (\mathrm{int}\widetilde{B} \cup \mathrm{int}\tau(\widetilde{B}))) \sqcup S^2 \times I}{x \times \{0\} \sim \phi(x) \text{ and } x \times \{1\} \sim \tau \circ \phi(x)}.$$

By construction, $W = \widetilde{Y} \# S^2 \times S^1$, and H naturally extends to the diffeomorphism $G : W \to W$ given by:

$$G(x) = \begin{cases} \widetilde{H}(x) & \text{if } x \notin S^2 \times [0,1], \\ x & \text{if } x \in S^2 \times [0,1]. \end{cases}$$

In particular, G is a composition of sphere twists, and so we are now in a position to appeal to the first case. Note that G is homotopic to id_W via an extension of h_t to $S^2 \times I$. Observe that all the following hold:

- W is orientable;
- $\widetilde{S}_1, \ldots, \widetilde{S}_p, \tau(\widetilde{S}_1), \ldots, \tau(\widetilde{S}_p)$ are 2–spheres embedded in W;
- $G = H_{\alpha_p}(\widetilde{S}_p) \circ \cdots \circ H_{\alpha_1}(\widetilde{S}_1) \circ H_{\alpha_p}(\tau\widetilde{S}_p) \circ \cdots \circ H_{\alpha_1}(\tau\widetilde{S}_1)$;
- G is homotopic to the identity map;
- $\widetilde{S}_1$ is non-separating in $W \setminus \{\widetilde{S}_2, \ldots, \widetilde{S}_p, \tau(\widetilde{S}_1), \ldots, \tau(\widetilde{S}_p)\}$.

Thus, by applying the first case, we see that $\alpha_1 = 0$. This completes the proof of Proposition 3.2.2. □

Remark 3.2.5. When $p = 1$, Theorem 3.2.1 gives a proof that the diffeotopy group (diffeomorphisms up to isotopy) of $S^2 \tilde{\times} S^1$ is equal to $\mathbb{Z}_2 \oplus \mathbb{Z}_2$, which is recorded as a corollary below. This group is generated by a reflection in the S^1 factor, and a non-trivial twist $H_\alpha(S^2)$ about a 2–sphere fiber, which we will simply denote τ. This was first computed by Kim and Raymond in [38], who also gave the corresponding analogue of Theorem 3.2.1 for $p = 1$. The reflection induces a non-trivial automorphism on $\pi_1(S^2 \tilde{\times} S^1)$, and the map τ is not homotopic to the identity by Proposition 3.2.2. This is analogous to the fundamental result of Gluck [26], who showed that the diffeotopy group of $S^2 \times S^1$ is equal to $\mathbb{Z}_2 \oplus \mathbb{Z}_2 \oplus \mathbb{Z}_2$, generated by a reflection in the S^1 factor, a reflection in the S^2 factor, and the twist map τ.

Corollary 3.2.6 ([38])**.** *The diffeotopy group of $S^2 \tilde{\times} S^1$ is generated by a reflection in the S^1 factor, and a sphere twist τ along a 2-sphere fibre. That is,* $\mathrm{Diff}(S^2 \tilde{\times} S^1) \cong \mathbb{Z}_2 \oplus \mathbb{Z}_2$.

Remark 3.2.7. The map τ is particularly important for constructing homotopy 4–spheres. Given an embedded 2–sphere S in S^4 with regular neighbourhood $\nu(S) \cong S^2 \times D^2$, the *Gluck twist of S* is the 4–manifold

$$\Sigma_S := (S^4 \setminus \nu(S)) \cup_\tau \nu(S),$$

i.e. the result of cutting out and regluing $\nu(S)$ by the map τ. In fact, Σ_S is a homotopy 4–sphere, and so by the groundbreaking work of Freedman [22], Σ_S is homeomorphic to S^4. However, despite study by many authors it remains an open question whether Σ_S is always *standard*, i.e. diffeomorphic to S^4.

If $S \subset S^4$ is an embedded 2–sphere, then $\partial\nu(S)$ is always diffeomorphic to $S^2 \times S^1$, and so there is not exactly a non-orientable analogue of a Gluck twist. However, τ can still be used to construct interesting (non-orientable) 4–manifolds. First, observe that $S^2 \tilde{\times} S^1 = \partial(D^2 \tilde{\times} \mathbb{RP}^2)$, the non-trivial disk bundle over $\mathbb{RP}^2$ obtained as the complement of an orientation reversing loop in $\mathbb{RP}^4$ (for an illustration, see Figure 3.5). Gluing this bundle to itself via either the identity map or τ yields $S^2 \tilde{\times} \mathbb{RP}^2$ or the 4–manifold $\mathbb{RP}^4 \#_{S^1} \mathbb{RP}^4$, sometimes called the *circle sum* of $\mathbb{RP}^4$ with itself. This process is analogous to gluing $S^2 \times D^2$ to itself via either the identity map or τ to produce $S^2 \times S^2$ or $S^2 \tilde{\times} S^2$. While $S^2 \times S^2$ and $S^2 \tilde{\times} S^2$ are distinguished easily by their intersection forms, $S^2 \tilde{\times} \mathbb{RP}^4$ and $\mathbb{RP}^4 \#_{S^1} \mathbb{RP}^4$ are somewhat harder to distinguish (they have the same $\mathbb{Z}_2$–intersection form). However, they are known to be homotopy inequivalent by the complete classification of non-orientable 4–manifolds with fundamental group $\mathbb{Z}_2$ by Hambleton-Kreck-Teichner [30], or the homotopy invariant for such manifolds given by Kim-Kojima-Raymond in [39].

As a last application of the results of this chapter, we show that there is a unique Heegaard splitting of $\#^k S^2 \tilde{\times} S^1$ up to isotopy. Waldhausen originally showed that S^3 admits a unique splitting up to isotopy, and that $\#^k S^2 \times S^1$ admits a unique splitting up to homeomorphism. In [10] Carvalho and Oertel showed that the result holds up to isotopy; the same method can be used to improve the statement of Proposition 1.3.12 to isotopy. To the best of our knowledge, this result is new and has not appeared in the literature.

Theorem 3.2.8. *Let $g \geq k \geq 0$. Any genus g Heegaard splitting of $\#^k S^2 \tilde{\times} S^1$ is isotopic to a stabilization of the standard Heegaard splitting.*

Proof. We will show that any two genus k Heegaard splittings of $\#^k S^2 \tilde{\times} S^1$ are isotopic. Since stabilization is well defined up to isotopy, this will complete the proof. To this end, let $\mathcal{H} = (\Sigma; H_1, H_2)$ and $\mathcal{H}' = (\Sigma'; H_1', H_2')$ be two genus k Heegaard splittings of $\#^k S^2 \tilde{\times} S^1$.

By Proposition 1.3.12, $\mathcal{H}$ and $\mathcal{H}'$ are equivalent. Choose any diffeomorphism $f : H_1 \to H_1'$. This doubles to a diffeomorphism $F : \#^k S^2 \tilde{\times} S^1 \to \#^k S^2 \tilde{\times} S^1$ which sends $\mathcal{H}'$ to $\mathcal{H}'$. We will show that F is isotopic to a diffeomorphism which preserves $\mathcal{H}$; the trace of such an isotopy will take Σ' to Σ, from which it follows that $\mathcal{H}$ and $\mathcal{H}$' are isotopic.

Consider the map $(F_1^{\#})^{-1} : \pi_1(\#^k S^2 \tilde{\times} S^1) \to \pi_1(\#^k S^2 \tilde{\times} S^1)$. Since $\pi_1(\#^k S^2 \tilde{\times} S^1) \cong \pi_1(H_1)$, by Lemma 3.1.4 we can find a map $g : H_1 \to H_1$ so that $g_1^{\#} = (F_1^{\#})^{-1}$. Doubling

this map, we obtain a map $G : \#^k S^2 \tilde{\times} S^1 \to \#^k S^2 \tilde{\times} S^1$. Letting $h = F \circ G$, we see that h takes $\mathcal{H}$ to $\mathcal{H}'$ and that $h_1^{\#} = \mathrm{id}$.

Let $S_1, \ldots, S_k$ be the k essential (non-separating) 2–spheres obtained by doubling non-separating disks in H_1. By Lemma 3.1.10, h is isotopic to a composition of sphere twists H along $S_1, \ldots, S_k$. However, we can clearly choose any such sphere twist so that it preserves $\mathcal{H}$.

Thus, the isotopy from h to H takes Σ' to Σ. We conclude that $\mathcal{H}$ and $\mathcal{H}'$ are isotopic, which completes the proof. □

3.2.2 Kirby diagrams for non-orientable 4–manifolds

In this section, we discuss Kirby diagrams of non-orientable 4–manifolds. While these have not enjoyed the same attention as the Kirby diagrams for orientable 4–manifolds, we can still work with them in much the same way. For more details, the reader is referred to [3], as well as [70]. The following result is an immediate corollary of Theorems 3.0.1 and 3.1.1, and is essential for descriptions of closed 4–manifolds. To the best of our knowledge, a proof of this statement does not appear in the literature.

Corollary 3.2.9. *Let X be a smooth, closed, and connected 4–manifold. Fix a handle decomposition of X, and let $X_{(n)}$ denote the union of the 0–, 1–, ... and n–handles of this decomposition. Then X is determined up to diffeomorphism by $X_{(2)}$.*

Since we only have to specify the 1– and 2–handles of a handle decomposition, we can effectively draw diagrams for closed 4–manifolds. For our purposes, a Kirby diagram is a depiction of a framed link in $\#S^2 \times S^1$ (or $\#S^2 \tilde{\times} S^1$), whose surgery is again $\#S^2 \times S^1$ or $\#S^2 \tilde{\times} S^1$. Equivalently, this is a drawing of the 1– and 2–handles of a handle decomposition without any extra information.

We will assume some familiarity with these diagrams, and refer the reader to [28] and [3] for extensive treatment. However, we will discuss how to draw 1–handles, since this depends on whether the 4–manifold is orientable.

As usual, we draw 1– and 2–handles attached to the boundary of a 0–handle, via their attaching regions in $\partial B^4 = S^3$. Both orientable and non-orientable 1–handles are attached along $S^0 \times B^3$, but the essential difference is how these 3–balls are identified. The usual convention is to draw orientable 1–handles as a pair of 3–balls, which are identified by a (orientation reversing) reflection across an equator. The reader may wish to compare this with the 2–dimensional case illustrated in Figure 3.3 and 3.4.

(a) (b)

Figure 3.3: Orientable 1–handles are drawn as a pair of 3–balls, identified by a reflection through the (vertical) equator. Attaching curves of 2–handles that enter on one side leave on the *opposite* side. The 4–dimensional case is illustrated in (a), and a 2–dimensional analogue is illustrated in (b).

Non-orientable handles are drawn as a pair of 3–balls, which are identified by the (orientation preserving) identity map. This convention differs slightly from [3], but is more convenient for our purposes.

We will record the framing of a 2–handle the same way as [3]. If a 2–handle runs over only orientable 1–handles, then we can specify a well defined framing with an integer. However, if it runs over non-orientable 1–handles, then we have to assign an integer to each arc of the 2–handle attaching circle minus the 1–handles. Indeed, if a twist is pushed through a non-orientable 1–handle, it becomes a twist of the opposite sign.

(a) (b)

Figure 3.4: Non-orientable 1–handles are drawn as a pair of 3–balls, identified by the identity map. We will color one half of the 3–ball as a reminder that 2–handle attaching curves that enter on one side leave on the *same* side. The 4–dimensional case is illustrated in (a), and a 2–dimensional analogue is illustrated in (b).

In preparation for their trisections, we will now draw Kirby diagrams for several well-known non-orientable 4–manifolds.

Example 3.2.10 ($\mathbb{RP}^4$)**.** We begin with the well known diagram for $D^2 \tilde{\times} \mathbb{RP}^2$ in Figure 3.5 (a) (see [3, Section 1.5] or [70]): it can be built with a single non-orientable 1–handle, and a 2–handle attached along a curve that runs across the 1–handle twice, attached with framing as described below.

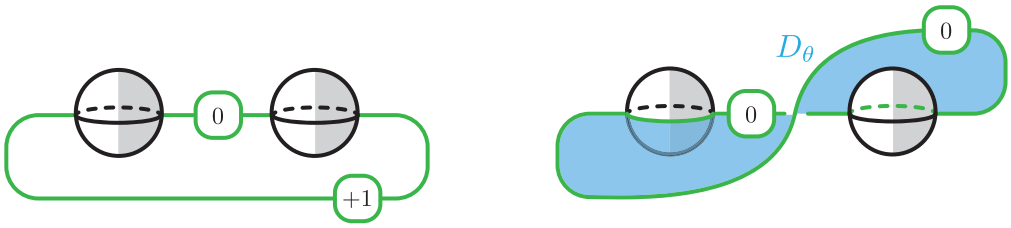

(a) (b)

Figure 3.5: In (a), a Kirby diagram for $D^2 \tilde{\times} \mathbb{RP}^2$, a neighbourhood of $\mathbb{RP}^2$ in $\mathbb{RP}^4$. In (b), an illustration of the fibration structure of the boundary showing that $\partial(D^2 \tilde{\times} \mathbb{RP}^2) = S^2 \tilde{\times} S^1$. Each pair of disks forms an annulus that meets a tubular neighbour of the 2–handle curve in two matching longitudes.

The boundary of this disk bundle over $\mathbb{RP}^2$ is $S^2 \tilde{\times} S^1$, whose fibration structure is illustrated in Figure 3.5 (b). The exterior of the 2–handle attaching curve is fibered by pairs of disks D_θ (one such disk is shaded blue); the disks D_θ and $D_{\theta+\pi}$ glue together to form an annulus which meets the boundary of a neighbourhood of the 2–handle curve in two longitudes. Since we attach the 2–handle with exactly the correct framing, we see the (twisted) S^2–bundle structure in $\partial(D^2 \tilde{\times} \mathbb{RP}^2)$. By adding a 3–handle (uniquely), we obtain a Kirby diagram for $\mathbb{RP}^4$.

Example 3.2.11 ($S^2 \times \mathbb{RP}^2$)**.** A relative Kirby diagram for $D^2 \times \mathbb{RP}^2$ is given in Figure 3.6 (a). We can obtain a Kirby diagram for the double of this manifold, $S^2 \times \mathbb{RP}^2$, in the usual way. To every 2–handle, we add a new 2–handle as a 0–framed meridian, corresponding to the core of each new (doubled) 2–handle. Consequently, a diagram for $S^2 \times \mathbb{RP}^2$ is given in Figure 3.6 (b).

(a) (b)

Figure 3.6: In (a), a Kirby diagram for $D^2 \times \mathbb{RP}^2$. In (b), a diagram for its double, $S^2 \times \mathbb{RP}^2$.

Example 3.2.12 (Gluing together copies of $D^2 \tilde{\times} \mathbb{RP}^2$)**.** We can obtain more interesting manifolds by gluing together copies of $D^2 \tilde{\times} \mathbb{RP}^2$.

A Kirby diagram of the double of this bundle may be obtained in the usual way, by simply adding a 0-framed meridian to the 2–handle attaching curve. Consequently, a diagram for $S^2 \tilde{\times} \mathbb{RP}^2$ is given in Figure 3.7 (a).

(a) (b)

Figure 3.7: In (a), a Kirby diagram for $S^2 \tilde{\times} \mathbb{RP}^2 = D^2 \tilde{\times} \mathbb{RP}^2 \cup_{\mathrm{id}} D^2 \tilde{\times} \mathbb{RP}^2$. In (b), a Kirby diagram for $D^2 \tilde{\times} \mathbb{RP}^2 \cup_{\tau^m} D^2 \tilde{\times} \mathbb{RP}^2$. The result only depends on m modulo 2.

To draw a diagram of $\mathbb{RP}^4 \#_{S^1} \mathbb{RP}^4 = D^2 \tilde{\times} \mathbb{RP}^2 \cup_{\tau} D^2 \tilde{\times} \mathbb{RP}^2$ (see Example 3.2.7), note that the map τ fixes γ pointwise, but adds (or subtracts) 2 to the framing. Thus we will add a ± 2–framed meridian, as illustrated in Figure 3.7 (b). What remains in both cases is a 3– and 4–handle, which do not need to be specified. The map τ has order two, so the framing of the meridian only matters modulo 4. The reader may also wish to check this by handle slides.

Chapter 4

Trisections of non-orientable 4–manifolds

In this chapter, we study trisections of non-orientable 4–manifolds. The goal will be to fill in any gaps for the non-orientable setting, and give many examples. Consequently, we will assume that the reader has at least some familiarity with trisections. Most of the theory carries over unchanged, but there are are few places where it is necessary to be careful. In particular, we will need several key results from Chapter 3. We will also give a self-contained discussion of relative trisections (4–manifolds with boundary) and bridge trisections (for surfaces embedded in 4–manifolds) that does not depend on orientability.

Trisections of non-orientable 4–manifolds may initially seem more complicated than their orientable counterparts. This is largely because even small non-orientable manifolds necessarily have non-trivial fundamental groups. However, they witness interesting exotic phenomena in dimension four: although it is currently unknown whether an exotic S^4 exists, there *are* known to be exotic versions of $\mathbb{RP}^4$. One might hope that these examples are more accessible for study by trisections, or that they might give some fresh insight into the relationship between trisections and exotic 4–dimensional behavior.

4.1 Existence, uniqueness, and diagrams

In what follows, manifolds are *not* assumed to be orientable. In particular, we will relax the assumption that parts[1] of a trisection are orientable.

[1] A part of a trisection is one of the 3– or 4–dimensional handlebodies, or the central surface.

Recall that an n–dimensional handlebody is a manifold which can be built from a single 0–handle and some number of 1–handles (see Definition 1.2.1). In other words, it is diffeomorphic to either $\natural^k B^n \times S^1$ or $\natural^k B^n \tilde{\times} S^1$. By sliding 1–handles it is easy to see that $(\natural^k B^n \times S^1) \natural (B \tilde{\times} S^1) \cong \natural^{k+1} B^n \tilde{\times} S^1$, i.e. the presence of a single non-orientable 1–handle makes a handlebody non-orientable.

The definition of a trisection from Chapter 2 carries over verbatim from the orientable setting. The following observation shows that either all parts of a trisection are orientable, or none of them are.

Lemma 4.1.1 ([69, Proposition 5])**.** *Suppose that $\mathcal{T}$ is a trisection of a smooth, closed, connected (but possibly not orientable) 4–manifold X. Then X is orientable if and only if any part of $\mathcal{T}$ is orientable.*

Proof. Suppose that the sectors of $\mathcal{T}$ are X_1, X_2, and X_3. If X is orientable, then each X_i is orientable, and so ∂X_i is orientable. Consequently, each $X_i \cap X_j$ and $X_1 \cap X_2 \cap X_3$ are also orientable.

Conversely, note that if any handlebody of $\mathcal{T}$ is orientable, then the above argument shows that $X_1 \cap X_2 \cap X_3$ is orientable. Moreover, if $X_1 \cap X_2 \cap X_3$ is orientable, then each of ∂X_i is orientable, and hence each X_i is orientable. We can thus orient X by starting with an orientation on X_1 and extending it across X_2 and X_3. □

Thus, the following definition is equivalent to Definition 2.1.1 in the non-orientable setting.

Definition 4.1.2 ([24])**.** Suppose that X is a smooth, non-orientable, closed, and connected 4–manifold. A $(g; k_1, k_2, k_3)$– *trisection* $\mathcal{T}$ of X is a decomposition $X = X_1 \cup X_2 \cup X_3$ such that

- X_i is diffeomorphic to $\natural^{k_i} B^3 \tilde{\times} S^1$;
- $X_i \cap X_j$ is diffeomorphic to $\natural^g B^2 \tilde{\times} S^1$;
- $\Sigma = X_1 \cap X_2 \cap X_3$ is diffeomorphic to $\#^g(\mathbb{RP}^2 \# \mathbb{RP}^2)$.

The proof of existence of trisections (Theorem 2.1.4) that begins with a handle decomposition carries over verbatim. As part of a more general treatment of multisections, Rubinstein and Tillman [66] give a proof of existence that does not require orientability. The proof of Proposition 2.1.5 also follows without any serious modifications.

Stable uniqueness in this setting requires more care, and has not previously appeared in the literature. Essentially the same technique from [24] can be used, but requires the strong version of Waldhausen's theorem for $\#^k S^2 \tilde{\times} S^1$ proved in Chapter 3 (Theorem 3.2.8).

Theorem 4.1.3. *Every smooth, closed, connected (but possibly not orientable) 4–manifold X admits a $(g;k)$–trisection for some $0 \leq k \leq g$. Any two trisections of X become isotopic after sufficiently many stabilizations.*

Proof of Uniqueness. We will only prove the stable uniqueness statement here. For existence, see the proof of Theorem 2.1.4 or [24].

Suppose that $\mathcal{T}$ and $\mathcal{T}'$ are two trisections of a fixed 4–manifold X. By Proposition 2.1.5, both $\mathcal{T}$ and $\mathcal{T}'$ induce handle decompositions of X, in which X_1 and X_1' are 1–handles for X. As noted in [24], Cerf theory guarantees that these handle decompositions are related by a sequence of:

- Adding cancelling 1/2 and 2/3 handles;
- Handle slides among handles of the same index;
- Isotopy of handles and handle attaching maps.

We have seen that we can add cancelling pairs of 1/2 or 2/3 handles by stabilizing the trisection. Moreover, isotopy or handle slides among 1–handles or 3–handles can be achieved without modifying the associated trisection, since they take place entirely within a sector. Consequently, we only need to check that we can realize 2–handle slides and isotopy of 2–handles, possibly up to trisection stabilization. As in Proposition 2.1.5, the trisections $\mathcal{T}$ and $\mathcal{T}'$ induce Heegaard splittings of ∂X_1 and $\partial X_1'$, in which the 2–handles attaching curves are a core of $H_{12} = X_1 \cap X_2$ or $H_{12}' = X_1' \cap X_2'$. Any 2–handle slide is performed along a framed arc, which we may assume is contained in the central surface. As in [24], stabilization of this Heegaard splitting (which may be achieved by trisection stabilization) allows us to assume that this framed arc is embedded and disjoint from any 2–handle curves or dual meridional curves for each 2–handle. Consequently, up to stabilization we can perform 2–handle slides while ensuring that the resulting handle decomposition is induced by a trisection.

Lastly, suppose $\mathcal{T}$ and $\mathcal{T}'$ are related only by isotopy of the corresponding 2–handle attaching maps. Since this isotopy extends to an isotopy of X, we can assume that the handle decompositions are identical and that the only difference between the trisections is

the induced Heegaard splittings on ∂X_1. Suppose that these are given by $\partial X_1 = H_{12} \cup H_{31}$ and $\partial X_1 = H'_{12} \cup H'_{31}$, respectively. Denote the 2–handle attaching link by L; in both cases L is dual to a system of meridional curves.

As noted in [24], either the strong version of Waldhausen's theorem or Theorem 3.2.8 guarantees that these Heegaard splittings are isotopic. This does *not* imply that the trisections are isotopic, since this process may move L. The process in [24] works verbatim; we can stabilize the Heegaard splittings of ∂X_1 to find an isotopy which also fixes L. Indeed, this is guaranteed by Cerf theory: we can pick Morse functions for ∂X_1 that agree on a tubular neighbourhood of L. These can be made to agree up to 3–dimensional 1/2 stabilizations and slides that occur away from L.

Isotoping the Heegaard splittings (after possibly further stabilizations of the trisection) to agree now completes the proof. □

As in the orientable case, we would like to be able to study non-orientable 4–manifolds via trisection diagrams. We can do so via the non-orientable version of Waldhausen's theorem, and the non-orientable version of the Laudenbach-Poénaru theorem.

Definition 4.1.4. A (non-orientable) $(g; k_1, k_2, k_3)$*–trisection diagram* is a tuple $\mathfrak{D} = (\Sigma; \alpha, \beta, \gamma)$, where Σ is a closed non-orientable surface of genus g (i.e. $\Sigma \cong \#^{2g}\mathbb{RP}^2$), and α, β, and γ are collections of g embedded closed curves such that:

- Each of α, β, and γ is a *cut system of curves* for Σ;
- Each pair of curves is standard, i.e. each of $(\Sigma; \alpha, \beta)$, $(\Sigma; \beta, \gamma)$, and $(\Sigma; \gamma, \alpha)$ is a genus g Heegaard diagram for $\#^{k_i} S^2 \tilde{\times} S^1$.

By Proposition 1.3.12, each pair of curves describes a Heegaard diagram for $\#^{k_i} S^2 \tilde{\times} S^1$ if and only if it is *standardizeable*, i.e. there is a sequence of handle slides and surface automorphisms which converts it to the diagram in Figure 4.8. As in the orientable case, we do not expect that the three sets of curves can be *simultaneously* standardized.

The same proof of Theorem 2.2.2 together with Theorem 3.1.1 shows that a trisection diagram determines a unique closed 4–manifold and vice versa. Combining this with the orientable case, we complete the diagrammatic theory of trisections for all 4–manifolds.

Theorem 4.1.5. *Let $\mathcal{T}$ be a trisection of a (possibly non-orientable) 4–manifold X. Then $\mathcal{T}$ determines a trisection diagram $(\Sigma; \alpha, \beta, \gamma)$ describing $\mathcal{T}$ that is well-defined up to automorphism of Σ and slides of α, β, γ. That is, there is a natural bijection*

$$\frac{\{\textit{trisection diagrams}\}}{\textit{surface automorphism, slides}} \leftrightarrow \frac{\{\textit{trisected 4–manifolds}\}}{\textit{diffeomorphism}}.$$

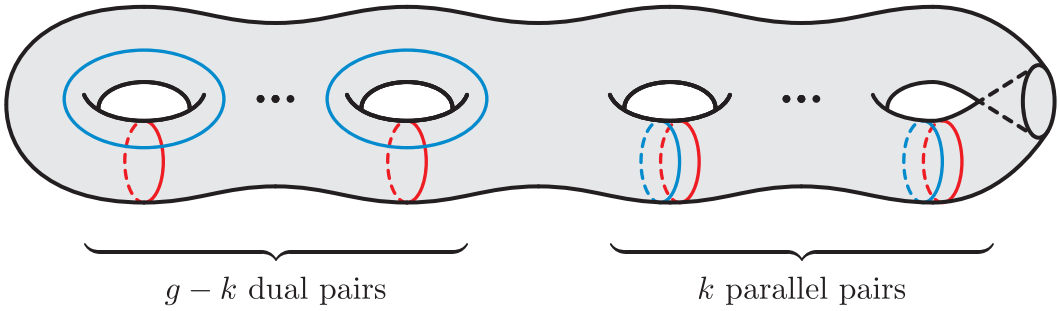

Figure 4.1: A standard diagram for a genus g Heegaard splitting of $\#^k S^2 \tilde{\times} S^1$. In a trisection diagram, every pair of curves $(\Sigma; \star, \star)$ is slide-diffeomorphic to this one.

4.2 Examples

In this section, we give many examples of non-orientable trisections. In a sense, these trisections tend to be more complicated than their orientable counterparts. By Lemma 4.1.1, if X is non-orientable, then so is any part of a trisection of X. In particular, the sectors cannot be 4–balls.

Example 4.2.1. The simplest non-orientable trisection is of $S^3 \tilde{\times} S^1$. As in the case of of $S^3 \times S^1$ (see Example 2.2.12), consider the trivial open book on S^3 with the unknot as binding and disk pages. Let D_1, D_2, and D_3 be three disjoint pages of this open book; these cobound 3-balls B_1, B_2, and B_3.

Now, note that $S^3 \tilde{\times} S^1$ can be built from $S^3 \times I$ by gluing the boundary components via a reflection r across the equatorial 2–sphere which intersects the unknot in two points. This reflection preserves each D_i and B_i *setwise*, but induces a reflection on each of ∂D_i and ∂B_i. Letting $X_i = B_i \times_r S_1 \cong B_i \tilde{\times} S_1$, we obtain a trisection of $S^3 \tilde{\times} S^1$. The central surface is a Klein bottle obtained by gluing the ends of $U \times I$ via r, and so this is a $(1;1)$–trisection. A diagram for this trisection is illustrated in Figure 4.2.

In fact, there are only *four* distinct isotopy classes of essential simple closed curves on the Klein bottle. Of these, only one curve is both non-separating and has an annular neighbourhood (rather than a Möbius band). Consequently, Figure 4.2 is the *only* possible $(1;1)$–trisection diagram.

Example 4.2.2. The next simplest non-orientable trisection is of $\mathbb{RP}^4$. We can reverse engineer a trisection diagram from the usual (non-orientable) Kirby diagram of $\mathbb{RP}^4$, using Algorithm 2.2.14 to check our work. In the non-orientable setting this needs only minor

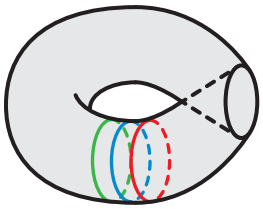

Figure 4.2: A $(1;1)$–trisection of $S^3 \tilde{\times} S^1$. This is the only trisection diagram that occurs on a Klein bottle.

modification; some 1–handles may be non-orientable. As usual, γ curves become 2–handle attaching curves with a framing induced by the surface (possibly on arcs). Non-orientable 1–handles arise from non-orientable portions of the trisection surface as in Figure 4.3. There are various ways to draw a Heegaard surface for $\#S^2 \tilde{\times} S^1$, and so we will use the most convenient one for the task at hand.

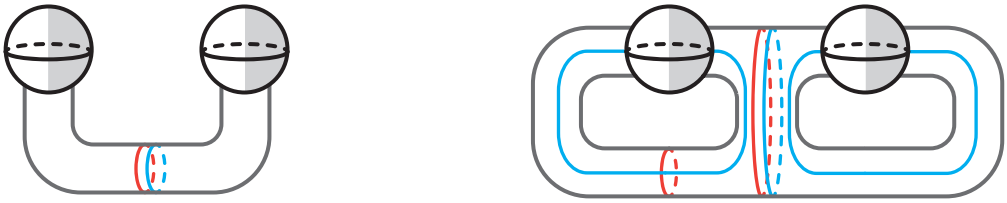

Figure 4.3: Two Heegaard surfaces in the boundary of $B^3 \tilde{\times} S^1$. The surface on the left has genus one, and the surface on the left has genus two. The reader may wish to check that the surface on the right is isotopic to a stabilization of the surface on the left, as guaranteed by Theorem 3.2.8.

Figure 4.4 (a) shows a genus two Heegaard surface for $S^2 \tilde{\times} S^1$, in which the attaching curves for the 2–handle for $\mathbb{RP}^4$ is a core of one of the handlebodies. In Figure 4.4 (b), the attaching curve has been isotoped to lie with surface framing, and so we can convert this to the trisection diagram. The other γ curve lies in the α handlebody, and one can check that the β and γ handlebodies share a common curve. Consequently, the model surface (obtained by a mild cut and paste) in Figure 4.4 (c) is a $(2;1)$–trisection diagram for $\mathbb{RP}^4$.

This trisection induces the usual handle structure on $\mathbb{RP}^4$ with a single 0–, 1–, 2–, 3–, and 4–handle.

Example 4.2.3. For more complicated examples, we consider the manifolds of the form $D^2 \tilde{\times} \mathbb{RP}^2 \cup_{\tau^m} D^2 \tilde{\times} \mathbb{RP}^2$ from Example 3.2.12, where τ is the twist map along a fiber of $S^2 \tilde{\times} S^1$. Like $\mathbb{RP}^4$, these admit relatively simple Kirby diagrams from which we can

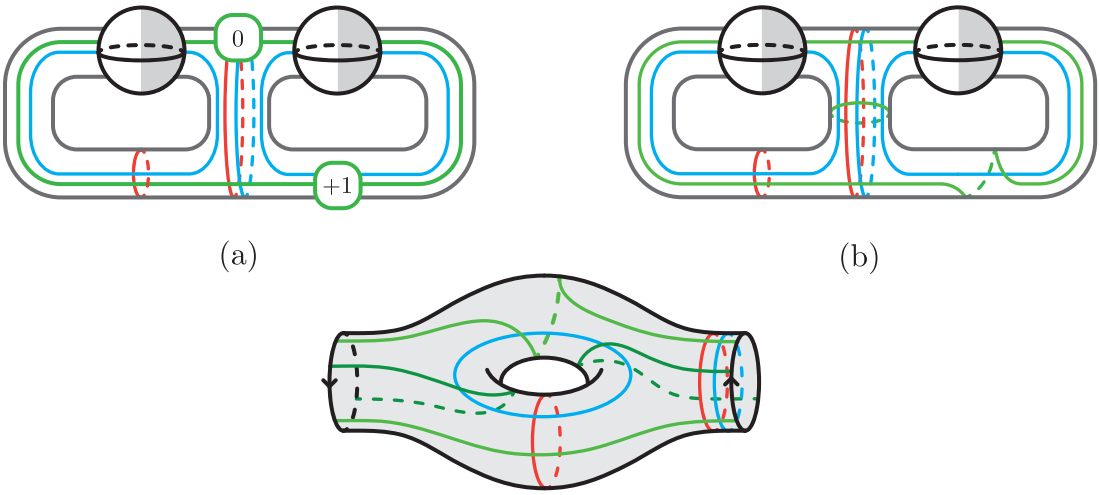

Figure 4.4: In (a) and (b), the process of arranging the 2–handle attaching curve to lie on a Heegaard surface for $S^2 \tilde{\times} S^1$. In (c), a trisection diagram for $\mathbb{RP}^4$. Opposite ends of the surface are identified to form a genus two non-orientable surface.

reverse engineer genus 3 trisection diagrams. This gives us a family of trisection diagrams describing $S^2 \tilde{\times} \mathbb{RP}^2$, and $\mathbb{RP}^4 \# \mathbb{RP}^4$. A diagram for $S^2 \times \mathbb{RP}^2$ can be obtained similarly.

These trisections are all minimal genus: the Euler characteristic of each of these manifolds is equal to 2, and so they cannot admit a $(g;k)$–trisection with $g < 3$.

Example 4.2.4. By lifting each sector, a trisection of a closed non-orientable 4–manifold X naturally lifts to a trisection of its orientation double cover $p : \widetilde{X} \to X$. Indeed, since p restricts to the orientation cover on each sector, the lifts $\widetilde{X}_i = p^{-1}(X_i)$ are each orientable 4–dimensional handlebodies with the correct intersection data.

Starting with a $(g;k)$–trisection for X, one obtains a $(2g-1; 2k-1)$–trisection for $\widetilde{X}$. Moreover, note that the central surface $\widetilde{\Sigma}$ for $\widetilde{X}$ double covers the central surface Σ for X. Thus, given a trisection diagram for X, we may easily draw the corresponding diagram for $\widetilde{X}$. Since each curve in Σ has an annular neighbourhood, it will lift to two disjoint curves in $\widetilde{\Sigma}$. One curve among the lifts of each of α, β, and γ will be homologically dependent, and so can be discarded.

As an example of this process, we produce a $(3;1)$–trisection of S^4 as the double cover of the trisection of $\mathbb{RP}^4$ from Example 4.2.2. This is illustrated in Figure 4.6. It is easy to

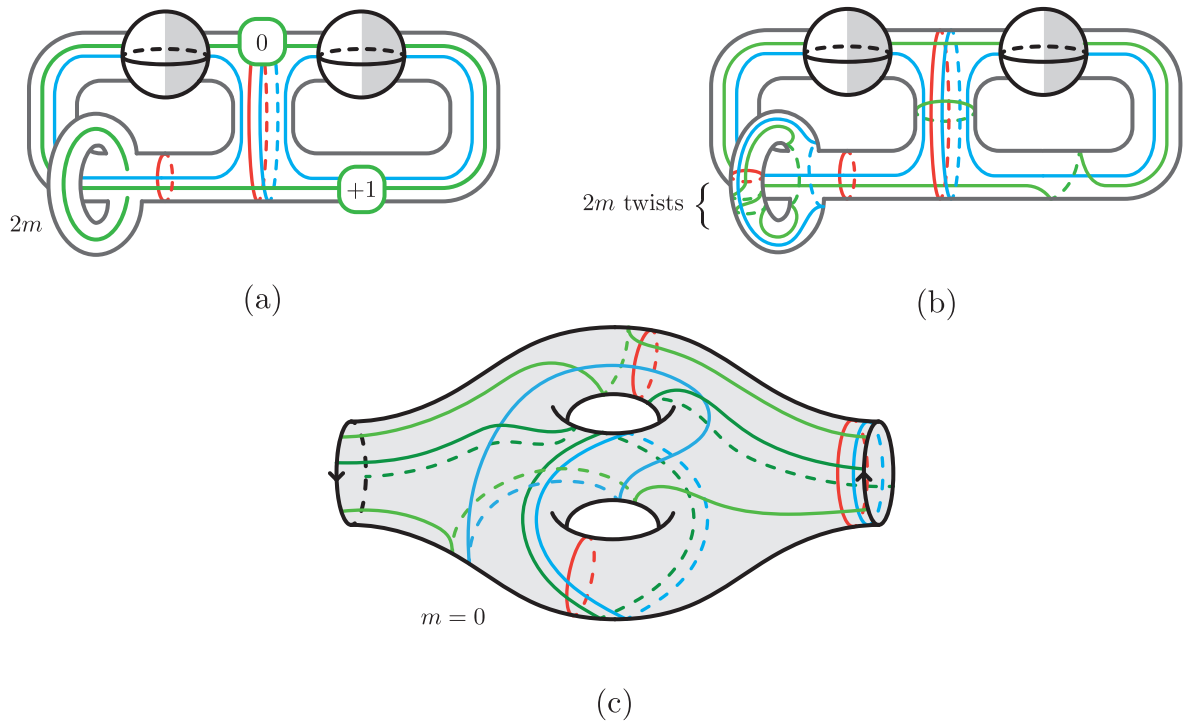

Figure 4.5: In (a) and (b), the process of arranging the 2–handle attaching curves to lie on a Heegaard surface for $S^2 \tilde{\times} S^1$ with surface framing. In (c), the case when $m = 0$. This is a $(3;1)$–trisection for $S^2 \tilde{\times} \mathbb{RP}^2$.

check that this trisection is handle slide diffeomorphic to the standard (balanced) stabilized trisection of S^4. For fun, we illustrate the sequence of handle slides and destabilizations in Figure 4.7.

Remark 4.2.5. As an interesting application of of Example 4.2.4, consider the Cappell-Shaneson homotopy 4–spheres [9], some of which double cover an exotic $\mathbb{RP}^4$. By lifting a trisection of such an exotic $\mathbb{RP}^4$, one would obtain a trisection of a Cappell-Shaneson homotopy 4–sphere. It remains an open question whether Cappell-Shaneson homotopy 4–spheres are always diffeomorphic to S^4, and so this could be useful as a possible technique for standardizing these manifolds.

This also has applications to Question 2.2.8; some Cappell-Shaneson homotopy spheres *are* known to be standard. By taking the double cover of a trisection of such an exotic $\mathbb{RP}^4$, we obtain a trisection of S^4 which at least cannot be equivariantly destabilized to the $(0;0)$–trisection. Since Question 2.2.8 is related to the Andrew-Curtis conjecture it

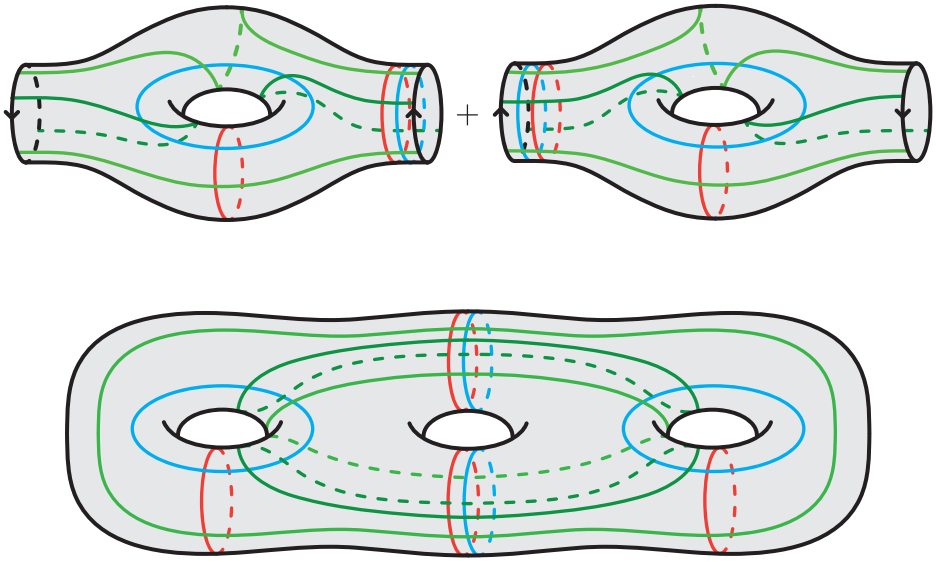

Figure 4.6: The double cover of the $(2;1)$–trisection of $\mathbb{RP}^4$.

is likely difficult to decide whether such a trisection is standard, but this construction produces many examples to test.

Explicitly obtaining a trisection of a homotopy $\mathbb{RP}^4$ (or S^4) is likely to be difficult. It would be particularly interesting to investigate whether any of the invariants use to distinguish the manifolds in [9] can be computed from a trisection diagram (although this is also likely to be very hard).

Question 4.2.6. Consider the trisections of S^4 which arise as double covers of an exotic $\mathbb{RP}^4$. Are these trisections standard?

A related question is whether one can use trisection diagrams to recover known results about exotic versions of $\mathbb{RP}^4$.

Question 4.2.7. Can trisection diagrams (or trisection genus) distinguish exotic non-orientable 4–manifolds?

We end this section with one last question. We will call a genus two trisection of a non-orientable 4–manifold *standard* if it is either reducible or the trisection of $\mathbb{RP}^4$ above.

Question 4.2.8. Are all genus two non-orientable trisections standard?

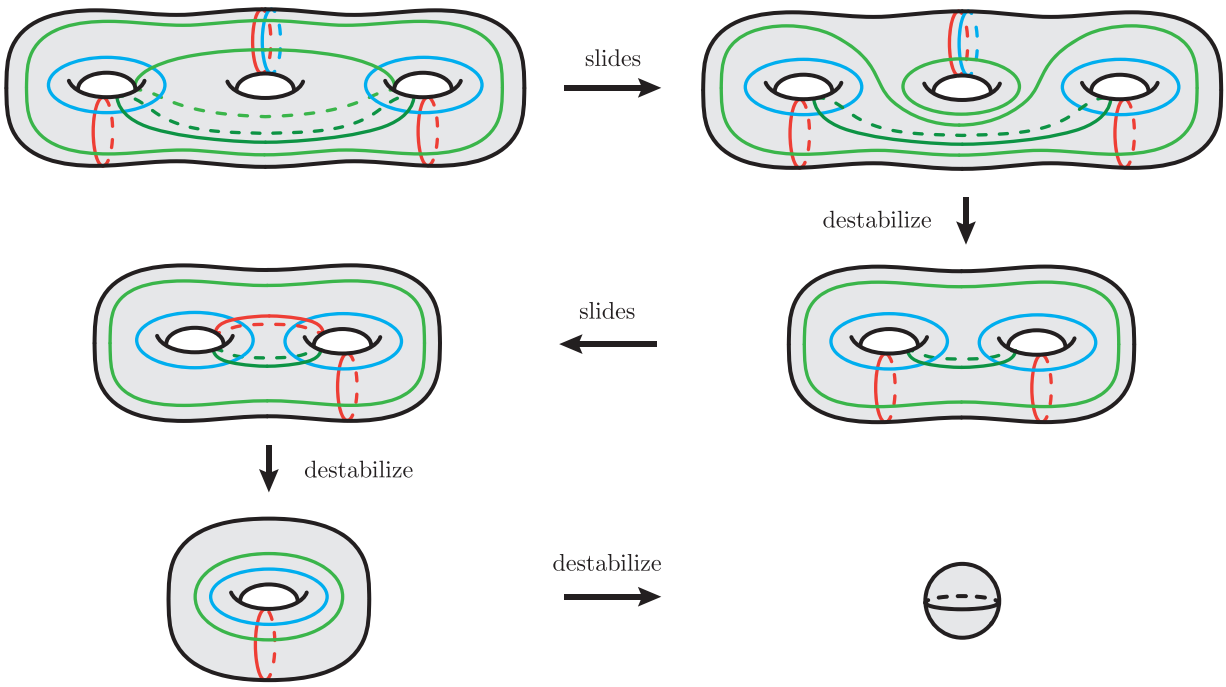

Figure 4.7: A sequence of handle slides and destabilizations that show that the $(3;1)$–trisection of S^4 arising as the double cover of the $(2;1)$–trisection of $\mathbb{RP}^4$ is standard.

Remark 4.2.9. The unique non-orientable $(2;2)$–trisection is a reducible trisection of $\#^2 S^3 \tilde{\times} S^1$, i.e. a connected sum of two genus one trisections of $S^3 \tilde{\times} S^1$. Indeed, in this case any pair (and hence all three) curves may be standardized simultaneously. Since there are no non-orientable $(2;0)$–trisections, Question 4.2.8 is specifically a question about $(2;1)$–trisections.

In the orientable case, we know that $(2;1)$–trisections are reducible by [57]. The main tool is the following theorem of Gabai [23], which guarantees that there are no non-trivial cosmetic surgeries of $S^2 \times S^1$.

Theorem 4.2.10 ([23])**.** *Suppose that K is a knot in $S^2 \times S^1$ with a cosmetic surgery. Then K is a (± 1)–framed unknot.*

However, we have seen that $S^2 \tilde{\times} S^1$ *does* admit at least one non-trivial cosmetic surgery (along the curve that wraps twice around the S^1 factor), a fact which produces the $(2;1)$–trisection of $\mathbb{RP}^4$. Whether or not this is the only cosmetic surgery is listed as a separate conjecture below, since it is likely interesting for other reasons. It would also be interesting

to see whether Conjecture 4.2.11 implies an positive answer to Question 4.2.8.

While $(2;0)$–trisections are known to be standard by [57], the proof uses deep results on Heegaard diagrams on genus two surfaces, and so may not have a non-orientable analogue. It also does not seem likely that Question 4.2.8 can be answered by lifting to the orientation cover. This would produce a $(3;1)$ trisection of an orientable 4–manifold, and these are only conjecturally classified by Meier [53]. In particular, it is not presently known if every $(3;1)$–trisection of S^4 is standard.

Conjecture 4.2.11. Suppose that K is a knot in $S^2 \tilde{\times} S^1$ with a cosmetic surgery. Then K is either a (± 1)–framed unknot, or the curve which wraps twice around the S^1 with (± 1)–framing.

At this point, the reader might believe that most orientable 3–manifold theorems carry over verbatim to the non-orientable setting. This conjecture illustrates that there are at least some differences.

4.3 Relative trisections

In this section, we will discuss relative trisections of 4–manifolds with boundary. This subject has been studied by several authors (e.g. see [12], [13], [14], [24]) in the orientable case. While the treatment is quite similar, the aim of this section is to give some self-contained exposition of the subject that also covers the non-orientable case. We will include proofs when they differ from the orientable case, but otherwise refer the reader to [12] and focus on new examples. For simplicity, we will *not* treat the case of multiple boundary components.

As an analogue for Heegaard splittings in the closed case, we will first discuss *compression bodies*. Using this language, we will construct specific decompositions of 4–dimensional handlebodies to use as the main building blocks for a trisection. One key feature of relative trisections is the *gluing theorem*, proved by Castro in his thesis: under sufficient conditions one can uniquely glue two relative trisections to obtain a trisected closed 4–manifold.

4.3.1 Compression bodies and definitions

Definition 4.3.1. Suppose that Σ is a connected surface with non-empty boundary. A *compression body* on Σ is a 3–manifold C obtained by attaching 3–dimensional 2–handles

to a thickening of Σ, i.e.

$$C = \Sigma \times [0,1] \cup_{\Sigma \times \{1\}} \{\text{3–dimensional 2–handles}\}.$$

The boundary of C decomposes as $\partial C = (\partial_- \Sigma) \cup (\partial \Sigma \times [0,1]) \cup (\partial_+ \Sigma)$, where

$$\partial_- C = \Sigma \times \{0\},$$

and

$$\partial_+ C = \partial \Sigma \setminus (\partial_- \Sigma \cup \partial \Sigma \times (0,1)).$$

We will assume that $\partial_+ C$ is connected unless otherwise indicated.

Note. Let C be a compression body. It is not hard to check that $C \times I \cong \natural^k B^3 \times S^1$ if C is orientable, and $C \times I \cong \natural^k B^3 \tilde{\times} S^1$ if C is non-orientable, where

$$k = 1 - \frac{\chi(\partial_+ C) + \chi(\partial_- C)}{2} = g(\partial_- \Sigma) + g(\partial_+ \Sigma) + |\partial \Sigma| - 1.$$

Indeed, we can alternatively view C as constructed from $\partial_+(C) \times I$ by adding 3–dimensional 1–handles. Consequently, this is a sensible object to use as a building block for Heegaard splitting of 3–manifolds with boundary. We will refer to this as a *generalized* Heegaard splitting.

We will now describe specific decompositions of a 4–dimensional handlebody. Like the closed case, these will make up the sectors of a relative trisection.

Definition 4.3.2. Let Σ be a connected surface with non-empty boundary, and let C be a compression body on Σ. Note that $Z = C \times [0,1]$ is a 4–dimensional handlebody. We decompose $\partial Z = \partial_{\text{in}} Z \cup \partial_{\text{out}} Z$, where

$$\partial_{\text{in}} Z = (C \times \{0\}) \cup (\partial_- C \times [0,1]) \cup (C \times \{1\}),$$

and

$$\partial_{\text{out}} Z = (\partial \Sigma \times [0,1] \times [0,1]) \cup (\partial_+ C \times [0,1]).$$

Note that $\partial_{\text{in}} Z$ admits a (generalized) Heegaard splitting as $\partial_{\text{in}} Z = Y_0^- \cup Y_0^+$, where

$$Y_0^- = (C \times \{0\}) \cup (\partial_- C \times [0,1/2])$$

and

$$Y_0^+ = (\partial_- C \times [1/2,1]) \cup (C \times \{1\}).$$

In particular, the splitting surface is $Y_0^- \cap Y_0^+ = \partial_- C \times \{1/2\}$. Any Heegaard splitting of $\partial_{\text{in}} Z$ obtained from this one by stabilization is called *standard*.

Note. In what follows, C will always denote a compression body on a surface Σ and Z will always denote $C \times I$. Whenever we write $\partial_{\text{in}} Z = Y^- \cup Y^+$, we mean that (Y^-, Y^+) is a standard splitting of $\partial_{\text{in}} Z$.

A diagram (i.e. a depiction of a model surface with standard 2–handle attaching curves) for this generalized Heegaard splitting is given in Figure 4.8 in the next section. With these models in mind, we can now define a relative trisection.

Definition 4.3.3. Let X be a smooth, compact, and connected 4–manifold with connected non-empty boundary. A relative trisection $\mathcal{T}$ of X is a a decomposition $X = X_1 \cup X_2 \cup X_3$ such that:

- There are diffeomorphisms $\phi_i : X_i \to Z$ such that $\phi_i(X_i \cap \partial X) = \partial_{\text{out}} Z$,
- For each i, $\phi_i(X_i \cap X_{i-1}) = Y^-$ and $\phi_i(X_i \cap X_{i+1}) = Y^+$.

In the literature, this often referred to as a $(g, k; p, b)$–relative trisection, where $g = g(X_1 \cap X_2 \cap X_3)$, $p = g(\partial_+ C)$, and $b = |\partial \Sigma|$. Depending on the author, the integer k is either the genus of the handlebody Z or the number of S^2–bundle summands in $\partial_{\text{in}} Z$. Since it is usually clear, we will generally avoid giving these parameters unless necessary.

4.3.2 Gluing relative trisections

At first glance, the definition of a relative trisection seems quite technical. However, one of the main features of these decompositions is that they induce a particularly nice structure on the boundary.

Proposition 4.3.4. *Suppose that $\mathcal{T}$ is a relative trisection of X. Then $\mathcal{T}$ induces a natural open book decomposition on ∂X.*

Proof. Let the sectors of $\mathcal{T}$ be X_1, X_2, and X_3, and note that $L := \partial(X_1 \cap X_2 \cap X_3)$ is a link in ∂X. By definition, $\phi_i(X_i \cap \partial X) = \partial_{\text{out}} Z = (\partial \Sigma \times I \times I) \cup (\partial_+ C \times I)$. Consequently, $X_i \cap \partial X$ consists of a tubular neighbourhood of L together with a thickened Seifert surface for L. Piecing these together, we see that $\partial X \setminus \nu(L)$ fibers over S^1, and that $X_i \cap X_{i+1} \cap (\partial X \setminus \nu(L))$ is a fiber for each i. In other words, L is the binding of an open book for ∂X for which each $X_i \cap X_{i+1}$ is a page. □

When X is orientable, then given an open book $\mathcal{O}$ on ∂X, there is a trisection of X inducing $\mathcal{O}$ [12]. Moreover, trisections that induce the *same* open book can be made isotopic after some number of *interior* stabilizations, i.e. stabilizations in the sense of Definition 2.1.3.

Theorem 4.3.5 ([24])**.** *Suppose that $\mathcal{T}_1$ and $\mathcal{T}_2$ are relative trisections of a 4–manifold X inducing isotopic open books on ∂X. Then after some number of interior stabilizations of each, $\mathcal{T}_1$ and $\mathcal{T}_2$ are isotopic.*

While Theorem 4.3.5 was only originally stated in the orientable case, the proof carries over verbatim, and so we will not discuss it here. The idea is to convert $\mathcal{T}_1$ and $\mathcal{T}_2$ to relative handle decompositions, and carry out the same proof of uniqueness as the closed case.

Remark 4.3.6. In the orientable case, there is a set of moves that relate trisections inducing *different* open books. Relative trisections inducing different open books are related by interior stabilization, relative double twists [15], and relative stabilization [12], in that order. For the definitions of these operations, see the cited papers.

However, this uniqueness result relies heavily on the classification of open books on orientable 3–manifolds and work of Giroux-Goodman. To prove such a result in the non-orientable case, one would need to find a complete set of moves relating any two open books of non-orientable 3–manifolds. Ozbagci [63] has shown that there are non-orientable open books that are *not* related by Hopf stabilization, and so in general any two relative trisections are not related by just interior and relative stabilizations in the above sense. In particular, there is a genus two open book decomposition on $\mathbb{RP}^2 \times S^1$ whose monodromy is a cross-cap transposition. It would be interesting to explicitly see this monodromy induced by a relative trisection.

Question 4.3.7. What moves are necessary to relate relative trisections of (possibly non-orientable) 4–manifolds? Is the cross-cap slide monodromy from [63] ever induced by a relative trisection?

One of the most important results on relative trisections is the *gluing theorem*, proved by Castro in his thesis. Essentially, under suitable conditions, relative trisections of two 4–manifolds can be naturally glued together.

Theorem 4.3.8 ([12])**.** *Let $\mathcal{T}$ and $\mathcal{T}'$ be relative trisections of 4–manifolds X and X', respectively. Let $\mathcal{O}$ and $\mathcal{O}'$ denote the open books of ∂X and $\partial X'$ (respectively) induced by $\mathcal{T}$ and $\mathcal{T}'$. Suppose there exists a diffeomorphism $f : \partial X \to \partial X'$ and that $f(\mathcal{O})$ is isotopic to $\mathcal{O}'$. Then there is a naturally induced trisection $\mathcal{T} \cup \mathcal{T}'$ of $X \cup_f X'$.*

While Castro only stated this theorem in the orientable setting, it carries over verbatim so we omit the proof.

4.3.3 Diagrams for relative trisections

As in the closed case, relative trisections can be represented by diagrams. We first define a *standard* set of curves.

Definition 4.3.9. Let Σ be a (possibly non-orientable) surface of genus g, and that α and β are cut systems for Σ. We say that the pair (α, β) is standard if there is a homeomorphism of Σ taking α to the red curves, and β to the blue curves in Figure 4.8. We say that the pair (α, β) is *slide-standard* if there is a pair (α', β') slide-equivalent to (α, β) which is standard.

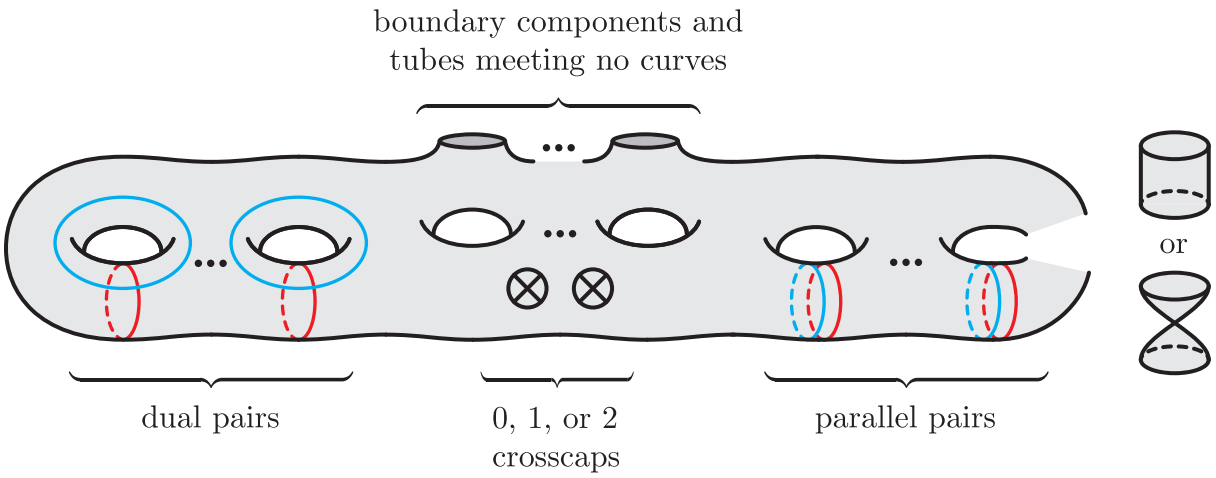

Figure 4.8: A slide-standard set of curves on a (possibly non-orientable) surface with boundary.

Lemma 4.3.10. *Let (α, β) be a slide-standard pair of cut systems on a surface Σ. Then $(\Sigma; \alpha, \beta)$ determines a standard splitting $\partial_{\text{in}} Z = Y^- \cup Y^+$.*

Proof. Let $V = \Sigma \times I \cup H_\alpha \cup H_\beta$, where H_α are 2–handles attached along $\alpha \times \{0\}$ and H_β are 2–handles attached along $\beta \times \{1\}$. Moreover, let $Y^- = H_\alpha \cup (\Sigma \times [0, 1/2])$ and $Y^+ = (\Sigma \times [1/2, 1]) \cup H_\beta$.

Then $V \cong \partial_{\text{in}} Z$, where $Z = C \times I$ and C is a compression body on a surface Σ' with $\chi(\Sigma') = \chi(\Sigma)+2n$ and $|\partial\Sigma'| = |\partial\Sigma|$, where n is the number of pairs of dual α, β curves. The surface Σ' is orientable if and only if Σ is orientable. Lastly, the pair (Y^-, Y^+) is obtained by stabilizing (Y_0^-, Y_0^+) a total of n times, and so is a standard splitting of $\partial_{\text{in}} Z$. □

Definition 4.3.11. A relative trisection diagram $\mathfrak{D}$ is a tuple $(\Sigma; \alpha, \beta, \gamma)$, where Σ is a (possibly non-orientable) connected surface of genus g with $b > 0$ boundary components, and each of (α, β),(β, γ), (γ, α) are slide-standard pairs.

Castro–Gay–Pinzón-Caicedo proved the following proposition in the orientable case. The proof here is essentially the same. Since we use Theorem 3.1.1 we include a short proof for convenience. The experienced reader may simply refer to Figure 4.9.

Proposition 4.3.12. *A relative trisection diagram $\mathcal{D} = (\Sigma; \alpha, \beta, \gamma)$ determines a relatively trisected 4–manifold $X(\mathfrak{D})$ up to diffeomorphism.*

Proof. We will proceed as in the closed case. Beginning with $\Sigma \times D^2$, let W be the 4–manifold obtained by attaching $H_\alpha \times I$, $H_\beta \times I$, and $H_\gamma \times I$ to neighbourhoods of $\Sigma \times \{1\}$, $\Sigma \times \{e^{2\pi i/3}\}$, and $\Sigma \times \{e^{4\pi i/3}\}$ respectively, where we view $D^2 \subset \mathbb{C}$. Denote the image of $H_* \times \{0\}$ by H_*^-, and the image of $H_* \times \{1\}$ by H_*^+, as illustrated in Figure 4.9

The resulting 4–manifold has 3–boundary components. The component $\partial W \cap (\Sigma \times [0, 2\pi/3] \cup H_\alpha^+ \cup H_\beta^-)$ is diffeomorphic to $\partial_{\text{in}} Z$ and determines a standard splitting (Y^-, Y^+). Consequently, there is a well-defined way to glue in a compression body Z_1 along this boundary component. Similarly, we may fill in the other two boundary components with compression bodies Z_2 and Z_3.

After gluing in three copies of Z, the resulting 4–manifold has a single boundary component. To see the relative trisection explicitly, consider the pieces

- $X_1 = \Sigma \times (\{0 \leq \theta \leq 2\pi/3\} \subset D^2) \cup Z_1$;
- $X_2 = \Sigma \times (\{2\pi/3 \leq \theta \leq 4\pi/3\} \subset D^2) \cup Z_2$;
- $X_3 = \Sigma \times (\{4\pi/3 \leq \theta \leq 0\} \subset D^2) \cup Z_3$.

This completes the proof. □

Conversely, every relative trisection induces a relative trisection diagram.

Proposition 4.3.13. *Let $\mathcal{T}$ be a relative trisection of a 4-manifold X. Then $\mathcal{T}$ determines a relative trisection diagram $(\Sigma; \alpha, \beta, \gamma)$ up to slides of α, β, γ and automorphisms of Σ.*

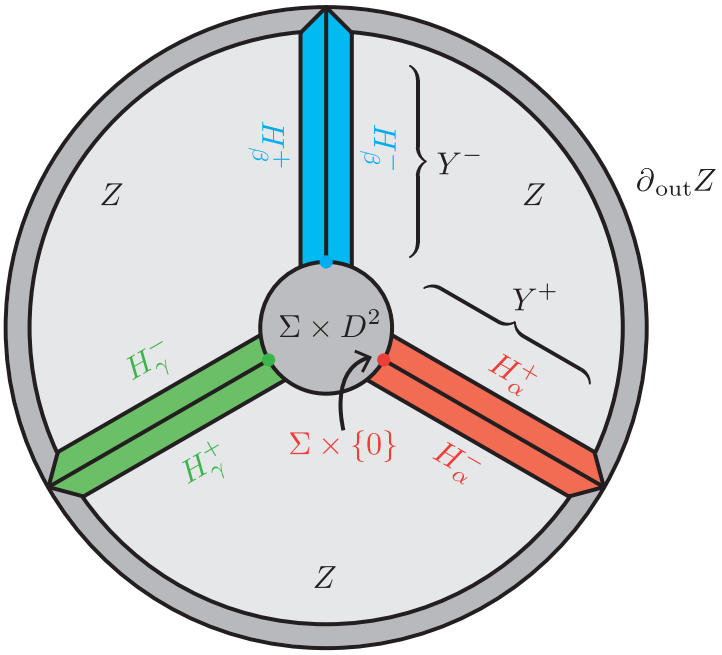

Figure 4.9: A schematic that describes how to build a relative trisection from a diagram. The process is similar to the closed case. The 4–dimensional compression bodies can be attached uniquely because the curves are slide-standard.

Proof. Let $\Sigma = X_1 \cap X_2 \cap X_3$. By definition, there is a diffeomorphism $\phi_i : X_i \to Z$, with $\phi_i(X_i \cap X_{i+1}) = Y^+$. Moreover, Y^+ is obtained by attaching 2–handles to $\phi_i(\Sigma) \times I$. Denote the corresponding attaching curves for the 2–handles on Σ by α, β, and γ respectively.

Since $\phi_1(X_3 \cap X_1) = Y^-$ and $\phi_1(X_1 \cap X_2) = Y^+$, the surface Σ determines a standard splitting of $\phi^{-1}(\partial_{\text{in}}Z)$, and so (γ, α) is a slide-standard pair. Similarly, (α, β) and (β, γ) are slide-standard. □

Remark 4.3.14. Proposition 4.3.12 illustrates a major difference between closed and relative trisections. In the closed case, it was enough to know that each pair of curves described a Heegaard diagram for $\#S^2 \times S^1$ or $\#S^2 \tilde{\times} S^1$, because Theorem 3.0.1 (or Theorem 3.1.1) guarantees that 4–dimensional handlebodies can be attached uniquely in this case. By a version Waldhausen's theorem we also know that the curves will be standardizeable. Because there is no analogue of either of these theorems for compression bodies, we need to assume that the curves are slide-standard to begin with.

This is one reason that the definition of a relative trisections is considerably more

technical. Practically, one would like a trisection diagram to produce a trisected 4–manifold to up to diffeomorphism, and vice versa. One might attempt to define a relative trisection of a 4–manifold X as in the closed case: a decomposition of X into three handlebodies X_1, X_2, X_3 which pairwise intersect in handlebodies, and so that the neatly embedded surface $X_1 \cap X_2 \cap X_3$ is the binding of an open book decomposition of ∂X (with pages $X_i \cap X_j$). While this turns out to be enough to glue relative trisections together, it is not enough to ensure a diagrammatic theory.

Like the closed case, we conclude with the standard bijection between relative trisections and relative trisection diagrams.

Corollary 4.3.15. *There is a natural bijection*

$$\frac{\{\textit{relative trisection diagrams}\}}{\textit{surface automorphism, slides}} \leftrightarrow \frac{\{\textit{relatively trisected 4-manifolds}\}}{\textit{diffeomorphism}}.$$

As in the closed case, we remark that diagrams only represent relative trisections of 4–manifolds up to diffeomorphism, and as such do not record information about isotopy of these decompositions.

4.3.4 Some new examples

In this section, we give some examples of non-orientable relative trisections and their diagrams.

Example 4.3.16 (Diagrams on a punctured $\mathbb{RP}^2$)**.** The simplest possible (non-orientable) relative trisection diagram is pictured in Figure 4.10 (a) (when $n = 0$); this is the diagram $(M, \emptyset, \emptyset, \emptyset)$, where M is the Möbius band. Since there are no non-separating curves on M with an annular neighbourhood, this is the unique diagram on the Möbius band. By Proposition 4.3.12 we see that this describes the manifold $M \times D^2 \cong B^3 \tilde{\times} S^1$.

If we add some number of boundary components to M, we still get a valid relative trisection diagram $(M_n; \emptyset, \emptyset, \emptyset)$, where M_n denotes the Möbius band with n open disks removed. Once again, this is the unique diagram on M_n, and via the same argument as above, we see that this diagram describes $M_n \times D^2 \cong \natural^{n+1} B^3 \tilde{\times} S^1$.

Example 4.3.17 (Diagrams on a punctured Klein bottle)**.** Let K_n denote the Klein bottle with $n \geq 1$ open disks removed. There is only one non-separating curve on K_n with an

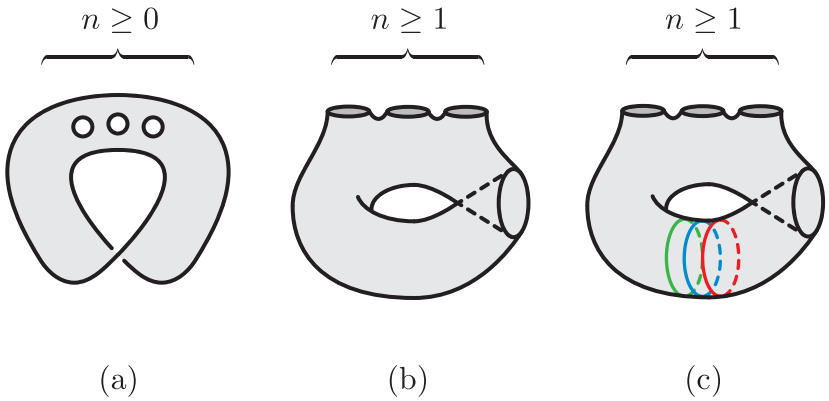

Figure 4.10: Three examples of simple relative trisection diagrams. In (a) and (b), diagrams for $\natural^{n+1} B^3 \tilde{\times} S^1$. In (c), a diagram for $(S^3 \tilde{\times} S^1 \setminus B^4) \natural (\natural^{n-1} B^3 \tilde{\times} S^1)$.

annular neighbourhood (which we will denote by c), and so there are two possible relative trisection diagrams on K_n: the diagram $(K_n; \emptyset, \emptyset, \emptyset)$ with no curves (Figure 4.10 (b)) and the diagram $(K_n; c, c, c)$ (Figure 4.10 (c)). It is easy to see that these are diagrams of $K_n \times D^2 \cong \natural^{n+1} B^3 \tilde{\times} S^1$ and $(S^3 \tilde{\times} S^1 \setminus \mathring{B}^4) \natural (\natural^{n-1} B^3 \tilde{\times} S^1)$.

Example 4.3.18 (A diagram of $D^2 \tilde{\times} \mathbb{RP}^2$)**.** Another irreducible trisection diagram is of $D^2 \tilde{\times} \mathbb{RP}^2$, pictured in Figure 4.11 below.

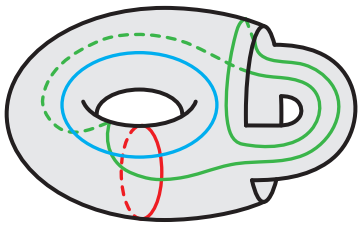

Figure 4.11: A relative trisection of $D^2 \tilde{\times} \mathbb{RP}^2$. The induced open book has Mobiüs band pages and trivial monodromy.

The α, β, and γ curves are each dual. We can use the algorithm of the next section to extract a Kirby diagram to verify that this diagram does indeed describe $D^2 \tilde{\times} \mathbb{RP}^2$.

The page of the induced open book decomposition on $S^2 \tilde{\times} S^1$ is a Möbius band, and the induced monodromy is trivial. In particular, it is the same as the induced monodromy of $(M; \emptyset, \emptyset, \emptyset)$ from Example 4.3.16. By the gluing theorem for diagrams in the next section,

we can "glue" these two diagrams and recover the familiar decomposition

$$D^2 \tilde{\times} \mathbb{RP}^2 \cup_{S^2 \tilde{\times} S^1} B^3 \tilde{\times} S^1 = \mathbb{RP}^4.$$

Example 4.3.19 (Puncturing closed diagrams)**.** In general, if $(\Sigma; \alpha, \beta, \gamma)$ is a trisection diagram for a closed 4–manifold X, then the diagram $(\Sigma^\circ; \alpha, \beta, \gamma)$ is a relative trisection diagram for $X \setminus B^4$, where Σ° denotes Σ with a small open disk removed. In fact, there is a unique diagram (up to slides and surface automorphism) determined by removing an open disk from Σ. The induced open book on $\partial X^\circ = S^3$ is the trivial one, with the unknot binding and disk pages. For example, the diagram in Figure 4.12 describes $\mathbb{RP}^4 \setminus B^4$ (rather than $\mathbb{RP}^4 \setminus B^3 \tilde{\times} S^1$ as above).

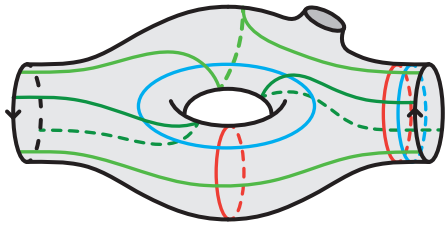

Figure 4.12: A relative trisection diagram for $\mathbb{RP}^4 \setminus \text{int} B^4$.

If $K \subset X$ is an embedded 2–sphere in *2–bridge position*, then there is a diagram for $X \setminus \nu(K)$ which can be obtained by removing two open disks from a trisection diagram for X. For example, the diagram in Figure 4.13 describes the complement of a neighbourhood of a 2–sphere fiber in $S^2 \tilde{\times} \mathbb{RP}^2$.

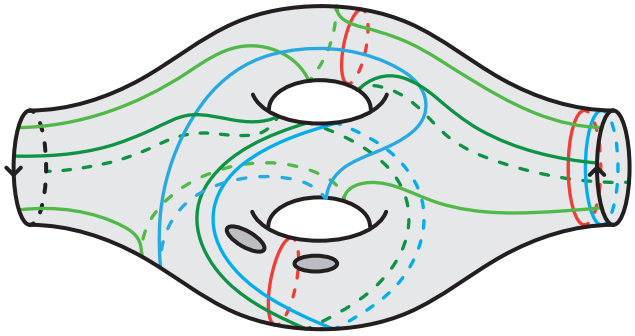

Figure 4.13: A relative trisection diagram for the complement of a fiber in $S^2 \tilde{\times} \mathbb{RP}^2$.

For more details on bridge position, see §2.3.2 and §4.4.

4.3.5 Gluing diagrams

In this section, we discuss the monodromy algorithm for gluing relative trisections, which works essentially the same as in the orientable case. Consequently, we will give the algorithm precisely and illustrate it with some non-orientable examples. Figure 4.14 contains an illustration which is likely more helpful than the ensuing wall of text.

Algorithm 4.3.20 (Monodromy algorithm)**.** The monodromy algorithm of [13] provides a way to compute the monodromy of the open book induced by a relative trisection diagram $(\Sigma; \alpha, \beta, \gamma)$. We compute the monodromy ϕ as an automorphism of the "α page" $P_\alpha := X_1 \cap X_3 \cap \partial X$ by identifying P_α with the result of compressing Σ along α.

- **Step 0.** Standardize the α β curves. Let a be a collection of disjoint properly embedded arcs in Σ, disjoint from α and from β, so that compressing $\Sigma \setminus (\nu(a))$ along α or along β yields a disk. (We say that a is a *cut system of arcs* for α and β).
- **Step 1.** Do slides of β, γ curves and slide a over β as necessary so that the arcs a are transformed into arcs c that are disjoint from γ. Note that the arcs c might intersect α many times. If β and γ are standard then we can avoid slides of β, γ curves, but otherwise we may have to perform many slides before obtaining c.
- **Step 2.** Let α' be another copy of α. Do slides of γ, α' curves and slide c over γ as necessary until transforming c into arcs a' that are disjoint from α'.
- **Step 3.** In practice, α' usually agrees with α. However, we may have performed many slides. Now undo the slides to α' from the previous step to make α' again agree with α while simultaneously sliding a' to remain disjoint from α'. The monodromy ϕ is now described by $\phi(a) = a'$.

For a first example, consider the well-known relative trisection for B^4 in Figure 4.14 below. This relative trisection induces the Hopf open book on S^3, i.e. has annular pages and monodromy equal to a left- (or right)-handed Dehn twist about the core of the annulus.

Monodromy calculations for non-orientable diagrams tend to be somewhat more complicated than their orientable counterparts, but simple non-orientable examples are illustrated in Figure 4.15 below. In particular, we can check that the monodromy of the open book on $S^2 \tilde{\times} S^1$ induced by the diagram in Figure 4.11 is indeed trivial. Note that while this diagram looks similar to the diagram for a punctured $\mathbb{RP}^4$, it is *not* the same. The page of the induced open book is a punctured Klein bottle, rather than a disk.

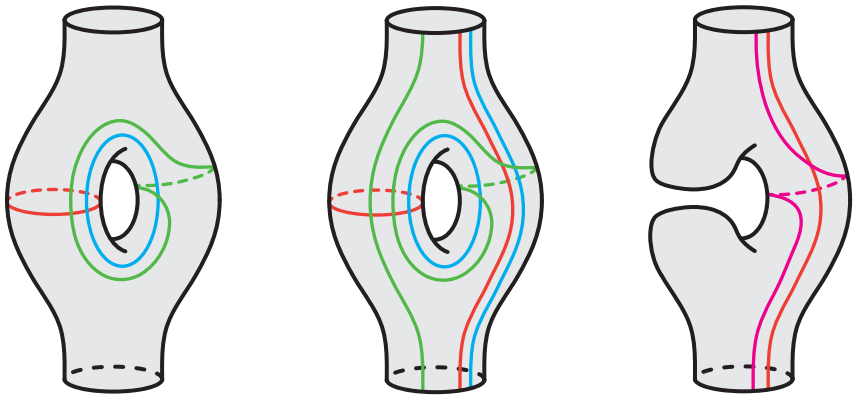

(a) (b) (c)

Figure 4.14: In (a), a well-known relative trisection diagram for B^4. In (b), the diagram is completed with arcs using Algorithm 4.3.20. In (c), the monodromy on the page P_α is a left-handed Dehn twist.

One of the most useful features of the monodromy algorithm is that it allows us to glue relative trisection diagrams. Let $\mathcal{D}_1 = (\Sigma_1, \alpha_1, \beta_1, \gamma_1)$ and $\mathcal{D}_2 = (\Sigma_2, \alpha_2, \beta_2, \gamma_2)$ be relative trisection diagrams of 4–manifolds X, Y inducing open books $\mathcal{O}_1, \mathcal{O}_2$ on $\partial X, \partial Y$ respectively. Assume there exists a homeomorphism ϕ from ∂X to ∂Y taking the pages of $\mathcal{O}_1$ to the pages of $\mathcal{O}_2$. In this case, we say that $\mathcal{D}_1$ and $\mathcal{D}_2$ are *gluable*.

By Theorem 4.3.8, we know that there is a naturally induced trisection of $X \cup_f Y$. In fact, we can glue the relative trisection diagrams in the following way. We begin by choosing a cut system of arcs a_1 in Σ_1 in the complement of α_1, as in Algorithm 4.3.20. We perform the monodromy algorithm to obtain arcs b_1 disjoint from β_1 (if α, β are not already standardized, in which case we can simply choose a_1 so $a_1 = b_1$ as in Algorithm 4.3.20) and c_1 disjoint from γ. Take the map $\phi : \partial X \to \partial Y$ to take the α page of the trisection induced by $\mathcal{D}_1$ to the α page of the trisection induced by $\mathcal{D}_2$. Then $a_2 := \phi(a_1)$ can be viewed as a cut system of arcs in Σ_2 for α_2. We perform the monodromy algorithm again in Σ_2 to obtain arcs b_2 disjoint from β_2 and c_2 disjoint from γ_2.

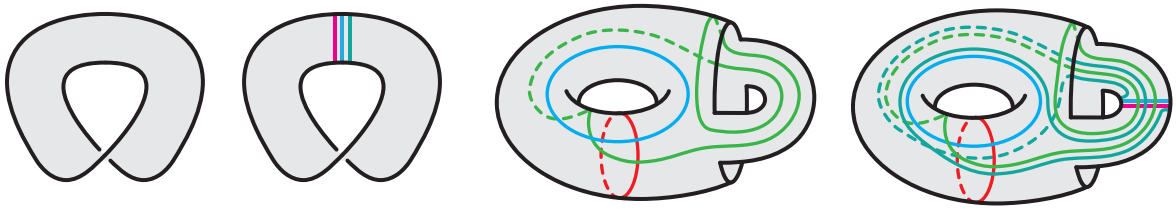

Figure 4.15: An illustration of the monodromy algorithm in two simple examples. **Left:** The monodromy induced by the diagram $(M;\emptyset,\emptyset,\emptyset)$ is trivial; the arc remains unchanged at each step. **Right:** The monodromy of the open book on $S^2 \tilde{\times} S^1$ induced by the genus one diagram for $D^2 \tilde{\times} \mathbb{RP}^2$ is also trivial, but the arcs produced by the algorithm are illustrated. The reader may wish to check that the monodromy is trivial by completing the last step of the monodromy algorithm.

Let $\Sigma := \Sigma_1 \cup_\partial \Sigma_2$, using ϕ to identify boundary components of Σ_1, Σ_2, and set

$$\begin{aligned} \alpha &:= \alpha_1 \cup \alpha_2 \cup (a_1 \cup a_2), \\ \beta &:= \beta_1 \cup \beta_2 \cup (b_1 \cup b_2), \\ \gamma &:= \gamma_1 \cup \gamma_2 \cup (c_1 \cup c_2). \end{aligned}$$

Then $(\Sigma;\alpha,\beta,\gamma)$ is a trisection diagram for $X \cup_\phi Y$.

Using the monodromy computed in Figure 4.15, we give various examples of this gluing operation in Figure 4.16. The simplest application of this procedure is to simply double a trisected 4–manifold with boundary, which we illustrate here. Some non-trivial examples of surgery along surfaces are illustrated in [40].

Remark 4.3.21. As in the closed case, there is an algorithm to convert a relative trisection diagram into a Kirby diagram containing a page of the induced open book decomposition of the boundary. This is described in the orientable case in [13], as well as [33]. Given a Kirby diagram together with a page of the induced open book, can also produce a relative trisection diagram inducing the given open book [14]. These algorithms work essentially the same way, except for the presence of non-orientable 1–handles. We will not use these algorithms in this thesis, and instead refer the reader to [59] for some examples if desired.

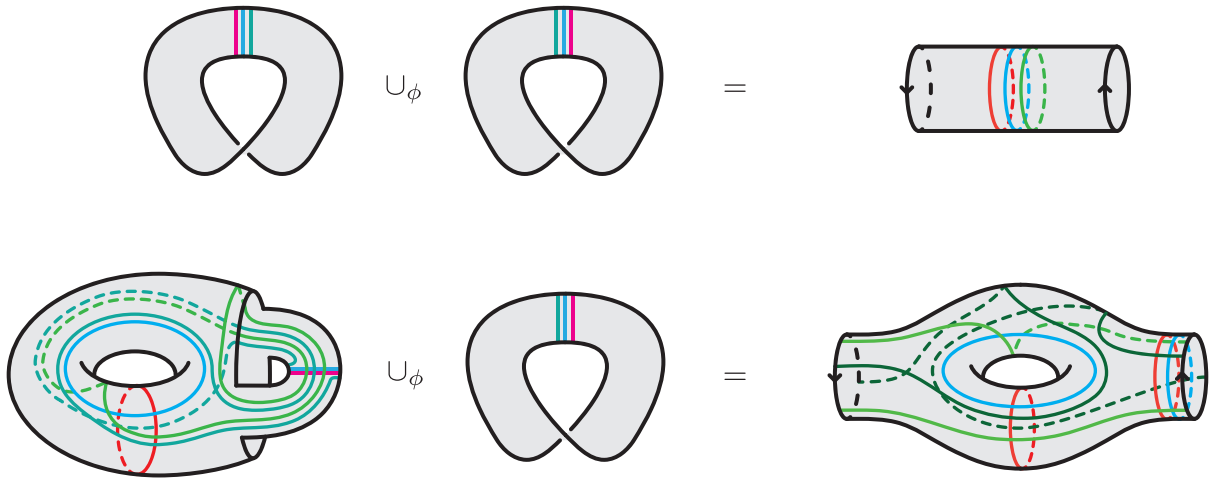

Figure 4.16: **Top:** We obtain a trisection diagram for $S^3 \tilde{\times} S^1$ by doubling a diagram for $B^3 \tilde{\times} S^1$. **Bottom:** We obtain a trisection diagram for $\mathbb{RP}^4$ by gluing diagrams for $D^2 \tilde{\times} \mathbb{RP}^2$ and $B^3 \tilde{\times} S^1$. It is easy to check that this diagram is slide equivalent to the one in Example 4.2.2. Note that we could also double the diagram for $D^2 \tilde{\times} \mathbb{RP}^2$ to obtain a diagram for $S^2 \tilde{\times} \mathbb{RP}^2$.

4.4 Bridge trisections

In this section, we give some self-contained treatment of bridge trisections with respect to non-orientable 4–manifolds. As in §4.3, the goal will be to give some exposition that does not depend on orientability. We will fill in any necessary gaps, but refer the reader to existing literature when the proofs carry over unchanged.

Bridge trisections are a 4–dimensional version of the notion of a bridge splitting of a knot in S^3.

Definition 4.4.1. A knot $K \subset S^3$ is said to be in *b–bridge position* if K intersects the equatorial $S^2 \subset S^3$ in $2b$ points, and each 3–ball in b boundary parallel arcs.

Equivalently, local minima of K appear before local maxima with respect to the radial height function. In fact, this definition makes sense with respect to a Heegaard splitting of any 3–manifold: if M admits a Heegaard splitting along the surface Σ, then $K \subset M$ is in b–bridge position if $K \cap \Sigma$ is $2b$ discrete points, and $K \cap (M \setminus \Sigma)$ consists of boundary parallel arcs.

Meier and Zupan showed that knotted surfaces in 4–manifolds admit analogous decompositions with respect to a trisection. After giving the basic definitions, we will sketch how to modify their existence proof for non-orientable 4–manifolds, and give some examples. Hughes, Kim and Miller have shown that bridge trisections for a fixed surface in a trisected 4–manifold are unique up to a suitable perturbation operation. Similarly, we will show how their proof can be modified to work in the non-orientable setting.

4.4.1 Definitions and diagrams

A collection $\mathcal{D}$ of properly embedded disks in a handlebody X is called *trivial* if the disks in $\mathcal{D}$ are simultaneously boundary parallel. The following lemma is well-known in the orientable case, but we give a short proof here.

Lemma 4.4.2. *Suppose that X is a (possibly non-orientable) 4–dimensional handlebody, and that $U \subset \partial X$ is an unlink. Then L bounds a unique collection of boundary-parallel disks in X up to isotopy rel L.*

Proof. Suppose that $\mathcal{D}$ and $\mathcal{D}'$ are two sets of disks with $L = \partial\mathcal{D} = \partial\mathcal{D}'$, and let $\mathcal{S} \subset \partial X$ be a collection of 2–spheres with the property that surgering ∂X along $\mathcal{S}$ yields S^3. Since L is an unlink, we may isotope $\mathcal{S}$ so that $\mathcal{S} \cap L = \emptyset$.

If $R \subset \partial X$ is any 2–sphere, we can attach 3–and 4–handles to $\partial X \times I$ to build a 4–manifold $X' \cong X$ with $\partial X'$ and ∂X identified so that R bounds a 3–ball into X'. We conclude from [51] or Theorem 3.1.1 that there is a diffeomorphism rel boundary from X' to X, so R also bounds a 3–ball in X.

Using this fact, a standard innermost argument (using the fact that any 2–sphere bounds a ball in X) shows that we may assume that $\mathcal{S} \cap \mathcal{D} = \mathcal{S} \cap \mathcal{D}' = \emptyset$. Thus by cutting along $\mathcal{S}$, we reduce to the case that $X \cong B^4$. The result now follows from the corresponding result of Livingston in [52]. □

Definition 4.4.3 ([58])**.** Let X be a closed, connected 4–manifold, and suppose that X has a trisection $\mathcal{T}$ with sectors X_1, X_2, and X_3. Let $S \subset X$ be a smoothly embedded surface. A *bridge trisection* of S with respect to $\mathcal{T}$ is a decomposition $(X, S) = (X_1, \mathcal{D}_1) \cup (X_2, \mathcal{D}_2) \cup (X_3, \mathcal{D}_3)$, where

- $\mathcal{D}_i$ is a collection of c_i trivial (boundary parallel) disks;
- $\tau_{ij} = \mathcal{D}_i \cap \mathcal{D}_j$ is a collection of trivial (boundary parallel) arcs in $X_i \cap X_j$;
- $X_1 \cap X_2 \cap X_3 \cap S$ is a collection of $2b$ points.

Such a decomposition is called a $(b; c_1, c_2, c_3)$–bridge trisection of S with respect to $\mathcal{T}$, or if $c = c_1 = c_2 = c_3$, simply a $(b; c)$–bridge trisection.

Note that each pairwise union $\tau_{ij} \cup \tau_{jk}$ is an unlink in bridge position with respect to the Heegaard splitting $X_1 \cap X_2 \cap X_3$ of ∂X_i.

Example 4.4.4. For a brief illustration of this idea, consider the decomposition in Figure 4.17 (a), which describes three trivial tangles in 3-balls. Since the pairwise union of any two tangles is an unlink in S^3, this describes a bridge trisection of some surface with respect to the trivial $(0; 0)$–trisection of S^4.

One can easily check that this surface is orientable and has Euler characteristic equal to 0, and so this diagram describes a torus embedded in S^4. In fact, all tangles have been arranged to have no crossings, and so this torus is unknotted.

(a) (b)

Figure 4.17: In (a), a schematic of a bridge trisection of an unknotted torus in S^4. In (b), a shadow diagram for this same bridge trisection.

Note. If S is a surface in $(b; c_1, c_2, c_3)$–bridge position, then from the obvious cell decomposition induced on S we see that $\chi(S) = c_1 + c_2 + c_3 - b$.

A *shadow* for a trivial arc t in a handlebody H is an embedded arc $s \subset \partial H$, with the property that t and s are isotopic in H rel endpoints. A collection of trivial arcs may admit non-isotopic sets of shadows (in ∂H), but these are related by slides of one shadow over another and over curves bounding disks into H. Unless H is a 3–ball, it is usually much easier to draw shadows for trivial arcs in ∂H than to try to depict a tangle in H. A shadow diagram on S^2 for the unknotted torus is given in Figure 4.17 (b).

Trisection diagrams can be augmented to also record information about a bridge trisection.

Definition 4.4.5 ([58])**.** Let X be a closed, connected 4–manifold, and suppose that $S \subset X$ is a smoothly embedded surface. A $(g, k_i; b, c_i)$-*bridge trisection diagram* (or *shadow diagram*) for $S \subset X$ is a diagram $(\Sigma_g; \alpha, \beta, \gamma; s_\alpha, s_\beta, s_\gamma)$, where:

- $(\Sigma; \alpha, \beta, \gamma)$ is a $(g; k_i)$–trisection diagram with $2b$ additional marked points;
- The arcs s_α,s_β, and s_γ are three collections of b shadows for trivial tangles $t_\alpha \subset H_\alpha$, $t_\beta \subset H_\beta$, and $t_\gamma \subset H_\gamma$, respectively;
- The pairwise unions $t_\alpha \cup t_\beta$, $t_\beta \cup t_\gamma$, and $t_\gamma \cup t_\alpha$ are c_1–, c_2–, and c_3– component unlinks.

By Lemma 4.4.2, the trivial disks in a bridge trisection are completely determined by the tangles t_{ij} (or equivalently, shadows $s_{ij} \subset \Sigma$), and so this information completely describes a surface S obtained by capping off each collection of unlinks with disk systems.

When studying knotted surfaces in S^4, it is common practice to use tangle diagrams (each tangle is a subset of B^3, and so can be drawn as such). When working with more complicated trisections, we are forced to use shadow diagrams.

In [58], Meier and Zupan gave a proof of the existence of bridge trisections for surfaces in any trisected oriented 4–manifold. They also gave a proof of uniqueness in the following precise sense for bridge trisections in S^4. The general proof of uniqueness in this sense is due to Hughes-Kim-Miller [33]. We will refer the reader to [58] and [33] for more details. We state this theorem here with *no* assumptions on orientability.

Theorem 4.4.6. *Let $\mathcal{T}$ be a trisection of a closed, connected 4–manifold X, and let $S \subset X$ a smoothly embedded surface. Then S may be isotoped to be in bridge trisected position with respect to $\mathcal{T}$. Moreover, if S' is isotopic to S, then any two bridge trisections for S and S' become isotopic after some sequence of perturbations and de-perturbations.*

We define the perturbation operation in §4.4.3, and sketch of a proof of this theorem.

4.4.2 Existence and examples

The existence of bridge trisections follows from the existence of *banded unlink diagrams*, which we will briefly outline here.

Definition 4.4.7. Let X be a closed and connected 4–manifold, and let $S \subset X$ a smoothly embedded surface. A function $f : X \to \mathbb{R}$ is a *Morse function for the pair* (X, S) if f is Morse, and $f|_S : S \to \mathbb{R}$ is also Morse. Moreover, f is called *self-indexing* if the image of all index k critical points for f are contained in $f^{-1}(k)$. We will always assume that f has a unique index 0 critical points and a unique index 4 critical point.

By a mild isotopy of S in X, $f|_S$ may be assumed to be Morse, so we will always work with a Morse function of the pair (X, S). When necessary, we will also fix a gradient-like vector field ∇ for f.

The proof of existence of trisections (Theorem 2.1.4) shows that a Morse function $f : X \to \mathbb{R}$ induces a trisection $\mathcal{T}$ of X. In particular, we chose a Heegaard splitting of $\partial X_{[3/2]} = H \cup_\Sigma H'$ so that the attaching link L for the 2–handles of X is a core of H. The trisection is then defined by:

- $X_1 = X_{[0,3/2]} \cup H'_{[3/2,2]}$;
- $X_2 = H_{[3/2,5/2]} = X \setminus (X_1 \cup X_3)$;
- $X_3 = H'_{[2,5/2]} \cup X_{[5/2,4]}$.

In what follows, when we consider a trisection of X, we will implicitly assume it is the one induced by a specified Morse function in this way. See Chapter 2 for more details.

By an ambient isotopy of S away from the critical points of f, we can arrange for $f|_S$ to be self-indexing. We will additionally push all index 1 critical points of $f|_S$ into $X_{[3/2]}$. This is essentially the definition of a surface in banded unlink position; for more details see [33] or [58].

Definition 4.4.8. Let X be a 4–manifold, and let $f : X \to \mathbb{R}$ be a self-indexing Morse function. Let $S \subset X$ be a smoothly embedded surface. We say that S is in *banded unlink position* if:

- $f(S) = [1/2, 5/2]$;
- $S_{[1/2]} \cap X_{[1/2]}$ and $S_{[5/2]} \cap X_{[5/2]}$ are collections of disjointly embedded disks;
- S is *vertical* on $(1/2, 3/2)$ and $(3/2, 5/2)$, i.e. $S \cap X_{(1/2,3/2)} = S_{(1/2,3/2)}$ and $S \cap X_{(3/2,5/2)} = S_{(3/2,5/2)}$;
- $S_{[3/2]}$ is a banded unlink (L, b), which is disjoint from the descending spheres of the index 2 critical points of f.

A *banded unlink* is an unlink $L \subset X_{[3/2]}$ together with bands $b = \{b_1, ..., b_m\}$ (corresponding to the index 1 critical points for S), attached with the property that resolving L along b is another unlink $L_b \subset X_{[3/2]}$. Here, a band attached to a link L is a copy of $[0, 1] \times [-\epsilon, \epsilon]$ meeting L along $\{0, 1\} \times [-\epsilon, \epsilon]$. A *banded unlink diagram* is a Kirby diagram $\mathcal{K}$ for X, together with L and $b_1, \ldots, b_m$. By Lemma 4.4.2, the triple $(\mathcal{K}, L, b)$ describes $S \subset X$. In [33], the authors study banded unlink diagrams in detail, and give a complete set of moves relating such diagrams.

Example 4.4.9. Figure 4.18 illustrates two very basic examples of banded unlink diagrams. On the left, we have a banded unlink diagram for one of two standard "unknotted" embeddings of an $\mathbb{RP}^2 \subset S^4$. The result of resolving the band is still an unknot in S^3 and so bounds a disk. On the right, we have a banded unlink diagram describing $\mathbb{CP}^1 \subset \mathbb{CP}^2$. In this case, the unlink bounds the obvious disk in S^3 as well as the core of the $(+1)$–framed 2–handle. For clarity, the unlinks in a banded unlink diagram will be coloured blue, and the bands will be colored red.

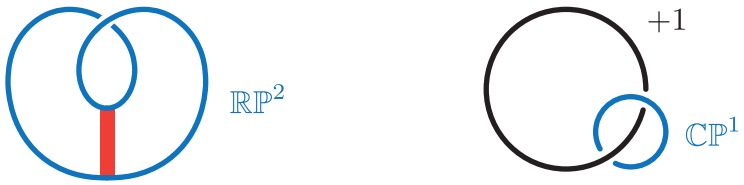

(a) (b)

Figure 4.18: In (a), a banded unlink diagram for the standard embedding of $\mathbb{RP}^2$ in S^4 with Euler number +2. In (b), a banded unlink diagram for a 2–sphere isotopic to $\mathbb{CP}^1 \subset \mathbb{CP}^2$.

Figure 4.19 illustrates two banded unlink diagrams in non-orientable 4–manifolds. On the left, we have a banded unlink diagram for $\mathbb{RP}^2 \subset \mathbb{RP}^4$. Note that there is always an induced handle decomposition for $\mathbb{RP}^k \subset \mathbb{RP}^n$ obtained from the k–dimensional cores of each n–dimensional handle. On the right, we have a banded unlink diagram for $S^2 \times \{\text{pt}\} \subset S^2 \times \mathbb{RP}^2$.

In each case, the unknot bounds a disk in the 0–handle. After possibly resolving a band, it also bounds a disk in the remaining higher index handles.

If a surface $S \subset X$ is in banded unlink position, we can further modify it so that it lies in bridge trisected position with respect to the induced trisection as in Definition 4.4.5. A banded unlink for $S \subset X$ is in *bridge position* with respect to the trisection $\mathcal{T}$ if:

- $L \subset X_{[3/2]}$ is in bridge position with respect to the central surface $\Sigma \subset X_{[3/2]}$;
- Each band is surface-framed with respect to Σ, i.e. for each i, $b_i \cap \Sigma$ is a single arc;
- The bands are *dual* to a set of shadows s_α for $L \cap H$, i.e. s_α and b intersect only at their ends, and $s_\alpha \cup (\Sigma \cap b_i)$ has no closed components.

This position is so named because it induces a bridge trisection of S with respect to $\mathcal{T}$. Meier and Zupan shows that every banded unlink decomposition of S can be upgraded to

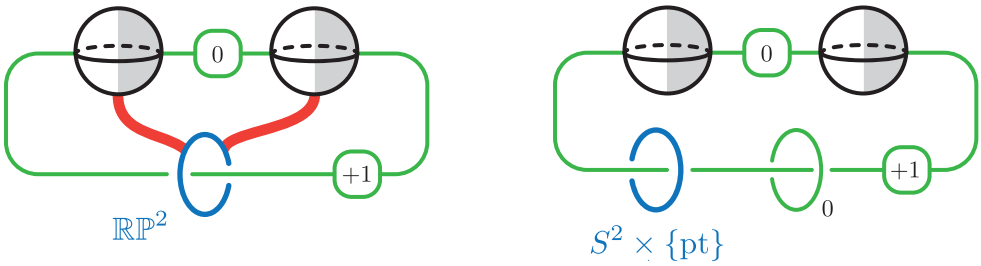

(a) (b)

Figure 4.19: In (a), a banded unlink diagram for $\mathbb{RP}^2 \subset \mathbb{RP}^4$. In (b), a banded unlink diagram describing $S^2 \times \{\text{pt}\} \subset S^2 \tilde{\times} \mathbb{RP}^2$.

be in bridge position, and so proved the following theorem. We state it with no assumptions about orientability.

Theorem 4.4.10 ([58])**.** *Suppose that X is a 4–manifold and $f : X \to \mathbb{R}$ is a self-indexing Morse function. If $S \subset X$ is a smoothly embedded surface, then S may be isotoped to lie in bridge position with respect to the trisection $\mathcal{T}$ induced by f.*

While Meier and Zupan only considered orientable manifolds, their proof does not use any orientability assumptions and so we will only sketch the proof. First, represent S by a banded unlink, and then further modify it to be in bridge position. Then, if $S \subset X$ is in banded unlink/bridge position as above, pushing the bands b_i into $H \subset \partial X_{[3/2]}$ produces a bridge trisection of S with respect to $\mathcal{T}$ [58, Lemma 3.1]. In other words, for each i the intersections $\mathcal{D}_i = S \cap X_i$ are trivial disk systems. It is easy to see that $\mathcal{D}_1$ and $\mathcal{D}_3$ are trivial disk systems, and the duality condition guarantees that $\mathcal{D}_2$ is also a trivial disk system. Similarly, t_α and t_β are trivial tangles by construction, and the duality condition guarantees that t_γ is also a trivial tangle.

Given a shadow diagram for $S \subset X$, we can use the following lemma to extract a banded unlink diagram together with a Kirby diagram for X.

Lemma 4.4.11. *Suppose that X is a 4–manifold and $S \subset X$ is a smoothly embedded surface described by a $(g, k_i; b, c_i)$-bridge trisection diagram $(\Sigma; \alpha, \beta, \gamma; s_\alpha, s_\beta, s_\gamma)$. Then we may extract a banded unlink diagram $(\mathcal{K}, L, b)$ for $S \subset X$ via the following procedure:*

1. *Standardize the α and β curves. Standardize the shadows so that $s_\alpha \cup s_\gamma$ is a collection of c_2 embedded closed curves on Σ.*

2. *Produce a Kirby diagram $\mathcal{K}$ from $(\Sigma;\alpha,\beta,\gamma)$ (e.g. see Chapter 3 or [24]). Moreover, let L be the link obtained by pushing the arcs s_α and s_β into H_α and H_β, respectively.*
3. *Let $\{s'_1,\dots,s'_{c_2}\}$ be a sub-collection of arcs from s_γ (one from each component of $s_\alpha\cup s_\gamma$). Add $b-c_2$ surface-framed arcs $b=\{b_i\}$ (bands) to L by pushing $s_\gamma-\{s'_1,\dots,s'_{c_2}\}$ into H_α.*

If $b=1$, then the resulting diagram is called a *doubly pointed trisection diagram* in analogy with doubly pointed Heegaard diagrams for knots in 3–manifolds, since $S\cap\Sigma$ consists of only two points. We need only draw these two points in a shadow diagram, since there is a unique way to connect them in the complement of each cut system. Note that in this case, no bands are added in Step 3, and a banded unlink diagram for the resulting 2–sphere may be obtained by simply pushing $s_\alpha\cup s_\beta$ (an unknot) into $H_\alpha\cup H_\beta$.

The proof of Lemma 4.4.11 is almost the same as [56, Lemma 3.3], but with one exception.

A key step in the proof of [58, Proposition 5.1] on the correspondence between banded unlink diagrams and bridge trisections is the fact every bridge splitting of the n–component unlink in $\#^k S^2\times S^1$ is *standard*. Such a bridge splitting is called standard if it is a perturbation of n copies of the 1–bridge splitting of the unlink in S^3 stabilized with k copies of $S^2\times S^1$. Since this result relies on work of Bachman-Schleimer [5] which is only stated for the orientable case, we give a proof of this fact.

Lemma 4.4.12. *Let F be a Heegaard surface for $\#^k S^2\tilde{\times}S^1$, and suppose that $L\subset\#^k S^2\tilde{\times}S^1$ is an n–component unlink. Assume that L is in bridge position with respect to F. Then L can be deperturbed with respect to F until each component of L is in 1–bridge position.*

Proof. If $M\cong S^3$, then this follows from [58]. As usual, we will proceed by induction and an application of Haken's lemma. Fix some $m>0$, and denote $M=\#^m S^2\tilde{\times}S^1$. Suppose that the claim holds whenever $k<m$. Further, assume the claim is true in $\#^m S^2\tilde{\times}S^1$ for any unlink of fewer than n components.

Note that $M\setminus\nu(L)\cong\#^m S^2\tilde{\times}S^1\#^n(S^1\times D^2)$, and that each component of $M\setminus(\nu(F)\cup\nu(L))$ is a compression body.

By Haken's lemma for 3–manifolds with boundary (see e.g. [6] or [11], or Chapter II of [37][2]), there is an essential 2–sphere S in $M\setminus L$ that intersects F in a connected simple

[2]The proof is only for closed manifolds, but the relative case is similar. Orientability does not play a role in the proof.

closed curve. Surger M along S (i.e. delete $\nu(S)$ and replace it with two disjoint 3–balls). There is a naturally induced Heegaard splitting of the resulting manifold M'.

If M' is connected, then it is homeomorphic to $\#^{m-1}S^2 \times S^1$ or $\#^{m-1}S^2 \tilde{\times} S^1$. In the first case, the claim holds by [58]; in the second it holds by inductive hypothesis.

On the other hand, suppose that $M' = M'_1 \sqcup M'_2$ is disconnected. Let $L_i = M'_i \cap L$. Since S is essential in $M \setminus L$, for each i we have either:

- $M'_i \cong \#^k S^2 \times S^1$ for $k < m$,
- $M'_i \cong \#^k S^2 \tilde{\times} S^1$ for $k < m$,
- L_i has fewer than n components.

In any case, the claim holds in M'_1 and M'_2 by [58] or the inductive hypothesis. □

Example 4.4.13. As an application, we convert shadow diagrams for $\mathbb{RP}^2 \subset \mathbb{RP}^4$ and $S^2 \times \{\text{pt}\} \subset S^2 \tilde{\times} \mathbb{RP}^2$ into banded unlink diagrams using Lemma 4.4.11, and so verify that they are correct. To obtain banded unlink diagrams, push s_α and s_β into H_α and H_β respectively. Then add a band corresponding to a framed arc from s_γ (in Figure 4.20 (b) no bands are added).

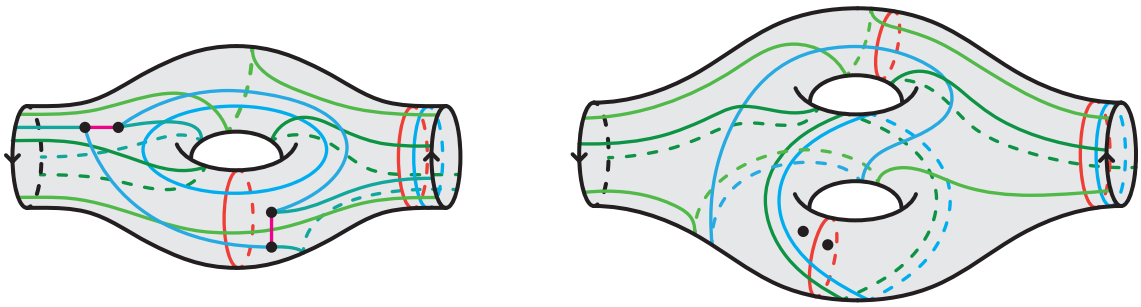

(a) (b)

Figure 4.20: In (a), a shadow diagram describing $\mathbb{RP}^2 \subset \mathbb{RP}^4$, obtained by arranging a banded unlink diagram to be in bridge position with respect to a Heegaard surface induced by the $(2;1)$–trisection of $\mathbb{RP}^4$. In (b), a shadow diagram for $S^2 \times \{\text{pt}\} \subset S^2 \tilde{\times} \mathbb{RP}^2$.

4.4.3 Perturbation and uniqueness

There is a natural way to perturb a knot in bridge position (see Figure 4.22). Similarly, there is an analogous operation on surfaces in bridge position, which is illustrated in Figure 4.21. The definition is somewhat technical, but simply describes this illustration.

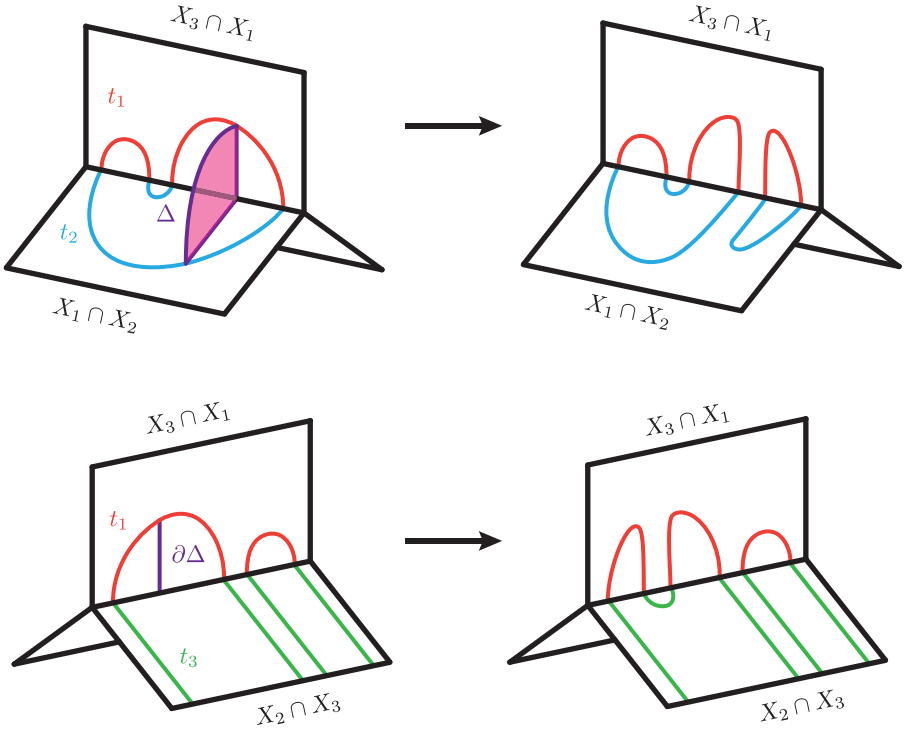

Figure 4.21: A schematic illustrating the process of perturbing a bridge trisection. In short, one does a Whitney move on a disk $\Delta \subset X_1$ satisfying certain conditions. Under these conditions, the resulting surface is still in bridge position.

Definition 4.4.14 ([56],[58])**.** Let $\mathcal{T}$ be a trisection of a 4–manifold X, with sectors X_1, X_2, and X_3. Let $\Sigma = X_1 \cap X_2 \cap X_3$ and suppose that $S \subset X$ is a surface in bridge position with respect to $\mathcal{T}$. Since $t_1 = S \cap X_3 \cap X_1$ and $t_2 = S \cap X_1 \cap X_2$ cobound boundary parallel disks in X_1, it follows that t_1 and t_2 have shadows s_1 and s_2 (respectively) in the central surface $\Sigma = \partial(X_3 \cap X_1) = \partial(X_1 \cap X_2)$ that are disjoint in their interiors, and so that $s_1 \cup s_2$ is an unlink bounding disks $D_1, \dots, D_c$ in Σ. Consequently $S \cap X_1$ is isotopic (rel ∂X_1) to $D_1 \sqcup \cdots \sqcup D_c$.

Let Δ be a disk in X_1 whose boundary can be decomposed into three arcs $\delta_1, \delta_2, \delta_3$ so that the following hold:

- The arc δ_1 is contained in $X_3 \cap X_1$ and has one endpoint on S and the other on Σ. Moreover, projecting δ_1 to Σ yields an embedded arc with one endpoint on the interior of s_1, one endpoint on $\Sigma \setminus S$, and the interior of δ_1 disjoint from s_1.
- The arc δ_2 is contained in $S \cap X_1 \cap X_2$ and has one endpoint on S and the other on Σ. Moreover, projecting δ_2 to Σ yields an embedded arc with one endpoint on the interior of s_2, one endpoint on $\Sigma \setminus S$, and the interior of δ_2 disjoint from s_2,
- The arc δ_3 is contained in S, and properly embedded in X_1.

Now let S' be the surface obtained by compressing S along Δ. That is, frame Δ so that $(\delta_1 \cup \delta_2) \times I \subset \partial X_1$ and $\delta_3 \times I \subset S$, and then let S' be the result of performing a Whitney move on S along Δ; see Figure 4.21. We say that S' is obtained from S by *perturbation*, and S is obtained from S' by *deperturbation*.

The roles of X_1, X_2, and X_3 may be permuted, i.e. we can obtain S' from compressing a disk in either X_2 or X_3. We still say S' is obtained from S by perturbation and that S is obtained from S' by deperturbation.

The point of this definition is to produce a surface which is still in bridge position.

Proposition 4.4.15. *[56, Lemma 5.2],[58] Let $\mathcal{T}$ be a trisection of a 4–manifold X, with sectors X_1, X_2, and X_3. Suppose $S \subset X$ is a surface in bridge position with respect to $\mathcal{T}$, and that S' is obtained from S by perturbation. Then S' is in bridge position with respect to $\mathcal{T}$.*

Perturbation of bridge trisections is (conveniently) very similar to perturbation of a banded link in bridge position (see Figure 4.22). There is a correspondence between bridge trisections of a surface S and bridge-split banded unlink diagrams of S [58],[33], in which the two notions of perturbations agree.

We will now discuss Theorem 4.4.6. The proof in [33] in the orientable case works almost verbatim. There, the authors use the correspondence between bridge trisections and banded unlink diagrams, and explicitly show how to induce any band move on a banded unlink via perturbations and deperturbations on the corresponding bridge trisection. In particular, they show that any two bridge trisections corresponding to isotopic banded unlinks are equivalent after a sequence of perturbations and deperturbations. However, the final step of their proof requires the following additional lemma in the non-orientable case.

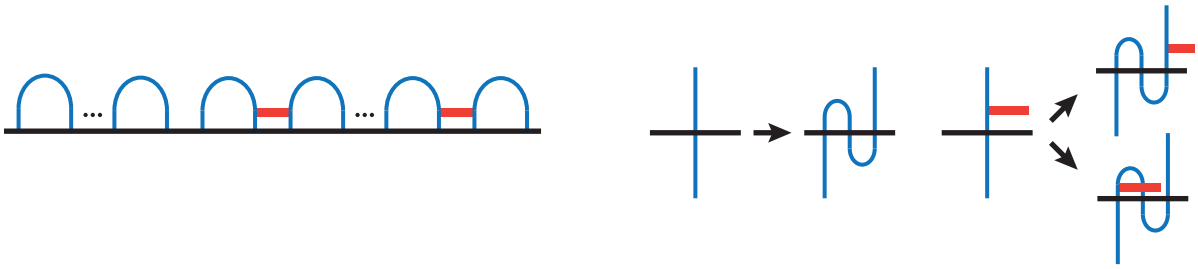

Figure 4.22: Right: a banded link (L, b) in a Heegaard split 3–manifold $H_1 \cup H_2$ is in *bridge position* with respect to $H_1 \cap H_2$ if each $(L, b) \cap H_i$ is isotopic to this picture. Left: perturbing a banded link in bridge position.

Lemma 4.4.16. *Let M be a non-orientable 3–dimensional handlebody of genus g, and let $M = H_1 \cup H_2$, where $H_1 \cong \Sigma \times I$ is a collar neighborhood of ∂M and $H_2 = \overline{M \setminus H_1}$.*

Let T be a boundary-parallel tangle in M that is in bridge position with respect to $H_1 \cap H_2$, (i.e. the closure of any component of $T \setminus (H_1 \cap H_2)$ is an arc properly embedded in H_1 or H_2 which is either parallel to an arc in $H_1 \cap H_2$ or of the form $\{pt\} \times I$ in $H_1 = \Sigma \times I$).

Then after a finite sequence of deperturbations applied to T and an isotopy fixing $H_1 \cap H_2$ setwise, T can be taken to intersect H_1 only in arcs of the form $\{pt\} \times I$.

When M is an orientable handlebody, 4.4.16 is a theorem of Hayashi and Shimokawa [31] (also see [73]). Their proof involves reducing the general case to when M is a 3–ball. For completeness, we repeat that argument for non-orientable handlebodies.

Proof of Lemma 4.4.16. Once again, the proof proceeds by induction and an application of Haken's lemma. If M is a 3–ball, the claim follows from [31]. Assume that the claim holds whenever the genus of M is less than g.

Observe that the claim is trivially true when T is the empty tangle. Further assume that the claim holds whenever T has fewer than n components for some fixed $n > 0$, and assume that T is an n-component tangle.

Since T is boundary parallel, $M \setminus \nu(T)$ is a non-orientable handlebody. By Haken's lemma for 3–manifolds with boundary (as in Lemma 4.4.12), there exists a disk D neatly embedded in M so that:

- D is disjoint from T,

- D intersects $H_1 \cap H_2$ in a connected simple closed curve,
- D is separating and each component of $M \setminus \nu(D)$ is either not a 3–ball or contains at least one component of T.

Let M_1 and M_2 be the components of $M \setminus \nu(D)$, and $T_i = M_i \cap T$. Note that M_i is a handlebody. Let F_i be a surface in M_i parallel to the boundary of M_i, with F_i agreeing with $H_1 \cap H_2$ away from D. Then T_i is in bridge position in M_i with respect to F_i. Moreover, for each i, either the genus of M_i is less than g (and M_i may be orientable) or T_i is a tangle of fewer than n components. Inductively, T_i can be deperturbed relative to F_i (and hence relative to $H_1 \cap H_2$ since F_i agrees with $H_1 \cap H_2$ near T_i), to intersect H_1 only in arcs of the form $\{\text{pt}\} \times I$ as desired. □

Using this lemma, we give a sketch of the proof of Theorem 4.4.6.

Sketch of the proof of Theorem 4.4.6. Suppose that S_1 and S_2 are isotopic surfaces that are each in bridge position with respect to a trisection $\mathcal{T}$ of a closed non-orientable 4–manifold X. Recall that there is a correspondence between bridge trisections of surfaces with respect to $\mathcal{T}$ and banded unlink diagrams in bridge position in a Heegaard-split Kirby diagram $\mathcal{K}$ related to $\mathcal{T}$. By [33], two banded unlink diagrams of a surface in a 4–manifold with respect to the same Kirby diagram are related by a sequence of band moves and isotopy. In [56] and [33], it is shown how to achieve band moves of the banded unlinks corresponding to S_1 and S_2 via a sequence of perturbations and deperturbations of S_1 and S_2. Thus, we can assume that the associated banded unlinks for S_1 and S_2 are isotopic.

Now consider the following perspective of the situation, in which we have isotoped the two banded unlinks to agree. We have a banded unlink (L, b) in $\#S^2 \tilde{\times} S^1$ and two Heegaard splittings $H_1 \cup_F H_2 = H_1' \cup_{F'} H_2'$ of $\#S^2 \tilde{\times} S^1$ so that (L, b) is in bridge position with respect to both splittings. We want to prove that F and F' become isotopic as bridge surfaces for (L, b) after a finite sequence of perturbations; we will use an argument from [73, Theorem 2.2].

Let C_1 and C_2' be wedges of circles so that H_1, H_2' deformation retract on C_1, C_2', respectively. Generically, we can take C_1 and C_2' to be disjoint. By isotoping F to lie close to C_1 and F' to lie close to C_2', we may therefore take F and F' to be disjoint, with H_1 and H_2' disjoint. Let $W := H_1' \setminus H_1 = H_2 \setminus H_2'$. Then W is homeomorphic to $F \times I$. Let $F^* = F \times \{1/2\} \subset W$. By Lemma 4.4.16 applied to the splitting (W, H_1) of $W \cup H_1$ and the tangle $L \cap (W \cup H_1)$, we find that F^* is obtained from F by perturbation. On the other hand, by Lemma 4.4.16 applied to the splitting (W, H_2') of $W \cup H_2'$ and the tangle

$L \cap (W \cup H_2')$, we find that F^* is obtained from F' by perturbation (without moving b, as in Figure 4.22). This completes the proof. □

References

[1] Aaron Abrams, David T. Gay, and Robion Kirby. Group trisections and smooth 4–manifolds. *Geometry & Topology*, 22(3):1537 – 1545, 2018.

[2] Selman Akbulut. A fake 4–manifold. In *Four-Manifold Theory*, volume 35 of *Contemporary Math.*, pages 75–141, 1984.

[3] Selman Akbulut. *4–manifolds*, volume 25 of *Oxford Graduate Texts in Mathematics*. Oxford University Press, Oxford, 2016.

[4] Anar Akhmedov and B. Doug Park. Exotic smooth structures on small 4–manifolds with odd signatures. *Inventiones Mathematicae*, 181(3):577–603, 2010.

[5] David Bachman and Saul Schleimer. Distance and bridge position. *Pacific Journal of Mathematics*, 219(2):221–235, 2005.

[6] Francis Bonahon and Jean-Pierre Otal. Scindements de Heegaard des espaces lenticulaires. *Annales Scientifiques de l'École Normale Supérieure. Quatrième Série*, 16(3):451–466, 1983.

[7] Tara Brendle, Nathan Broaddus, and Andrew Putman. The mapping class group of connect sums of $S^2 \times S^1$. *arXiv e-prints*, page arXiv:2012.01529, December 2020.

[8] Clarisson Rizzie Canlubo. The Heegaard splitting of S^3 and the Hopf fibration. *Matimyás Matematika*, 40(1-2):13–18, 2017.

[9] Sylvain E. Cappell and Julius L. Shaneson. Some new four-manifolds. *Annals of Mathematics*, 104(1):61–72, 1976.

[10] Leonardo N. Carvalho and Ulrich Oertel. A classification of automorphisms of compact 3–manifolds. *arXiv Mathematics e-prints*, page math/0510610, October 2005.

[11] A. J. Casson and C. McA. Gordon. Reducing Heegaard splittings. *Topology and its Applications*, 27(3):275–283, 1987.

[12] Nicholas A. Castro. *Relative trisections of smooth 4–manifolds with boundary*. PhD thesis, University of Georgia, 2015.

[13] Nickolas Castro, David Gay, and Juanita Pinzón-Caicedo. Diagrams for relative trisections. *Pacific Journal of Mathematics*, 294(2):275–305, 2018.

[14] Nickolas A. Castro, David T. Gay, and Juanita Pinzón-Caicedo. Trisections of 4–manifolds with boundary. *Proceedings of the National Academy of Sciences*, 115(43):10861–10868, 2018.

[15] Nickolas A. Castro, Gabriel Islambouli, Maggie Miller, and Maggy Tomova. The relative $\mathcal{L}$-invariant of a compact 4–manifold. *arXiv e-prints*, page arXiv:1908.05371, August 2019.

[16] Nickolas A. Castro and Burak Ozbagci. Trisections of 4–manifolds via Lefschetz fibrations. *Mathematical Research Letters*, 26(2):383–420, 2019.

[17] Jean Cerf. Sur les difféomorphismes de la sphère de dimension trois ($\Gamma_4 = 0$). *Lecture notes in Math*, 53, 1968.

[18] Jean Cerf. La stratification naturelle des espaces de fonctions différentiables réelles et le théoreme de la pseudo-isotopie. *Publications Mathématiques de l'Institut des Hautes Études Scientifiques*, 39(1):7–170, 1970.

[19] John B Etnyre. Lectures on open book decompositions and contact structures. In *Floer Homology, Gauge Theory, and Low-Dimensional Topology: Proceedings of the Clay Mathematics Institute 2004 Summer School, Alfréd Rényi Institute of Mathematics, Budapest, Hungary, June 5-26, 2004*, volume 5, page 103. American Mathematical Soc., 2006.

[20] Peter Feller, Michael Klug, Trenton Schirmer, and Drew Zemke. Calculating the homology and intersection form of a 4–manifold from a trisection diagram. *Proceedings of the National Academy of Sciences*, 115(43):10869–10874, 2018.

[21] Vincent Florens and Delphine Moussard. Torsions and intersection forms of 4–manifolds from trisection diagrams. *Canadian Journal of Mathematics*, pages 1–24, 2020.

[22] Michael H. Freedman. The topology of four-dimensional manifolds. *Journal of Differential Geometry*, 17(3):357–453, 1982.

[23] David Gabai. Foliations and surgery on knots. *Bulletin (New Series) of the American Mathematical Society*, 15(1):83 – 87, 1986.

[24] David Gay and Robion Kirby. Trisecting 4–manifolds. *Geometry & Topology*, 20(6):3097 – 3132, 2016.

[25] David Gay and Jeffrey Meier. Doubly pointed trisection diagrams and surgery on 2–knots. *arXiv e-prints*, page arXiv:1806.05351, June 2018.

[26] Herman Gluck. The embedding of two-spheres in the four-sphere. *Transactions of the American Mathematical Society*, 104(2):308–333, 1962.

[27] Robert E. Gompf. Stable diffeomorphism of compact 4–manifolds. *Topology and its Applications*, 18(2-3):115–120, 1984.

[28] Robert E. Gompf and András Stipsicz. *4–manifolds and Kirby calculus*, volume 20. American Mathematical Soc., 1999.

[29] Wolfgang Haken. Some results on surfaces in 3–manifolds. *Studies in Modern Topology*, 5:39–98, 1968.

[30] Ian Hambleton, Matthias Kreck, and Peter Teichner. Nonorientable 4–manifolds with fundamental group of order 2. *Transactions of the American Mathematical Society*, 344(2):649–665, 1994.

[31] Chuichiro Hayashi and Koya Shimokawa. Heegaard splittings of trivial arcs in compression bodies. *Journal of Knot Theory and its Ramifications*, 10(1):71–87, 2001.

[32] Sebastian Hensel and Jennifer Schultens. Strong Haken via Sphere Complexes. *arXiv e-prints*, page arXiv:2102.09831, February 2021.

[33] Mark Hughes, Seungwon Kim, and Maggie Miller. Isotopies of surfaces in 4–manifolds via banded unlink diagrams. *Geometry & Topology*, 24(3):1519–1569, 2020.

[34] William H. Meeks III. Representing codimension-one homology classes on closed nonorientable manifolds by submanifolds. *Illinois Journal of Mathematics*, 23(2):199 – 210, 1979.

[35] Gabriel Islambouli. Nielsen equivalence and trisections. *Geometriae Dedicata*, 2021.

[36] Gabriel Islambouli and Patrick Naylor. Multisections of 4–manifolds. *arXiv e-prints*, page arXiv:2010.03057, October 2020.

[37] William Jaco. *Lectures on three-manifold topology*, volume 43 of *CBMS Regional Conference Series in Mathematics*. American Mathematical Society, 1980.

[38] M. Ho Kim and Frank Raymond. The diffeotopy group of the twisted 2–sphere bundle over the circle. *Transactions of the American Mathematical Society*, 322(1):159–168, 1990.

[39] Myung Ho Kim, Sadayoshi Kojima, and Frank Raymond. Homotopy invariants of nonorientable 4–manifolds. *Transactions of the American Mathematical Society*, 333(1):71–81, 1992.

[40] Seungwon Kim and Maggie Miller. Trisections of surface complements and the Price twist. *Algebraic & Geometric Topology*, 20(1):343–373, 2020.

[41] Robion Kirby and Abigail Thompson. A new invariant of 4–manifolds. *Proceedings of the National Academy of Sciences*, 115(43):10857–10860, 2018.

[42] Dale Koenig. Trisections of 3–manifold bundles over S^1. *arXiv e-prints*, page arXiv:1710.04345, October 2017.

[43] Peter Lambert-Cole. Symplectic trisections and the adjunction inequality. *arXiv e-prints*, page arXiv:2009.11263, September 2020.

[44] Peter Lambert-Cole. Stein trisections and homotopy 4–balls. *arXiv e-prints*, page arXiv:2104.02003, April 2021.

[45] Peter Lambert-Cole and Jeffrey Meier. Bridge trisections in rational surfaces. *Journal of Topology and Analysis*, pages 1–54, 2020.

[46] Peter Lambert-Cole, Jeffrey Meier, and Laura Starkston. Symplectic 4–manifolds admit Weinstein trisections. *Journal of Topology*, 14(2):641–673, 2021.

[47] Peter Lambert-Cole and Maggie Miller. Trisections of 5–manifolds *in 2019-20 MATRIX Annals*, volume 4 of *MATRIX Book Series*, pages 117–134. Springer, 2021.

[48] François Laudenbach. Sur les 2–spheres d'une variete de dimension 3. *Annals of Mathematics*, 97(1):57–81, 1973.

[49] François Laudenbach. *Topologie de la dimension trois: homotopie et isotopie*. Société Mathématique de France, 1974.

[50] François Laudenbach. A proof of Reidemeister-Singer's theorem by Cerf's methods. *Annales de la Faculté des Sciences de Toulouse. Mathématiques.*, XXIII(1):197 – 221, 2014.

[51] François Laudenbach and Valentin Poénaru. A note on 4–dimensional handlebodies. *Bulletin de la Société Mathématique de France*, 100:337–344, 1972.

[52] Charles Livingston. Surfaces bounding the unlink. *The Michigan Mathematical Journal*, 29(3):289–298, 1982.

[53] Jeffrey Meier. Trisections and spun 4–manifolds. *Mathematical Research Letters*, 25(5):1497–1524, 2018.

[54] Jeffrey Meier, Trent Schirmer, and Alexander Zupan. Classification of trisections and the Generalized Property R Conjecture. *Proc. Amer. Math. Soc.*, 144:4983–4997, 2016.

[55] Jeffrey Meier, Abigail Thompson, and Alexander Zupan. Cubic graphs induced by bridge trisections. *arXiv e-prints*, page arXiv:2007.07280, July 2020.

[56] Jeffrey Meier and Alexander Zupan. Bridge trisections of knotted surfaces in S^4. *Transactions of the American Mathematical Society*, 369(10):7343–7386, 2017.

[57] Jeffrey Meier and Alexander Zupan. Genus-two trisections are standard. *Geometry & Topology*, 21(3):1583 – 1630, 2017.

[58] Jeffrey Meier and Alexander Zupan. Bridge trisections of knotted surfaces in 4–manifolds. *Proceedings of the National Academy of Sciences*, 115(43):10880–10886, 2018.

[59] Maggie Miller and Patrick Naylor. Trisections of non-orientable 4–manifolds. *arXiv e-prints*, page arXiv:2010.07433, October 2020.

[60] J. Milnor. *Morse Theory. (AM-51), Volume 51*. Princeton University Press, 1969.

[61] Edwin E. Moise. Affine structures in 3–manifolds: V. The triangulation theorem and Hauptvermutung. *Annals of Mathematics*, pages 96–114, 1952.

[62] William E. Olsen. Trisections and Ozsvath-Szabo cobordism invariants. *arXiv e-prints*, page arXiv:2102.00910, February 2021.

[63] Burak Ozbagci. On open books for nonorientable 3–manifolds. *arXiv e-prints*, page arXiv:2004.08173, April 2020.

[64] Kurt Reidemeister. Zur dreidimensionalen topologie. *Abhandlungen aus dem Mathematischen Seminar der Universität Hamburg*, 9(1):189–194, 1933.

[65] José Román Aranda and Jesse Moeller. Diagrams of *–Trisections. *arXiv e-prints*, page arXiv:1911.06467, November 2019.

[66] Hyam Rubinstein and Stephan Tillmann. Multisections of piecewise linear manifolds. *Indiana University Mathematics Journal*, 69(6):2209–2239, 2020.

[67] J. Hyam Rubinstein and Stephan Tillmann. Generalized trisections in all dimensions. *Proceedings of the National Academy of Sciences*, 115(43):10908–10913, 2018.

[68] James Singer. Three-dimensional manifolds and their Heegaard diagrams. *Transactions of the American Mathematical Society*, 35(1):88–111, 1933.

[69] Jonathan Spreer and Stephan Tillmann. Determining the trisection genus of orientable and non-orientable PL 4–manifolds through triangulations. *Experimental Mathematics*, pages 1–11, 2020.

[70] Rafael Torres. Smooth structures on nonorientable four-manifolds and free involutions. *Journal of Knot Theory and Its Ramifications*, 26(13):1750085, 2017.

[71] Friedhelm Waldhausen. Heegaard-zerlegungen der 3–sphäre. *Topology*, 7(2):195–203, 1968.

[72] C. T. C. Wall. On simply-connected 4–manifolds. *Journal of the London Mathematical Society*, 1(1):141–149, 1964.

[73] Alexander Zupan. Bridge and pants complexities of knots. *Journal of the London Mathematical Society*, 87(1):43–68, 2013.